

On-line Calibration of Instrument Transformers Using Synchrophasor Measurements

Paroma Chatterjee

Thesis submitted to the faculty of Virginia Polytechnic
Institute and State University in partial fulfillment
of the requirements for the degree of

Master of Science
In
Electrical Engineering

Jaime De La Ree, Chair
James S. Thorp, Co-Chair
Virgilio A. Centeno, Member

December 08, 2015
Blacksburg, VA

Keywords - Calibration, Current Transformers (CTs),
Optimal placement, Phasor Measurement Units (PMUs),
Quantized errors, Voltage Transformers (VTs)

On-line Calibration of Instrument Transformers Using Synchrophasor Measurements

Paroma Chatterjee

ABSTRACT

The world of power systems is ever changing; ever evolving. One such evolution was the advent of Phasor Measurement Units (PMUs). With the introduction of PMUs in the field, power system monitoring and control changed for the better. Innovative and efficient algorithms that used synchrophasors came to be written. To make these algorithms robust, it became necessary to remove errors that crept into the power system with time and usage. Thus the process of calibration became essential when practical decisions started being made based on PMU measurements.

In the context of this thesis ‘calibration’ is the method used to estimate a correction factor which, when multiplied with the respective measurement, negates the effect of any errors that might have crept into them due to the instrument transformers located at the inputs of a PMU or the PMU device itself. Though this thesis mainly deals with the calibration of instrument transformers, work has been done previously for calibrating other components of a power system. A brief description of those methods have been provided along with a history on instrument transformer calibration.

Three new methodologies for instrument transformer calibration have been discussed in details in this thesis. The first method describes how only voltage transformers can be calibrated by placing optimal number of good quality voltage measurements at strategic locations in the grid, in presence of ratio errors in the instrument transformers and Gaussian errors in the PMUs. The second method provides a way to calibrate all instrument transformers (both current and voltage) in presence of only one good quality voltage measurement located at the end of a tie-line. This method assumes that all the instrument transformers have ratio errors and the PMUs have quantization errors. The third method attains the same objective as the second one, with the additional constraint that the data obtained from the field may be contaminated. Thus, the third method shows how calibration of all the instrument transformers can be done with data that is intermittent and is therefore, the most practical approach (of the three) for instrument transformer calibration.

To my mother, Tanima Chatterjee, my father, Goutam Chatterjee and my sister, Preeti Chatterjee, for believing in me even when I stumbled

ACKNOWLEDGEMENTS

I would like to express my sincere gratitude to the ECE department of Virginia Tech, for letting me fulfill my dream of being a student here and completing my Master's Thesis. I would like to thank my advisor, Dr. Jaime De La Ree, for his continuous support, patience and motivation. I would like to extend my sincere gratitude to Dr. James Thorp, for without his guidance, this thesis would not have been possible. I would also like to thank Dr. Virgilio Centeno for his insightful comments and encouragement.

I would also like to thank my fellow graduate students for their continued support and encouragement. I am thankful to Ming Zhou and Zhongyu Wu, as the beginning of this thesis was based on the foundation that has been laid by them. I would like to extend my thanks to Anamitra Pal for his inputs that proved extremely helpful and helped me learn a lot.

Last, but not the least, my family has been a great pillar of support for me. I would not have been here if not for their support, guidance and unwavering faith in me.

December 8th, 2015

Paroma Chatterjee

TABLE OF CONTENTS

Abstract	ii
Dedication	iii
Acknowledgements	iv
List Of Figures	vii
List Of Tables	ix
Chapter 1: Introduction	1
1.1 Phasor Measurement Units and their applications	2
1.1.1 Monitoring based applications	3
1.1.2 Control based applications	4
1.1.3 Protection based applications.....	4
1.2 Need for Calibration	6
1.3 Process of Calibration	7
1.4 Structure of the Thesis	10
Chapter 2: History behind Calibration	11
2.1 Previous Research	13
2.2 On-line Calibration of VTs Using Synchrophasor Measurements	16
2.2.1 Formulation	18
2.2.2 Simulations and Results	27
Chapter 3: A New Approach to Instrument Transformer Calibration	31
3.1 Error Model	33
3.2 PMU data based Voltage & Current Transformer Calibration	34
3.2.1 Voltage and Current Transformer Calibration	38
3.2.2 Simulation and Results for Voltage and Current Transformer Calibration	39
Chapter 4: Calibrating Instrument Transformers in Presence of Incomplete Data	45
4.1 Methodology	45
4.2 Simulation and Results	48
Chapter 5: Conclusion and Future Scope of Work	57
5.1 Thesis Summary	57
5.2 Future Scope of work	58
References	60

Appendices	64
Appendix A	65
MATLAB simulations for Chapter-3	65
Appendix B	74
MATLAB simulations for Chapter-4	74

LIST OF FIGURES

Figure 1.1: Block diagram of a Phasor Measurement Unit (PMU)	3
Figure 1.2: High voltage transmission system with two buses X and Y	7
Figure 1.3: The IEEE 118 bus system with the high voltage network highlighted [26]	8
Figure 1.4: The IEEE 300 bus system with the high voltage network highlighted [27]	9
Figure 2.1: Two-bus pi-network model of the power system	14
Figure 2.2: Two pi-sections with dual-use line relays acting as PMUs	19
Figure 2.3: Flowchart for finding optimal locations of good quality measurements	26
Figure 2.4: High-voltage network of IEEE-118 bus system	27
Figure 2.5: High-voltage network of IEEE-300 bus system	27
Figure 2.6: Growth of standard deviation (σ) when only one reliable measurement is present in the systems; the dashed line shows the pre-defined threshold (T0) of 0.01	28
Figure 2.7: All the standard deviations (σ) for both test systems are below the pre-defined threshold (T0) where T0 = 0.01	30
Figure 3.1(a): Field data-Voltages	31
Figure 3.1(b): Field data-Voltages (magnified view)	32
Figure 3.2(a): Field data-Currents	32
Figure 3.2(b): Field data-Currents (magnified view)	33
Figure 3.3: Two-bus π -network model of the power system	35
Figure 3.4: A Comparison of condition numbers when A is voltages (blue) instead of currents (red)	37
Figure 3.5: Two pi-sections with dual-use line relays acting as PMUs	39
Figure 3.6: Standard deviation (σ) of the ratio errors in voltage transformers of the IEEE 118 bus system with good quality measurements only at bus 10	41
Figure 3.7: Standard deviation (σ) of the ratio errors in voltage transformers of the IEEE 300 bus system with good quality measurements only at bus 242	41
Figure 3.8: Standard deviation (σ) of the ratio errors in current transformers of the IEEE 118 bus system with good quality measurements only at bus 10	42
Figure 3.9: Standard deviation (σ) of the ratio errors in current transformers of the IEEE 300 bus system with good quality measurements only at bus 242	42
Figure 3.10: Standard deviation (σ) of the ratio errors in voltage transformers of the IEEE 300 bus system with good quality VT at bus 242 and bus 28	43
Figure 3.11: Standard deviation (σ) of the ratio errors in current transformers of the IEEE 300 bus system with good quality VT at bus 242 and bus 28	44

Figure 4.1: Snapshot of a part of the field data obtained from a utility with data missing from it	49
Figure 4.2: The 3D matrix created for both voltages and currents	50
Figure 4.3: Solution of each pi-section available as pieces of a jigsaw puzzle	51
Figure 4.4: Putting the jigsaw puzzle together	52
Figure 4.5: Standard deviation (σ) of the errors in estimating the ratios of ratio errors of the voltage transformers in the IEEE-118 bus system	54
Figure 4.6: Standard deviation (σ) of the errors in estimating the ratios of ratio errors of the current transformers in the IEEE-118 bus system	54
Figure 4.7: Standard deviation (σ) of the errors in estimating the ratios of ratio errors of the voltage transformers in the IEEE-300 bus system	55
Figure 4.8: Standard deviation (σ) of the errors in estimating the ratios of ratio errors of the current transformers in the IEEE-300 bus system	56

LIST OF TABLES

TABLE 2.1: Optimal Locations of Good Measurements for Different Pi-section Lengths of IEEE-300 Bus System	29
TABLE 2.2: Optimal Locations of Good Measurements for Test Systems	29
TABLE 4.1: Ratio of Ratio Errors in Voltages for the IEEE-118 bus system for the first iteration	52
TABLE 4.2: Ratio of Ratio Errors in Voltages for the IEEE-118 bus system for the Thousandth iteration.....	53

CHAPTER 1: INTRODUCTION

Since its inception, the power system has played a key role in industrialization and urbanization. Till date, it plays a socially responsible role in bridging disparities by improving provision of affordable commercial energy access. Power sector has come of age through radical changes related to the competition scenario and focus on green energy which have progressively evolved over the last decade. For the US, the genesis of these changes occurred after the blackout of 1965. Till that point in time, the power sector was controlled and protected by analog instruments: meters, breakers, etc. The sub-station operators had only their manuals and experience to count on. They had no way of looking at the entire grid as a whole and be able to plan for contingencies. But, even then, electricity was an irreplaceable part of life. People and economy were heavily dependent on reliable power supply. Homes, offices and factories had all been transformed by electricity. Elevators, lights, air-conditioners, the upcoming computer industry, everything depended on electricity.

Then came the US North-East blackout of 1965. It blacked out parts of Ontario, Canada as well as Connecticut, Massachusetts, New Hampshire, New Jersey, New York, Rhode Island and Vermont in the United States on 9th of November, 1965. A relatively minor error resulted in this massive disruption that affected over 30 million people and spread across 80,000 square miles with some people being left without electricity for up to 13 hours [1]. The cause of the blackout was that the relays had been set according to the load conditions of 1956. In the 9 years that followed, the load had increased to such a level that the usual loads on that fateful day became larger than the maximum overload that the relays had been designed to operate at. Thus the relays of one of the five transmission lines carrying power north from the Sir Adam Beck Station of the Hydro-Electric Power Commission of Ontario tripped thinking that it was a fault instead of the norm. This put the load of that line on the rest four, overloading them in turn [2]. This caused a domino effect and brought down the entire North-Eastern grid. Soon after normalcy was restored and the mistake corrected, utilities across the country started looking for answers to solving the big issue: How to make sure such a cascading failure not repeat itself? The answer lay in integrating information systems and power electronics with the power grid. This eventually led to the beginning of the concept of a smart grid.

1.1 Phasor Measurement Units and their applications

The massive blackout of 1965 had many ramifications. It forced the people to rethink their way of life, their dependence on the power grids and also propelled electrical engineers to re-engineer the current grid system. It took the Federal Power Commission almost a week to find the root cause of the black-out. This got power engineers all across the country thinking that there had to be a way of knowing the states of the power system at all times, so that a quicker diagnosis can be carried out.

The state of a power system is the magnitudes and phase angles of the voltages at all network buses. A central control system was initially proposed, which could help improve the security and thus, the reliability of the electric power system, both at the generation as well as transmission levels. The central control system would operate in two steps: (1) a digital computer which would be able to process the collected data, and (2) either the computer or a human operator could make the control decisions based on the processed data [3]. In accordance with this logic, Fred Schweppe came up with the idea of a static-state estimator algorithm in the late 1960s-early 70s. His idea was to create a data processing algorithm which would work by processing redundant meter readings and any other form of information available and estimate the state vector.

Utilities were especially interested in wide-area view provided by such an estimator as they would get a snap-shot of the entire power systems operation sitting in the comforts of an air-conditioned room. Thus came the supervisory control and data acquisition (SCADA) system, which was used at first to support these static-state estimators. But, these estimators worked for steady state applications only. Also, these estimators had to perform complex calculations. Hence, they were slow, and would often lag behind.

With advancement in information systems and communication technology and the advent of microprocessors around 1982, it became easier to monitor, control and protect the power grid as a whole. In 1983, synchrophasor technology was introduced with the invention of phasor measurement units (PMUS) [4]. By 1988, PMUs were being commercially produced [5] [6]. This technology enabled power engineers to have access to real-time snapshots of the entire system, thus making real-time monitoring possible. There can be two different types of PMUs. The

traditional PMUs provide GPS time synchronized values of the phasors (voltage magnitudes and phase angles) of the bus they are on, as well as the branch currents of all the transmission lines connected to the bus. The newer dual use line relay PMUs (DULR PMUs) are placed on every line connected to high voltage transmission buses, and provide the currents on the lines as well as a look at the phasors on the bus as output. The block diagram of a PMU is shown in fig. 1.1. These were the first devices that gave hope that the entire power system can be monitored, controlled and protected in real-time. There was minimal time delay between the actual measurement at the field and those reported at the control center. So the control center operators always had the whole picture in front of them, to make decisions and take actions in case of any faults.

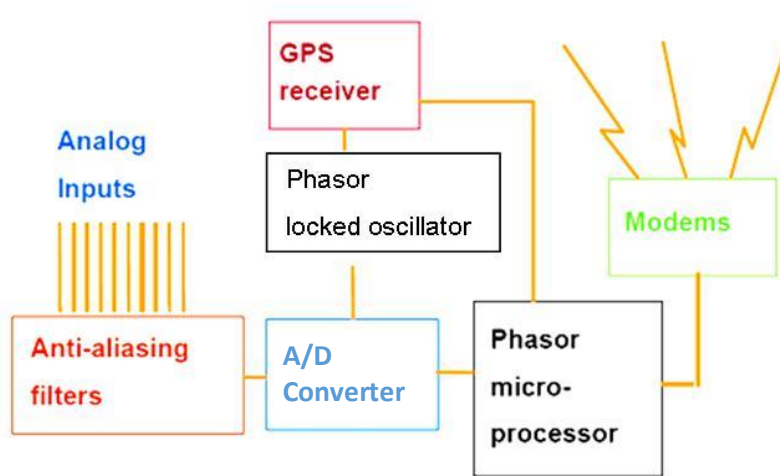


Figure 1.1: Block diagram of a Phasor Measurement Unit (PMU)

Some downstream applications, like state estimation (hybrid/linear), base-lining studies (computing alert/alarm limits), protection (security assessment, adaptive relaying), control (damping oscillations), etc. that use PMU data for their operation have been explained below.

1.1.1 Monitoring based applications

With the introduction of PMUs, hybrid state estimators came to be proposed [7]-[9]. Although superior to purely static state estimators, hybrid estimators were non-linear and iterative and hence, slow. As more and more PMUs were added to the network, a PMU-only state estimator became possible. One type of “linear state estimator” has already been developed for Dominion Virginia

Power and is being currently used in their high-voltage network and is working quite successfully [10]-[11]. The voltage phasor output of such a linear state estimator has also been used for fault classification in [12].

The idea of partitioned linear state estimator (PLSE) as an alternative to the traditional linear state estimator (LSE) has also been presented in [13]. PLSE would have applications in large power systems, like the independent system operators (ISOs) which have different utilities functioning under them, without compromising the individual privacy requirements of the utilities.

1.1.2 Control based applications

For a power system, the power flow has to be monitored as well as controlled. The key quantities to be controlled are: frequency, voltage and current. Uncontrolled variations in any one will affect the other two, which in turn will affect the transmission network which can potentially lead to a cascading blackout scenario.

PMUs have come a long way in assisting the monitoring and control of high voltage transmission systems. To counter the effects of inter-area oscillations on the stability of a power system [14], [15] describe a polytopic approach for damping numerous operating conditions simultaneously. But it was observed in [16] that a single polytope is not able to guarantee reliable performance over a large number of operating points. A multi-polytope based adaptive damping control using PMU data was proposed in [17] that used classification and regression tree (CART) for making control decisions.

1.1.3 Protection based applications

The protection system of a power system is traditionally designed to respond to faults in a predetermined manner. That is, its behavior is based on *some* assumptions that have been made regarding the power system. Synchrophasor-based adaptive relaying emphasizes the need to change the characteristics of a relay to suit prevailing system conditions. Collectively called adaptive protection, it is defined as follows: “*Adaptive protection is a protection philosophy which*

permits and seeks to make adjustments in various protection functions automatically in order to make them more attuned to prevailing power system conditions” [18].

Adaptive protection encompasses a large number of applications. The use of apparent impedance trajectory obtained from PMUs for transient stability prediction was proposed in [19]. System stress was assessed using synchrophasor-based metrics in [20]. A dynamic state prediction mechanism using PMU data was developed in [21]. A variety of studies have also been done to make the protection system more reliable. Reliability in power system protection encompasses two aspects: dependability and security. Dependability can be defined as *“the measure of the certainty that the relays will operate correctly for all of the faults for which the relays have been designed”*. Security, on the other hand, can be defined as *“the measure of the certainty that the relays will not operate incorrectly for any fault”* [18]. According to NERC outage reports, hidden failures are involved in more than 70% of cascading outages [6] [22]. Hence, the aim of adaptive protection is to reduce the likelihood of hidden failure manifestation and potential cascading events by adjusting the security and dependability balance of protective relays according to existing system conditions. When the power system is in a “safe” state, a bias toward dependability is desired. Under these conditions, not clearing a fault with primary protection has a greater impact on the system than a relay mis-operation due to a lack of security. However, when the power system is in a “stressed” state, unnecessary line trips can greatly exacerbate the severity of the outage, contribute to the geographical propagation of the disturbance, and may even lead to a cascading event and subsequent blackout. Under these states, it is desirable to alter the reliability balance in favor of security.

To be able to achieve the balance between dependability and security, a voting scheme can be implemented. This voting scheme consists of three independent and redundant relays in each phase; hence nine relays in three phases. Optimally positioned PMUs on strategic buses provide the required wide-area measurements. These measurements can be used to infer the state of the power system which can be classified as either “stressed” or “safe.” If the system is found to be stressed, the proper course of action would be to enable the voting scheme and, therefore, bias the protection system toward security. On the other hand, if the system is found to be safe, the voting scheme would be disabled and only one relay will perform the protective function, resulting in a favorable bias toward dependability [23].

PMU data are complex numbers, both the attributes—real and imaginary—should be considered simultaneously for making critical decisions. In order to more accurately classify the system as safe or stressed, [24] provides a method to utilize the complex number nature of PMU data for building the required decision tree. This paper allows the complex plane to be split into two sections, say the “safe” and “stressed” sections by treating the complex numbers as a single entity. Thus, depending on which side of the split the data lies, the state of the system can be determined with great accuracy.

1.2 Need for Calibration

Since the introduction of phasor measurement units (PMUs) in 1988, a variety of applications have been proposed that use synchrophasor measurements for operational decision-making, as discussed above. However, un-calibrated instrument transformers present at the inputs of phasor measurement units (PMUs) can significantly degrade their outputs. This can then cause problems in the downstream applications which use PMU data.

Current and voltage instrument transformers located at the inputs of a PMU step down the levels of current (e.g. from 10 kAmps to 5 Amps) and voltage (e.g. from 500 kV to 5 V) measurements to the levels that the PMU’s electronic circuits can bear. However, the nominal transformer ratios specified on the name plates of these devices may differ from the actual conversion ratios due to age, environmental conditions, and prevailing burdens. Many of the downstream applications previously mentioned, suggest applying results obtained from simulated data to the field. However, due to the differences that exist between nominal transformer ratios and actual conversion ratios, results obtained from simulated data can cause problems when applied directly to the field. A base-lining example has been shown below to illustrate this.

Consider the case shown in fig. 1.3, where there are two buses connected via a transmission line. For this example, it is assumed that according to the simulated data (i.e. angle difference of the respective voltages between the two buses, as seen by PMUs, in a simulation software such as PSS/E or PSLF), the alert limit has been calculated to be 20° while the alarm limit is calculated to be 25° . According to [25], the ratio errors in the voltage angles can be as high as $\pm 4^\circ$. Now, let the real time angle at bus X be 68° while that at bus Y be 50° . Then the real time actual angle

difference is $68 - 50 = 18^\circ$. Now, considering the worst case scenario, let the instrument transformer at bus X have a ratio error (angle) of 4° and bus Y have a ratio error (angle) of -4° . Hence, the real time angle difference observed will be $(68 + 4) - (50 - 4) = 26^\circ$. As a result, if the simulated data is the basis for setting the alert/alarm limits, this case would set off the alarm. But, it is evident that the system is safe.

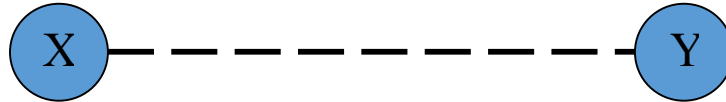


Figure 1.2: High voltage transmission system with two buses X and Y

It is worse for the other way round, i.e., a system is considered safe when it actually is stressed! Thus this example clearly illustrates that calibrating instrument transformers is necessary for the smooth operation of modern power systems.

1.3 Process of Calibration

In the context of this thesis, calibration is the process of estimating unknown ratio-errors present in the instrument transformers used by PMUs. Early research regarding calibration mostly involved off-line methods, some of which included the usage of precise equipment to compare and determine the errors in field equipment. The concept of calibration with respect to PMUs was not limited to instrument transformers but was applied to other areas as well, such as generator model validation, PMU device calibration, etc. The most recent developments in instrument transformer calibration has been discussed (Chapter-2). This thesis also presents two new methodologies which can be applied in the field to calibrate both voltage and current transformers in the presence of PMU errors (Chapters-3 and 4 respectively). All the simulations done in this thesis have been done on two test systems: the IEEE 118 bus and 300 bus systems. The original systems have been shown in figs. (1.4) and (1.5) with the high voltage (345kV) networks highlighted. For ease of understanding and calculation, these figures have been replaced by only their high voltage networks later on in this thesis. These are the networks used to provide the simulated results in the following chapters.

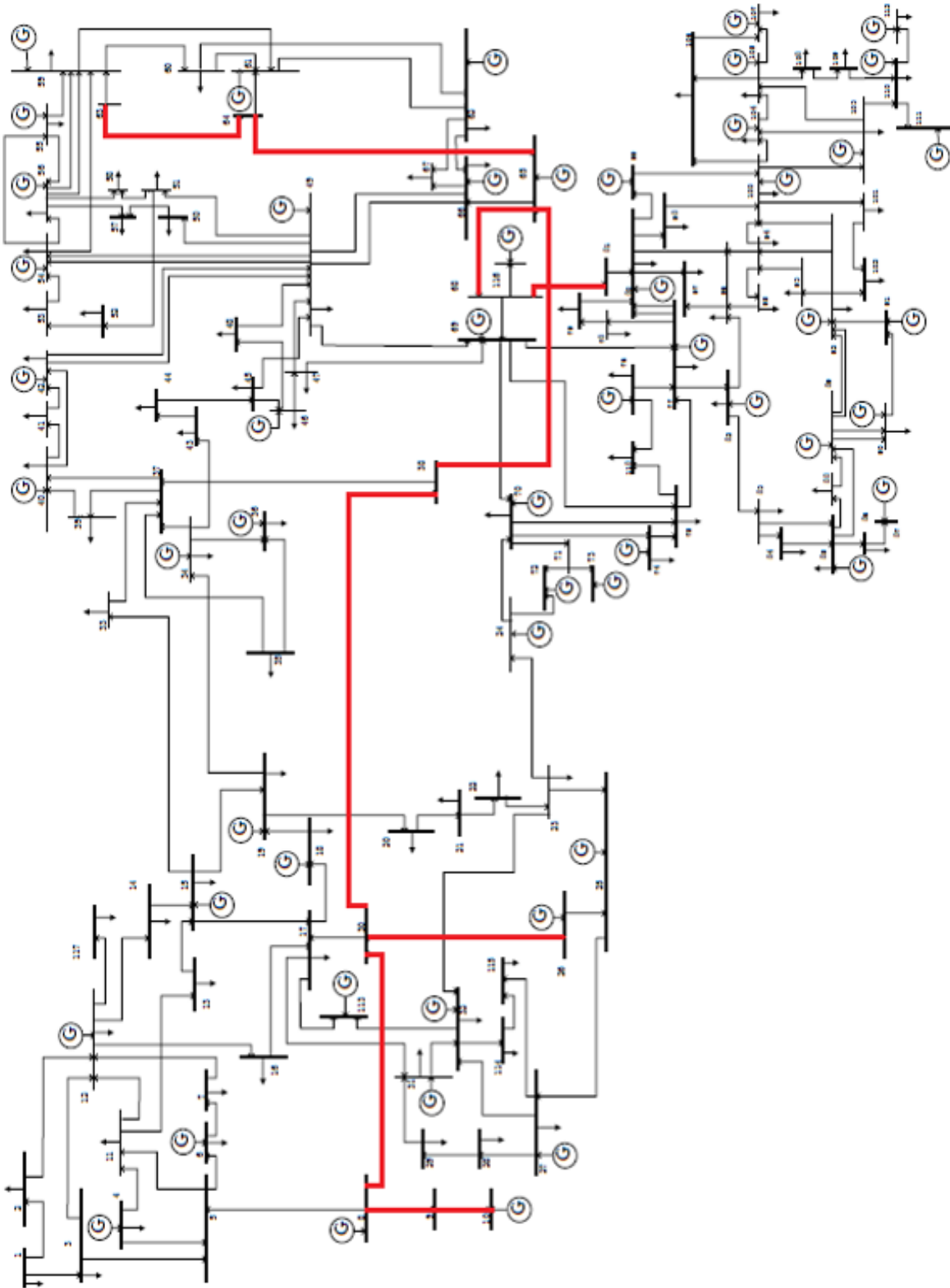


Figure 1.3: The IEEE 118 bus system with the high voltage network highlighted [26]

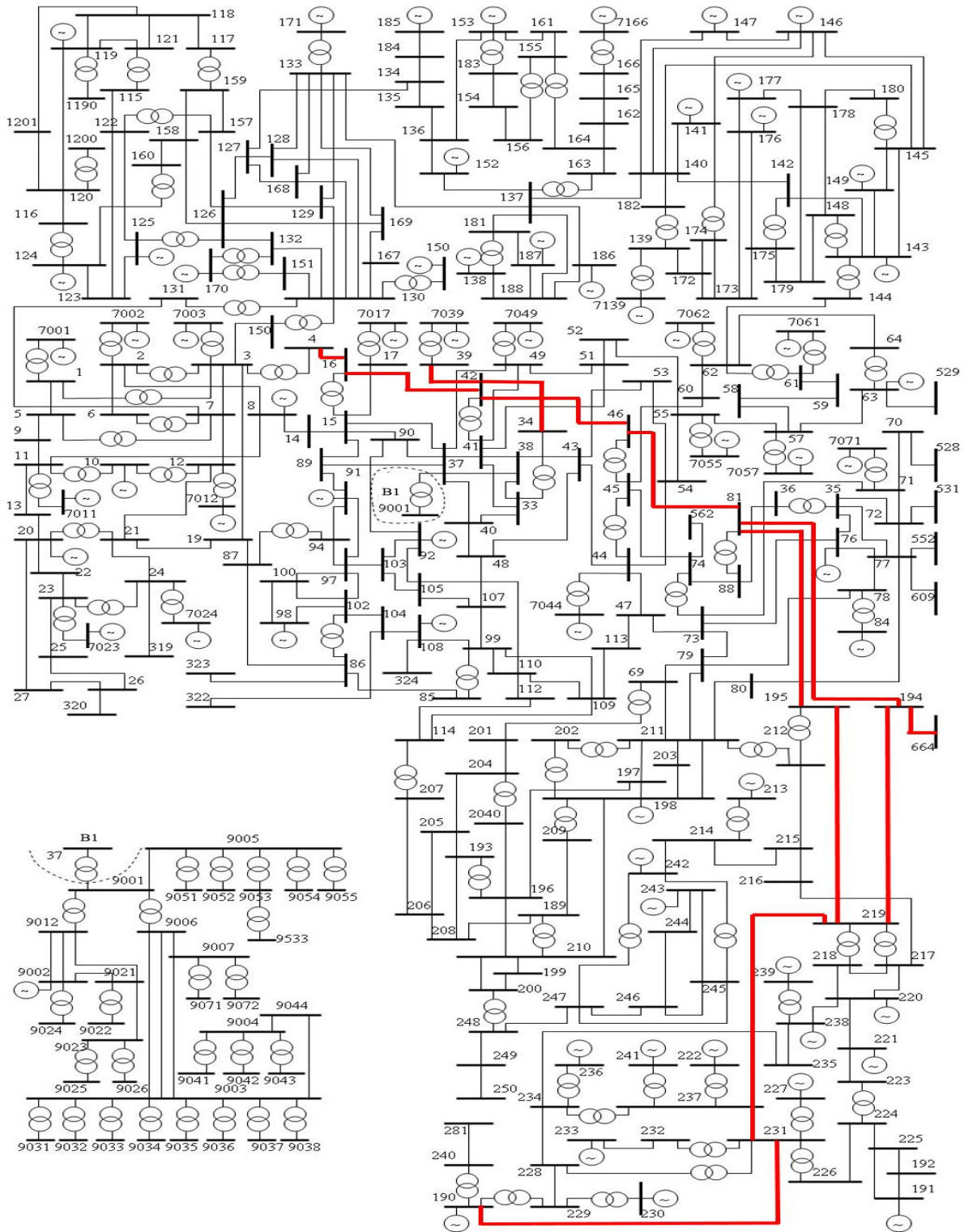


Figure 1.4: The IEEE 300 bus system with the high voltage network highlighted [27]

1.4 Structure of the Thesis

This thesis has been structured as follows. The first chapter introduced the concept of calibration of instrument transformers. The second chapter gives a brief history on calibration, its importance and previous work done in that direction. The third chapter describes the new method of calibration of both voltage and current transformers in the presence of PMU errors. It explains the error model used and includes the results of the simulations for calibrating the instrument transformers starting from one good quality voltage transformer (VT) at a tie-line. The fourth chapter presents a methodology for calibrating both current and voltage transformers, with only one good quality VT present at a tie-line. In this chapter, the data collected from the field is incomplete which results in islanding, thus forming a disconnected tree. The methodology takes into account all of that and still calibrates the instrument transformers of the entire network quite efficiently. This chapter presents the results of various scenarios that can be implemented in the field according to the availability of equipment and/or data. The last chapter provides the conclusions, i.e. it summarizes all the topics discussed in this thesis and also talks about future scope of work in calibration.

CHAPTER 2: HISTORY BEHIND CALIBRATION

For the past two decades, in the field of power systems, there has been a growing interest in calibration. Hence, a lot of research has been done in this area. While some of these methods are for calibrating instrument transformers, mostly in the absence of PMUs, or for calibrating the PMU devices themselves, others have used calibration for modeling and parameter identification of generators [28] [29].

One of the earliest attempts at calibration of instrument transformers was made by using on-site methods, i.e., the instrument transformers had to be taken down from the network to test them. One such example of this would be applying impedance synthesis method to active, hybrid and phantom burdens [30]. Active burdens in that paper referred to the linear devices which were fully programmable by the digital control of analog signal processors. Combining these active burdens with high power inductors and resistors would result in hybrid burdens. A phantom voltage burden or power controller comprised of an active voltage burden and an auxiliary voltage source for reduction of the power dissipation of the controlled current source.

Another example of the on-site calibration process is given in [31]. The idea presented there is to use more accurate devices for performing calibration. This accurate device would be used to compare with the one already in use in the field to determine the “ratio errors” present. Instrument transformers used in high voltage transmission networks are essentially step-down transformers used to step down high-voltages from the transmission lines to low voltages suitable for the PMU devices, as these devices have electronic components which can handle very low voltages (typically 5V). The nominal transformer ratios mentioned on the nameplates of the transformers do not remain constant. They change due to various external factors such as age, weather conditions, etc, thus introducing an error termed as the “ratio error”.

Most of the on-site calibration methods are used for the calibration of current and/or voltage instrument transformers. The drawbacks of these on-site tests are that they are quite expensive and time consuming, and as a result, applying these methods on a system-wide basis is difficult and uneconomical.

Some researchers even tried calibrating in the presence of PMUs. One example would be the approach which uses synchrophasor measurements for generating unit model validation and calibration [32]. But this method is only interested in the generator model calibration by observing the behavior of synchronous machine and governor parameters and does not talk about calibrating the instrument transformers themselves.

Another approach for calibration has been discussed in [33]. In this paper, a method to calibrate the voltage, current and time measurements of the PMU device has been devised and the total vector error uncertainty of that device was calculated to be 0.05%. Yet another method proposed in [34] uses nonlinear optimal estimation theory to calculate calibration factor using a traditional model of an un-transposed transmission line with unbalanced load. This method is intended to work as a pre-filtering scheme that can significantly improve the accuracy of the PMU measurement for further use in their down-stream applications. Such methods could be helpful, but quite expensive at the same time. Also, taking down the PMUs from the network and taking the communication systems off-line for the purpose of calibration would be quite time consuming.

The use of a three-phase reference grade calibrator, developed by the METAS for the European Metrology Research Program (EMRP) to calibrate PMUs has been discussed in [35]. Since a part of the process followed in [35] is offline, it would be cumbersome to use this method on a commercial level.

The method proposed by [36] calibrates the transformers online, without having to take them off the network and can be performed as frequently as required. But the dependence on heavy and light load conditions results in limited practical use, since the load conditions cannot be controlled in real systems. It also does not account for the presence of PMU errors.

Research is also being done for estimation of line parameters of high voltage transmission systems. A method of estimating line parameters has been provided in [37], but this paper does not account for the shunt elements, which are crucial for high voltage transmission lines. In [38], state estimation methods have been used to estimate line parameters of new lines right before their commissioning, using data from PMUs at the ends of these lines. In this paper, the state estimator calculates the optimal bus voltages based on the redundant data available using the quadratic weighted least squares approach. Bad data is filtered out based on measurement accuracies and the chi-square test. Unfortunately, for this method to work, the transmission line in question has to be

taken offline and tested. Also, the test can be performed on one line at a time. Thus making this method time consuming and uneconomical to be performed on a system-wide basis.

Another method has been described in [39], which uses both PMU and SCADA data and provides a non-linear weighted least square algorithm to estimate line parameters of multi-terminal transmission lines. But, PMUs provide data at the rate of 30 times a second, while SCADA data is obtained once in five minutes. It will be difficult to time synchronize the two to obtain the required set of data for a particular line in question. Moreover, using SCADA data entails the introduction of SCADA errors. Also, a non-linear approach gets quite complicated when it has to be applied to large systems.

One of the earliest attempts at calibrating instrument transformers using PMUs was made in [40]. But the model in [40] did not include the PMU errors that were present in the individual measurement sets. Three-phase line parameter estimation using a PMU data driven recursive Kalman filter was proposed in [41]. But [41] assumed that the instrument transformers were free from errors. An improvement to [36] was made in [42] in which the dependence on load conditions was removed. But both [36] and [42] required at least one highly accurate calibrated VT used as the reference for all other transformers. Combined with a highly calibrated current measurement the logic developed in [42] could also estimate line parameters [43], [44].

2.1 Previous Research

Considering the challenges for solving the calibration problem, the approach developed in [44] was significant because with the least number of assumptions, it was able to simultaneously calibrate voltage and current transducers as well as estimate line parameters. A brief overview of that approach is provided here. Although, the algorithm developed in [44] works for both three-phase and positive sequence, for simplicity of notations, the positive sequence version is presented below.

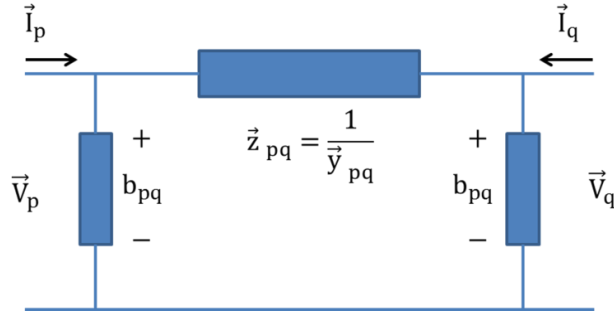


Figure 2.1: Two-bus pi-network model of the power system

Considering the two-bus pi-network model pq shown in fig. 2.1, PMUs placed on both ends of the line provide direct measurements of two complex voltages (\vec{V}_p and \vec{V}_q) and two complex currents (\vec{I}_p and \vec{I}_q). For this method dual use line relay PMUs (DULR PMUs) have been used. Using Kirchoff's laws in fig. 2.1, the following equations can be realized,

$$\begin{aligned}\vec{I}_p &= b_{pq}\vec{V}_p + (\vec{V}_p - \vec{V}_q)\vec{y}_{pq} \\ \vec{I}_q &= b_{pq}\vec{V}_q - (\vec{V}_p - \vec{V}_q)\vec{y}_{pq}\end{aligned}\quad (2.1)$$

On multiplying both equations of eq. (2.1) by \vec{z}_{pq} we get eq. (2.2).

$$\begin{aligned}\vec{z}_{pq}\vec{I}_p &= b_{pq}\vec{z}_{pq}\vec{V}_p + (\vec{V}_p - \vec{V}_q) \\ \vec{z}_{pq}\vec{I}_q &= b_{pq}\vec{z}_{pq}\vec{V}_q - (\vec{V}_p - \vec{V}_q)\end{aligned}\quad (2.2)$$

On multiplying the first equation of eq. (2.2) by \vec{W}_{pq} where $\vec{W}_{pq} = (1 + b_{pq}\vec{z}_{pq})$ and rearranging we get eq. (2.3).

$$\begin{aligned}\vec{W}_{pq}^2\vec{V}_p - \vec{W}_{pq}\vec{V}_q - \vec{W}_{pq}\vec{z}_{pq}\vec{I}_p &= 0 \\ \vec{W}_{pq}\vec{V}_q - \vec{z}_{pq}\vec{I}_q &= \vec{V}_p\end{aligned}\quad (2.3)$$

The voltages and currents in eq. (2.3) are the true voltages and currents of the network. Now, if voltage of the "p" side is known, then in absence of PMU errors, the measured voltages and currents can be written as shown in eq. (2.4).

$$\begin{aligned}\vec{V}_{pm}(j) &= \vec{V}_p(j) & ; & \quad \vec{V}_{qm}(j) = \overline{RE}\vec{V}_q\vec{V}_q(j) \\ \vec{I}_{pm}(j) &= \overline{RE}\vec{I}_p\vec{I}_p(j) & ; & \quad \vec{I}_{qm}(j) = \overline{RE}\vec{I}_q\vec{I}_q(j)\end{aligned}\quad (2.4)$$

In eq. (2.4), \overline{REV}_q , \overline{REI}_p and \overline{REI}_q are the unknown voltage and current ratio errors, and $j = \{1, 2, \dots, N\}$ where N is the total number of measurements made. Now, if $\overline{KV}_q = \frac{1}{\overline{REV}_q}$, $\overline{KI}_p = \frac{1}{\overline{REI}_p}$ and $\overline{KI}_q = \frac{1}{\overline{REI}_q}$ are the ratio correction factors, then using eq. (2.4), for the j^{th} measurement, eq. (2.3) can be rewritten as

$$\begin{aligned} \overline{W}_{pq} \overline{V}_{pm}(j) - \overline{W}_{pq} \overline{KV}_q \overline{V}_{qm}(j) - \overline{W}_{pq} \overline{z}_{pq} \overline{KI}_p \overline{I}_{pm}(j) &= 0 \\ \overline{W}_{pq} \overline{KV}_q \overline{V}_{qm}(j) - \overline{z}_{pq} \overline{KI}_q \overline{I}_{qm}(j) &= \overline{V}_{pm}(j) \end{aligned} \quad (2.5)$$

Now, if N such measurements are made, where $N > 2$, then an over-determined set of equations can be written for the pi-section pq as shown in eq. (2.6).

$$\begin{bmatrix} \overline{V}_{pm}(1) & -\overline{V}_{qm}(1) & -\overline{I}_{pm}(1) & 0 \\ 0 & \overline{V}_{qm}(1) & 0 & -\overline{I}_{qm}(1) \\ \overline{V}_{pm}(2) & -\overline{V}_{qm}(2) & -\overline{I}_{pm}(2) & 0 \\ 0 & \overline{V}_{qm}(2) & 0 & -\overline{I}_{qm}(2) \\ \vdots & \vdots & \vdots & \vdots \\ \overline{V}_{pm}(N) & -\overline{V}_{qm}(N) & -\overline{I}_{pm}(N) & 0 \\ 0 & \overline{V}_{qm}(N) & 0 & -\overline{I}_{qm}(N) \end{bmatrix} \begin{bmatrix} \overline{W}_{pq} \\ \overline{W}_{pq} \overline{KV}_q \\ \overline{z}_{pq} \overline{W}_{pq} \overline{KI}_p \\ \overline{z}_{pq} \overline{KI}_q \end{bmatrix} = \mathbf{b} \quad (2.6)$$

In eq. (2.6), $\mathbf{b} = [0 \ \overline{V}_{pm}(1) \ 0 \ \overline{V}_{pm}(2) \ \dots \ 0 \ \overline{V}_{pm}(N)]^T$ and the numbers within brackets represent different measurement sets. Eq. (2.6) is of the form $\mathbf{Ax} = \mathbf{b}$ in which \mathbf{A} and \mathbf{b} are known and \mathbf{x} is unknown. Hence, eq. (2.6) can be solved in the least-square sense to compute for \mathbf{x} . An example showing how eq. (2.6) can be used for computing for the unknown ratio errors is provided below.

Consider the case where all line parameters are known and all ratio errors except that of the pre-calibrated voltage measurement are unknown. That is, there is only one known voltage measurement ($\overline{V}_{pm} = \overline{V}_p$) present in the system. Then, for the pi-section pq , \overline{z}_{pq} and \overline{W}_{pq} are known and hence \overline{W}_{pq} is known, while \overline{KV}_q , \overline{KI}_p and \overline{KI}_q are unknown. Then, if $\overline{\mathbf{x}} = [\overline{\mathbf{x}}(1) \ \overline{\mathbf{x}}(2) \ \overline{\mathbf{x}}(3) \ \overline{\mathbf{x}}(4)]^T$ is the solution to eq. (2.6), we get eq. (2.7).

$$\overline{KV}_q = \frac{\overline{\mathbf{x}}(2)}{\overline{W}_{pq}} \quad ; \quad \overline{KI}_p = \frac{\overline{\mathbf{x}}(3)}{\overline{z}_{pq} \overline{W}_{pq}} \quad ; \quad \overline{KI}_q = \frac{\overline{\mathbf{x}}(4)}{\overline{z}_{pq}} \quad (2.7)$$

Using $\overline{K\vec{V}}_q$ obtained from eq. (2.7), \vec{V}_q can be calculated using eq. (2.4). Then, for the next pi-section, say qr, a similar procedure can be followed to compute \vec{V}_r . This process can then be repeated for subsequent pi-sections.

It is important to note here that eqs. (2.4) - (2.7) do not contain PMU errors in the measured voltages and currents. In the presence of PMU errors in the measurements, the unknown ratio correction factors of pi-section pq cannot be computed accurately. This implies that \vec{V}_q also cannot be estimated precisely. Now, since \vec{V}_q is used in the computation of subsequent pi-sections, as one keeps moving further away from the pre-calibrated measurement, the errors in the estimates of the ratio errors keep growing. Moreover, since the *true* measurement is difficult to know in practice, eq. (2.6) cannot be used directly in the field. A methodology that is capable of containing the growth in error of the estimates of the ratio errors is presented in the next section.

2.2 *On-line Calibration of VTs Using Synchrophasor Measurements*

This section focuses on the online calibration of only the voltage instrument transformers. Major control and measurement systems, such as the supervisory control and data acquisition (SCADA) system and the PMU based hybrid/ linear state estimation system depend on accurate voltage measurements for their proper functioning. The voltage instrument transformers are typically assumed to have very high accuracy levels [25]. However, as the error values vary with the manufacturer and increase over time and usage, the resulting biased measurements become an inherent component of input data errors for both SCADA and PMU data based applications. Since the accuracy of modern intelligent electronic devices (IEDs) is constantly improving, it becomes important to also calibrate the instrument transformers so as to take full advantage of these devices.

The computation of ratio errors in the presence of PMU errors is not straightforward. The reason for this is that the two errors are multiplicative and when combined with the unknown *true* measurement results in three unknowns being multiplied together. Mathematically, for the voltage of the i^{th} bus, this is described by eq. (2.8)

$$\vec{V}_{\text{meas}_{ij}} = \vec{\alpha}_{ij}\vec{\beta}_i\vec{V}_{\text{true}_{ij}} \quad (2.8)$$

In eq. (2.8), $j = \{1, 2, \dots, N\}$ where N is the total number of measurements made, $\vec{V}_{\text{meas}_{ij}}$ is the j^{th} measured voltage, $\vec{\alpha}_{ij}$ is the unknown PMU error for the j^{th} measurement, $\vec{\beta}_i$ is the ratio error of the voltage of the i^{th} bus, and $\vec{V}_{\text{true}_{ij}}$ is the j^{th} true voltage. The symbol \rightarrow on top of a variable indicates that it is a complex number. If N is sufficiently large, then the PMU errors can be approximated by a Gaussian distribution having zero mean and a small standard deviation (σ). However, since the ratio error (which follows a uniform distribution) and the true voltage values are not known, the number of unknowns still exceeds the number of equations. Under such circumstances, the previous researches either did not consider the PMU errors [40], or made the assumption that there is one measurement whose errors are known and computed the rest on the basis of that measurement [36]-[44]. This section explains the methodology developed in [45] which shows that by placing sufficient number of good quality measurements, the errors in the computation of the ratio errors of all the voltages can be kept below a pre-defined threshold.

The problem associated with *un-calibrated* measurements surfaced during the research performed for a DOE-demonstration project of a three phase, linear PMU-only state estimator developed for Dominion Virginia Power (DVP) [10], [11]. Because of this, the characteristics of the solution match problems/constraints specific to DVP as described below.

- 1) *Focus is on calibrating voltage transformers:* As DVP is interested in improving the accuracy of their linear state estimator, the primary focus of this research is on calibrating voltage instrument transformers.
- 2) *PMUs are placed on all buses that need to be calibrated:* Since phasor measurements are used for calibrating the instrument transformers, it is necessary that a PMU is placed at the locations where calibration is needed. For the DVP system calibration was intended for the high-voltage network and PMUs were placed on all high-voltage buses.
- 3) *A connected tree is present:* If $\{i, j\} \in \mathbf{B}$ where \mathbf{B} is the set of buses whose voltages need to be calibrated, then for all i and j there has to be at-least one path connecting them (called *constraint-approved path*) such that all buses that lie between i and j belong to \mathbf{B} .
- 4) *Some good quality measurement instruments are already present in the system:* Typical examples are revenue quality meters that are placed on the tie-line buses that join two

utilities.

- 5) *Use of dual-use line relay PMUs (DULR PMUs) instead of traditional PMUs:* DVP is placing dual-use line relay PMUs in their high-voltage network. While a traditional PMU installed at a particular bus is assumed to measure currents of all lines connected to that bus and voltage of that bus, a dual use line relay acting as a PMU when placed on a line measures the voltage of the bus that it is protecting and the current in that line. Thus, when choosing locations for good measurements, end-points of the lines were selected rather than the nodes.

2.2.1 Formulation

The objective here is to compute the voltage ratio errors when PMU errors are present and the practical constraints are satisfied. To do so, a modified version of eq. (2.6) was derived as shown below. Since the known voltage measurement at p is replaced by an unknown but relatively good measurement, eq. (2.4) becomes

$$\begin{aligned}\vec{V}_{pm}(j) &= \overline{RE}\vec{V}_p\vec{V}_p(j) \quad ; \quad \vec{V}_{qm}(j) = \overline{RE}\vec{V}_q\vec{V}_q(j) \\ \vec{I}_{pm}(j) &= \overline{RE}\vec{I}_p\vec{I}_p(j) \quad ; \quad \vec{I}_{qm}(j) = \overline{RE}\vec{I}_q\vec{I}_q(j)\end{aligned}\tag{2.9}$$

However, since the p side voltage is a *good* quality measurement in comparison to the other *normal* measurements, $\overline{RE}\vec{V}_p$ is smaller than the other ratio errors. Now, if $\overline{KV}_p = \frac{1}{\overline{RE}\vec{V}_p}$, $\overline{KV}_q = \frac{1}{\overline{RE}\vec{V}_q}$, $\overline{KI}_p = \frac{1}{\overline{RE}\vec{I}_p}$ and $\overline{KI}_q = \frac{1}{\overline{RE}\vec{I}_q}$ are the ratio correction factors, then using eq. (2.9), for the j^{th} measurement eq. (2.2) can be re-written as shown in eq. (2.10).

$$\begin{aligned}\vec{z}_{pq}\overline{KI}_p\vec{I}_{pm}(j) &= \overline{W}_{pq}\overline{KV}_p\vec{V}_{pm}(j) - \overline{KV}_q\vec{V}_{qm}(j) \\ \vec{z}_{pq}\overline{KI}_q\vec{I}_{qm}(j) &= \overline{W}_{pq}\overline{KV}_q\vec{V}_{qm}(j) - \overline{KV}_p\vec{V}_{pm}(j)\end{aligned}\tag{2.10}$$

where, $\overline{W}_{pq} = (1 + b_{pq}\vec{z}_{pq})$. By dividing both equations in eq. (2.10) by \overline{KV}_p and rearranging, we get eq. (2.11).

$$\begin{aligned} \frac{\overline{KV}_q}{\overline{KV}_p} \vec{V}_{qm}(j) + \frac{\overline{KI}_p}{\overline{KV}_p} \vec{z}_{pq} \vec{I}_{pm}(j) &= \vec{W}_{pq} \vec{V}_{pm}(j) \\ \frac{\overline{KV}_q}{\overline{KV}_p} \vec{W}_{pq} \vec{V}_{qm}(j) - \frac{\overline{KI}_q}{\overline{KV}_p} \vec{z}_{pq} \vec{I}_{qm}(j) &= \vec{V}_{pm}(j) \end{aligned} \quad (2.11)$$

Now, if N such measurements are made, where $N > 2$, then an over-determined set of equations can be written for the pi-section pq as shown in eq. (2.12).

$$\begin{aligned} \overbrace{\begin{bmatrix} \vec{V}_{qm}(1) & \vec{z}_{pq} \vec{I}_{pm}(1) & 0 \\ \vec{W}_{pq} \vec{V}_{qm}(1) & 0 & -\vec{z}_{pq} \vec{I}_{qm}(1) \\ \vec{V}_{qm}(2) & \vec{z}_{pq} \vec{I}_{pm}(2) & 0 \\ \vec{W}_{pq} \vec{V}_{qm}(2) & 0 & -\vec{z}_{pq} \vec{I}_{qm}(2) \\ \vdots & \vdots & \vdots \\ \vec{V}_{qm}(N) & \vec{z}_{pq} \vec{I}_{pm}(N) & 0 \\ \vec{W}_{pq} \vec{V}_{qm}(N) & 0 & -\vec{z}_{pq} \vec{I}_{qm}(N) \end{bmatrix}}^{A_1} \underbrace{\begin{bmatrix} x_1 \\ \frac{\overline{KV}_q}{\overline{KV}_p} \\ \frac{\overline{KI}_p}{\overline{KV}_p} \\ \frac{\overline{KI}_q}{\overline{KV}_p} \end{bmatrix}}_{x_1} &= \overbrace{\begin{bmatrix} \vec{W}_{pq} \vec{V}_{pm}(1) \\ \vec{V}_{pm}(1) \\ \vec{W}_{pq} \vec{V}_{pm}(2) \\ \vec{V}_{pm}(2) \\ \vdots \\ \vec{W}_{pq} \vec{V}_{pm}(N) \\ \vec{V}_{pm}(N) \end{bmatrix}}^{b_1} \end{aligned} \quad (2.12)$$

Eq. (2.12) solves for the other ratio errors in pi-section pq with respect to the ratio error in voltage of bus p . This implies that for subsequent pi-sections, the estimates of the ratio errors will also be a function of \overline{KV}_p . In order to accommodate for dual-use line relay PMUs and PMU errors, the following changes are made to eq. (2.12).

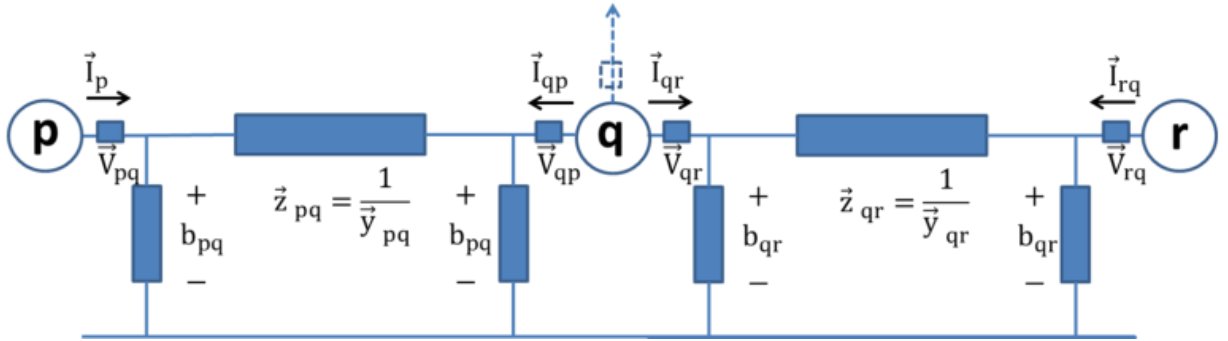


Figure 2.2: Two pi-sections with dual-use line relays acting as PMUs

1) *When dual-use line relays are present:* Let the two neighboring pi-sections be pq and qr as shown in Fig. 2.2. The small rectangles depict the dual-use line relays while the dotted shapes at q indicate the possibility of an injection. For the pi-section pq shown in fig. 2.2, eq. (2.12) will become eq. (2.13).

$$\begin{bmatrix} \vec{V}_{qpm}(1) & \vec{z}_{pq}\vec{I}_{pqm}(1) & 0 \\ \vec{W}_{pq}\vec{V}_{qpm}(1) & 0 & -\vec{z}_{pq}\vec{I}_{qpm}(1) \\ \vec{V}_{qpm}(2) & \vec{z}_{pq}\vec{I}_{pqm}(2) & 0 \\ \vec{W}_{pq}\vec{V}_{qpm}(2) & 0 & -\vec{z}_{pq}\vec{I}_{qpm}(2) \\ \vdots & \vdots & \vdots \\ \vec{V}_{qpm}(N) & \vec{z}_{pq}\vec{I}_{pqm}(N) & 0 \\ \vec{W}_{pq}\vec{V}_{qpm}(N) & 0 & -\vec{z}_{pq}\vec{I}_{qpm}(N) \end{bmatrix} \begin{matrix} \overbrace{\hspace{10em}}^{A_2} \\ \underbrace{\hspace{10em}}^{x_2} \\ \left[\begin{matrix} \overline{KV}_{qp} \\ \overline{KV}_{pq} \\ \overline{KI}_{pq} \\ \overline{KV}_{pq} \\ \overline{KI}_{qp} \\ \overline{KV}_{pq} \end{matrix} \right] \end{matrix} = \mathbf{b}_2 \quad (2.13)$$

In eq. (2.13),

$$\mathbf{b}_2 = \left[\vec{W}_{pq}\vec{V}_{pqm}(1) \quad \vec{V}_{pqm}(1) \quad \vec{W}_{pq}\vec{V}_{pqm}(2)\vec{V}_{pqm}(2) \quad \dots \quad \vec{W}_{pq}\vec{V}_{pqm}(N) \quad \vec{V}_{pqm}(N) \right]^T$$

Now, if \vec{V}_q is the actual voltage of bus q then

$$\begin{aligned} \vec{V}_q &= \overline{KV}_{qp}\vec{V}_{qpm} \\ \vec{V}_q &= \overline{KV}_{qr}\vec{V}_{qrm} \end{aligned} \quad (2.14)$$

Using eq. (2.14), a variable $\vec{\gamma}_q$ can be defined where,

$$\vec{\gamma}_q = \frac{\vec{V}_{qrm}}{\vec{V}_{qpm}} = \frac{\overline{KV}_{qp}}{\overline{KV}_{qr}} \quad (2.15)$$

If N measurements are made, then the complex quantity $\vec{\gamma}_q$ can be calculated experimentally from the measurements of \vec{V}_{qpm} and \vec{V}_{qrm} as shown in eq. (2.16).

$$\vec{\gamma}_q = \frac{1}{N} \sum_{j=1}^N \frac{\vec{V}_{qrm}(j)}{\vec{V}_{qpm}(j)} \quad (2.16)$$

Then, since \overline{KV}_{qp} as a function of \overline{KV}_{pq} can be estimated from eq. (2.13), using $\vec{\gamma}_q$ obtained from eq. (2.16), \overline{KV}_{qr} can be computed using eq. (2.15). The \overline{KV}_{qr} thus obtained (also as a function of \overline{KV}_{pq}) can be used in the next pi-section (qr of Fig. 2.2). This process can then be repeated for subsequent pi-sections.

2) *When PMU errors are present:* In the presence of PMU errors in measurements, there will be further degradation in the quality of the estimates. The over-all deterioration in the quality is quantified by the growth in standard deviation of the difference in the actual ratio error and its estimate (defined *sigma* from henceforth). One contributing factor that was identified for this was the ill-conditioning of the \mathbf{A}_2 matrix of eq. (2.13). The ill-conditioning was reduced by splitting the impedance term in eq. (2.13) between \mathbf{A}_2 and \mathbf{x}_2 . The resulting matrices \mathbf{A}_3 and \mathbf{x}_3 are shown in eq. (2.17). The \sim symbol over the measurements in eq. (2.17) indicate that PMU errors are embedded in them.

$$\begin{array}{c} \mathbf{A}_3 \\ \left[\begin{array}{ccc} \widetilde{\vec{V}}_{qpm}(1) & \sqrt{2} \widetilde{\vec{z}}_{pq} \widetilde{\vec{I}}_{pqm}(1) & 0 \\ \widetilde{\vec{W}}_{pq} \widetilde{\vec{V}}_{qpm}(1) & 0 & -\sqrt{2} \widetilde{\vec{z}}_{pq} \widetilde{\vec{I}}_{pqm}(1) \\ \widetilde{\vec{V}}_{qpm}(2) & \sqrt{2} \widetilde{\vec{z}}_{pq} \widetilde{\vec{I}}_{pqm}(2) & 0 \\ \widetilde{\vec{W}}_{pq} \widetilde{\vec{V}}_{qpm}(2) & 0 & -\sqrt{2} \widetilde{\vec{z}}_{pq} \widetilde{\vec{I}}_{pqm}(2) \\ \vdots & \vdots & \vdots \\ \widetilde{\vec{V}}_{qpm}(N) & \sqrt{2} \widetilde{\vec{z}}_{pq} \widetilde{\vec{I}}_{pqm}(N) & 0 \\ \widetilde{\vec{W}}_{pq} \widetilde{\vec{V}}_{qpm}(N) & 0 & -\sqrt{2} \widetilde{\vec{z}}_{pq} \widetilde{\vec{I}}_{pqm}(N) \end{array} \right] \begin{array}{c} \mathbf{x}_3 \\ \left[\begin{array}{c} \overline{\vec{K}}\overline{\vec{V}}_{qp} \\ \overline{\vec{K}}\overline{\vec{V}}_{pq} \\ \sqrt{2} \overline{\vec{z}}_{pq} \overline{\vec{K}}\overline{\vec{I}}_{pq} \\ \overline{\vec{K}}\overline{\vec{V}}_{pq} \\ \sqrt{2} \overline{\vec{z}}_{pq} \overline{\vec{K}}\overline{\vec{I}}_{qp} \\ \overline{\vec{K}}\overline{\vec{V}}_{pq} \end{array} \right] = \mathbf{b}_3 \end{array} \quad (2.17) \end{array}$$

In eq. (2.17),

$$\mathbf{b}_3 = \left[\widetilde{\vec{W}}_{pq} \widetilde{\vec{V}}_{pqm}(1) \quad \widetilde{\vec{V}}_{pqm}(1) \quad \widetilde{\vec{W}}_{pq} \widetilde{\vec{V}}_{pqm}(2) \quad \widetilde{\vec{V}}_{pqm}(2) \quad \dots \quad \widetilde{\vec{W}}_{pq} \widetilde{\vec{V}}_{pqm}(N) \quad \widetilde{\vec{V}}_{pqm}(N) \right]^T$$

As an example of the improvement in conditioning, typical condition numbers of the \mathbf{A}_2 matrices of eq. (2.13) for different pi-sections were of the order of few thousands. By splitting the impedance term, as was done in eq. (2.17), the condition numbers of the \mathbf{A}_3 matrices for the same pi-sections were found to be below fifty. However, even after improving the conditioning of \mathbf{A}_3 , due to their being only one reliable measurement, the results did not improve significantly. This was especially found to be true for estimating the ratio errors that were more than 3-4 pi-sections away from that reliable measurement. Therefore, it was realized that more reliable measurements must be added to the system.

Before identifying the optimal locations where good measurements can be added, the following Lemma is defined.

Lemma 1: *The advantage of adding multiple good measurements to a system is that as long as the measurements are independent, their combination will give a better estimate.*

Proof of Lemma 1: Let n measurements be made of an unknown quantity x . For the given problem, x is a scalar that denotes the standard deviation. Then for the k^{th} measurement, we have

$$z_k = x + e_k \quad (2.18)$$

where $e \sim N(0, \sigma^2)$. The residual is given by (19).

$$[\mathbf{r}]_{n \times 1} = \hat{x}[\mathbf{1}]_{n \times 1} - [\mathbf{z}]_{n \times 1} \quad (2.19)$$

In eq. (2.19), \hat{x} is the optimal estimate of x and $[\mathbf{1}]_{n \times 1}$ is a $n \times 1$ vector of ones. In order to find \hat{x} , weighted least squares approach is used which minimizes $[\mathbf{r}]^T[\mathbf{Q}]^{-1}[\mathbf{r}]$ where $[\mathbf{Q}]$ is the error covariance matrix. On solving, the desired value of \hat{x} comes out to be

$$\hat{x} = \frac{[\mathbf{1}]_{n \times 1}^T [\mathbf{Q}]^{-1} [\mathbf{z}]_{n \times 1}}{[\mathbf{1}]_{n \times 1}^T [\mathbf{Q}]^{-1} [\mathbf{1}]_{n \times 1}} \quad (2.20)$$

Then, the covariance of \hat{x} is given by

$$\text{cov}(\hat{x}) = E \left[\frac{[\mathbf{1}]_{n \times 1}^T [\mathbf{Q}]^{-1} [\mathbf{z}]_{n \times 1} [\mathbf{z}]_{n \times 1}^T [\mathbf{Q}]^{-1} [\mathbf{1}]_{n \times 1}}{([\mathbf{1}]_{n \times 1}^T [\mathbf{Q}]^{-1} [\mathbf{1}]_{n \times 1})^2} \right] \quad (2.21)$$

Simplifying the RHS of eq. (2.21) gives

$$\text{cov}(\hat{x}) = \frac{1}{([\mathbf{1}]_{n \times 1}^T [\mathbf{Q}]^{-1} [\mathbf{1}]_{n \times 1})} \quad (2.22)$$

Now, if measurements are independent, $[\mathbf{Q}] = \text{diag}(\sigma_k^2)$ and so $[\mathbf{1}]_{n \times 1}^T [\mathbf{Q}]^{-1} [\mathbf{1}]_{n \times 1} = \sum_{k=1}^n \frac{1}{(\sigma_k)^2}$ which gives

$$\text{cov}(\hat{x})_{\text{independent}} = \frac{1}{\frac{1}{(\sigma_1)^2} + \frac{1}{(\sigma_2)^2} + \dots + \frac{1}{(\sigma_n)^2}} \quad (2.23)$$

Therefore, as long as the measurements are independent, the net variance will be lower than

the variance of the individual measurements; thereby resulting in an improvement of the over-all estimate. For example, let measurements be made independently of end-point v from good measurements located at end-points u and w . Now, if the sigma of the difference between the actual ratio error and its estimate at v for u and w be σ_{vu} and σ_{vw} , respectively, then the combined sigma at end-point v denoted by σ_v is

$$\sigma_v = \sqrt{\frac{1}{\frac{1}{(\sigma_{vu})^2} + \frac{1}{(\sigma_{vw})^2}}} \quad (2.24)$$

From eq. (2.24), it is easy to see that $\sigma_v < \sigma_{vu}$ and $\sigma_v < \sigma_{vw}$.

However, if the n measurements are not independent then the resulting covariance of \hat{x} is a function of the correlation between the measurements. In the context of the given problem, dependence occurs only when there is more than one constraint-approved path to reach one end-point from another end-point. However, since the degree of correlation between parallel paths is difficult to compute in practice, a definite upper-bound on the value of the net variance is obtained based on the premise that being able to observe a particular entity by a different path can only increase the over-all accuracy (and not decrease it). Therefore, the net-variance is set equal to the minimum variance obtained along any one of the parallel paths as shown in eq. (2.25).

$$\text{cov}(\hat{x})_{\text{dependent}} = \min(\sigma_k^2) \text{ for } k = \{1, 2, \dots, n\} \quad (2.25)$$

For example, let measurements be made of end-point v from the good measurement located at end-point u via paths 1 and 2. Now, if the sigma of the difference between the actual ratio error and its estimate at v for u via paths 1 and 2 are σ_{vu1} and σ_{vu2} , respectively, where $\sigma_{vu2} > \sigma_{vu1}$ then the combined sigma at end-point v due to the good measurement at u denoted by σ_{vu} is

$$\sigma_{vu} = \sigma_{vu1} \quad (2.26)$$

On the basis of Lemma 1, the calibration problem reduces to choosing optimal locations for adding good measurements to the network. This can be done through a binary integer programming (BIP) formulation as shown below.

Let the connected undirected graph of buses whose voltages need to be calibrated be described by $\mathcal{G}(\mathbf{V}, \mathbf{E})$ where \mathbf{V} is the set of vertices, and \mathbf{E} is the set of edges. Let $[\mathbf{S}]$ be a $2|\mathbf{E}| \times 2|\mathbf{E}|$ matrix

whose columns correspond to the locations where the good measurements can be placed and whose rows denote the standard deviation obtained for all the other locations with respect to a good measurement at the column to which the row belongs to. Let $[\mathbf{X}_{init}]$ be a $2|\mathbf{E}| \times 1$ binary integer matrix such that the indices of the non-zero entries of $[\mathbf{X}_{init}]$ denote locations of initial good measurements. Also, let the variable T denote the value below which all the standard deviation must lie. Then, the objective of the optimization problem is the minimization of the L1 – norm of a $2|\mathbf{E}| \times 1$ binary integer matrix $[\mathbf{X}]$ such that the indices of the non-zero entries of $[\mathbf{X}]$ denote locations of good measurements. The constraints further imposed on this objective are given by eqs. (2.27) - (2.28).

$$[\mathbf{A}]_{2|\mathbf{E}| \times 2|\mathbf{E}|} [\mathbf{X}]_{2|\mathbf{E}| \times 1} \geq [\mathbf{B}]_{2|\mathbf{E}| \times 1} \quad (2.27a)$$

where

$$\mathbf{A}(i, j) = \frac{1}{(\mathbf{S}(i, j))^2} \quad (2.27b)$$

$$[\mathbf{B}]_{2|\mathbf{E}| \times 1} = \frac{1}{T^2} [\mathbf{1}]_{2|\mathbf{E}| \times 1}$$

$$[\mathbf{X}_{init}]^T_{2|\mathbf{E}| \times 1} [\mathbf{X}]_{2|\mathbf{E}| \times 1} = \text{nnz}([\mathbf{X}_{init}]_{2|\mathbf{E}| \times 1}) \quad (2.28)$$

Eq. (2.27) ensures that the combined standard deviation are below the desired threshold while eq. (2.28) guarantees that the locations of the initial good measurements are retained and accounted for in the final solution.

The flowchart based on this BIP formulation for finding the optimal locations is shown in fig. 2.3 and described below in more details.

Step 1: Find good measurements initially present in the system. If there are no good measurements initially present, then **GO TO Step 5**.

Step 2: Taking one good measurement at a time, find standard deviation for end-points that are P pi-sections away from the end-point where the good measurement is placed.

Step 3: For the initial good measurements, find combined standard deviation for all end-points using eq. (2.22). Call initial set of good measurement end-points as the *Starting Set*.

Step 4: Define T_0 as the pre-defined threshold for the standard deviation, where T_0 is a constant

scalar quantity independent of the test systems. If the maximum of the combined standard deviation for all end-points computed based on the Starting Set is less than T_0 , then no more good measurements need to be added to the system; **GO TO Step 12**.

Step 5: For all the end-points that do not have good measurements initially, taking one end-point at a time, find standard deviation for end-points that are P pi-sections away from that end-point by assuming that a good measurement will be placed only on that end-point.

Step 6: In presence of dependent measurements, find net standard deviation using eq. (2.25).

Step 7: Set $T = T_0$.

Step 8: Perform the optimization using eqs. (2.27) - (2.28). This gives the minimum *number* of good measurements that must be present in the system to keep the standard deviation for all the end-points below T_0 .

Step 9: Reduce T by a small amount (say 1%).

Step 10: Re-do the optimization using eqs. (2.27) - (2.28). If the number of good measurements required is equal to the number obtained in **Step 8**, then **GO TO Step 9**.

Step 11: The location set corresponding to the *smallest* value of T (called T_{\min}) for which the number of good measurements is equal to the number of good measurements obtained in **Step 8** is the *best location set*.

Step 12: Stop.

Steps 1-4 of the flowchart cater to the initial good measurements present in the system. The optimal number of good measurements is computed in **Steps 5-8**. **Steps 9-11** increase the robustness of the solution. The results obtained by applying this methodology to different test systems are described next.

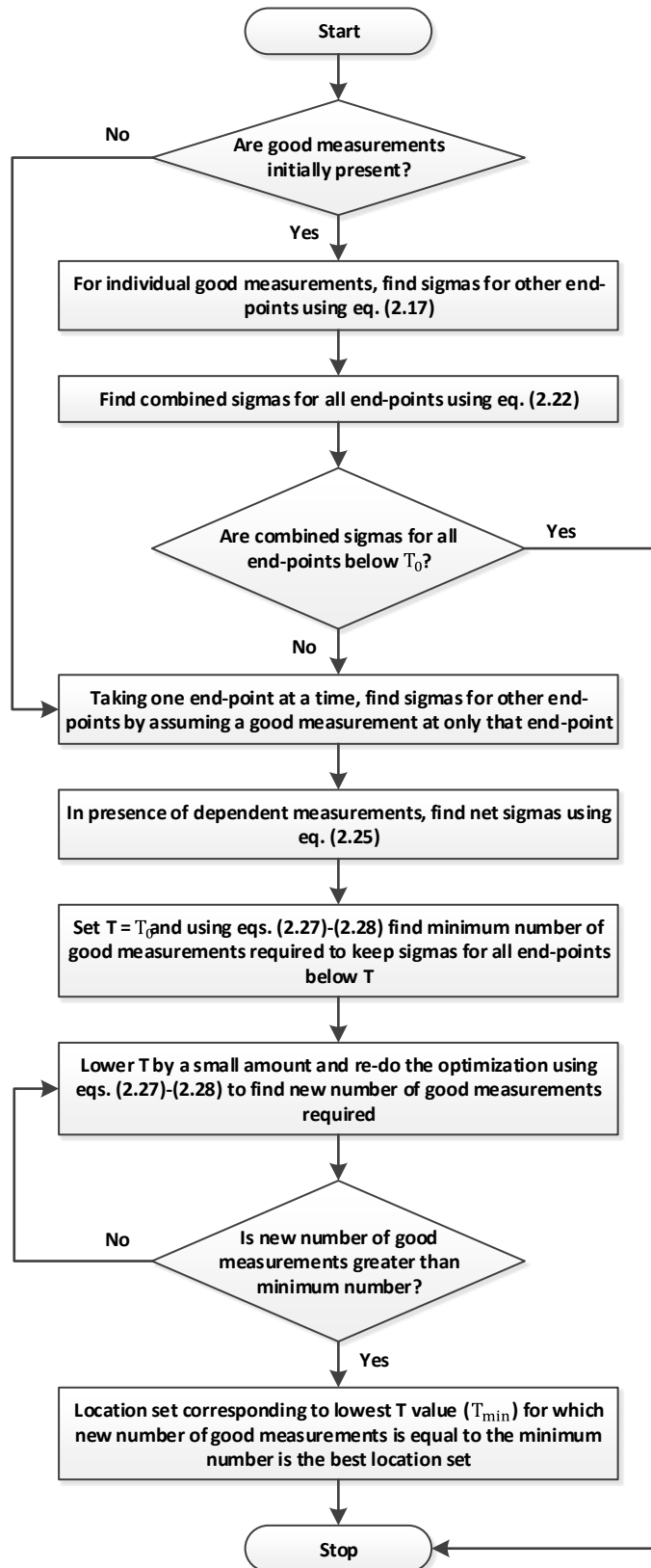


Figure 2.3: Flowchart for finding optimal locations of good quality measurements

2.2.2 Simulations and Results

The IEEE-118 bus system and the IEEE-300 bus system were selected for the analysis done here. The characteristics of the test systems which make them relevant for this study are that both the systems have a distinct high voltage (HV) network which forms the backbone of the respective systems; also the IEEE-300 bus system has closed loops in it, which makes dependent measurements possible. For illustration purposes, the HV network of the IEEE-118 and 300 bus systems are shown in figs. 2.4 and 2.5.

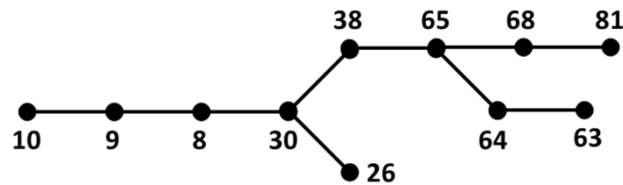


Figure 2.4: High-voltage network of IEEE-118 bus system

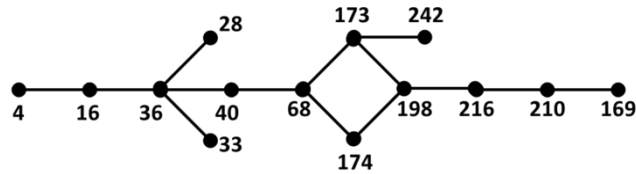


Figure 2.5: High-voltage network of IEEE-300 bus system

For each system, the simulation was run 1000 times to generate the standard deviation. During each run, for every measurement a different ratio error was picked at random from the range given in [25]. Moreover, for every run, 12 different operating conditions were created, that is $N = 12$. The perfect measurements were assumed to have no ratio errors or PMU errors in them. The smaller ratio errors of the good quality measurements were chosen from a uniform distribution having zero mean and standard deviation of 0.15% for magnitudes and 0.1° for angles [25]. All PMU errors were chosen from a Gaussian distribution having zero mean and standard deviation of 0.2% for magnitudes and 0.104° for angles. It was assumed in the simulations that the standard deviation were to be kept below 1%. Accordingly, T_0 was set at 0.01. The test system data can be found in the MATPOWER [47] toolbox of MATLAB [48], while the integer optimization was performed using GUROBI [49]. The results obtained are as follows.

Fig. 2.6 depicts the growth in standard deviation if one *reliable* measurement (either good quality or perfect quality) is placed at different locations in the IEEE-118 and 300-bus systems. In order to create fig. 2.6, all possible locations where a reliable measurement could be placed were initially identified. For instance, the IEEE-118 bus system had 20 such locations (either end of the ten HV lines shown in fig. 2.4). Then taking one location at a time, the standard deviation were computed for all the other locations by assuming that the reliable measurement was placed only at that location. So, for the IEEE-118 bus system, the whole set-up (1000 runs with randomly chosen ratio errors for 12 sets of measurements) was repeated 20 times with the reliable measurement at one of those 20 locations at each time.

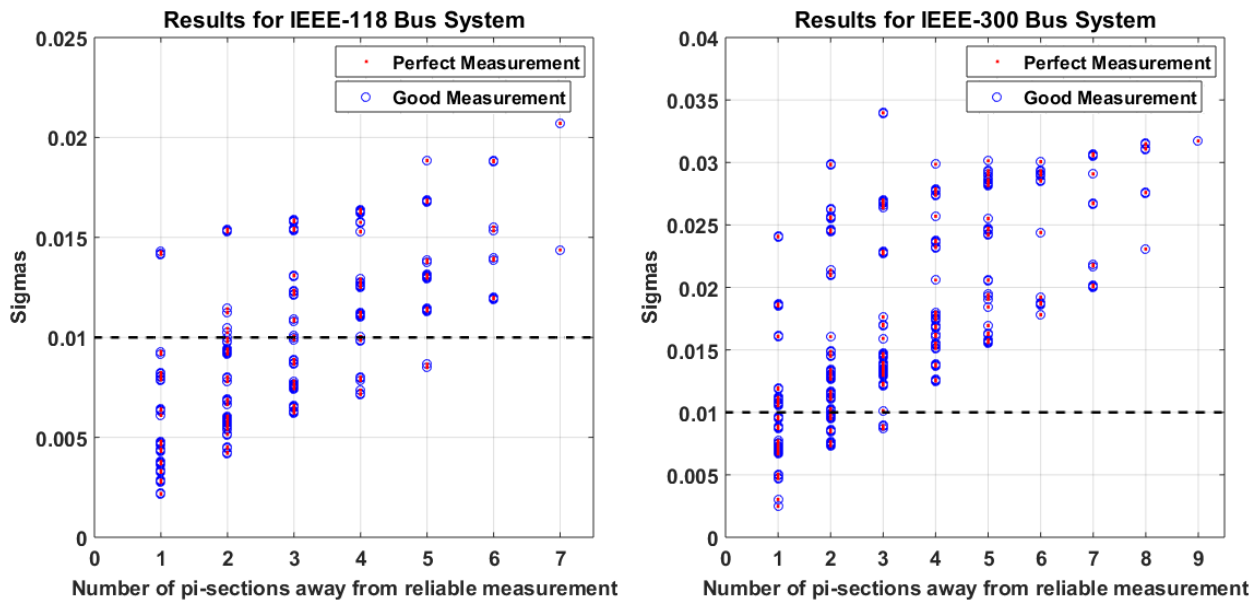


Figure 2.6: Growth of standard deviation (σ) when only one reliable measurement is present in the systems; the dashed line shows the pre-defined threshold (T_0) of 0.01

From fig. 2.6, it is realized that good quality and perfect quality measurements have similar performances (almost all dots lay inside circles). Another observation that is made from fig. 2.6 is that one reliable measurement is not able to keep most of the standard deviation below 0.01 beyond 3-4 pi-sections. This observation is important because it meant that it was not necessary to compute standard deviation for end-points that were far away as their combination would not have significant influence on the net variance. This theory was further tested for the IEEE-300 bus system and the results obtained are shown in Table 2.1.

TABLE 2.1: OPTIMAL LOCATIONS OF GOOD MEASUREMENTS FOR DIFFERENT PI-SECTION LENGTHS OF IEEE-300 BUS SYSTEM

All pi-section	4 pi-section	5 pi-section	6 pi-section	7 pi-section	8 pi-section
4-16	4-16	4-16	4-16	4-16	4-16
36-16	16-4	16-4	28-36	36-40	36-16
28-36	36-28	36-33	40-68	28-36	28-36
68-173	28-36	28-36	242-173	242-173	68-173
242-173	242-173	242-173	198-173	216-198	242-173
	210-169	210-216			
0.0094	0.0087	0.0085	0.0098	0.0095	0.0094

Table 2.1 compares the optimal locations obtained when standard deviation for *all pi-section* lengths are considered, and when standard deviation up to 4 to 8 *pi-section* lengths are considered. An entry $i - j$ in Table 2.1 means that the good measurement is placed on the i end of line $i - j$. The location of the initial good measurements are shown in red. They were so chosen because the i^{th} node of those lines was connected to only one other node of the network (the j^{th} node). Therefore, in all practicality, they could be assumed to be the tie-lines that join the test system with its neighbors, with the i^{th} nodes becoming the tie-line buses. The numbers in the disconnected row of Table 2.1 indicate the value of T_{\min} obtained for the location set given in the corresponding column. From the table it is realized that the numbers and locations are identical for *all pi-section* and 8 *pi-section* lengths. This meant that standard deviation computed up to a length of 8 *pi-sections* was sufficient for finding optimal locations where new good measurements can be added. This result is particularly important for large systems where it is computationally complex to consider all possible *pi-section* lengths.

In the final set of simulations, the optimal locations for adding good quality measurements for both test systems were computed using the proposed approach. Table 2.2 shows the results obtained with the disconnected row listing the T_{\min} values for both the systems.

TABLE 2.2: OPTIMAL LOCATIONS OF GOOD MEASUREMENTS FOR TEST SYSTEMS

118-Bus System	300-Bus System
10-9	4-16
30-26	36-16
63-64	28-36
	68-173
	242-173
0.0073	0.0094

The results of Table 2.2 are also validated by fig. 2.7. In fig. 2.7, the dots correspond to the standard deviation while the dashed line depicts T_0 . From the figure it becomes clear that by using the proposed approach the growth in standard deviation has been contained for both the systems.

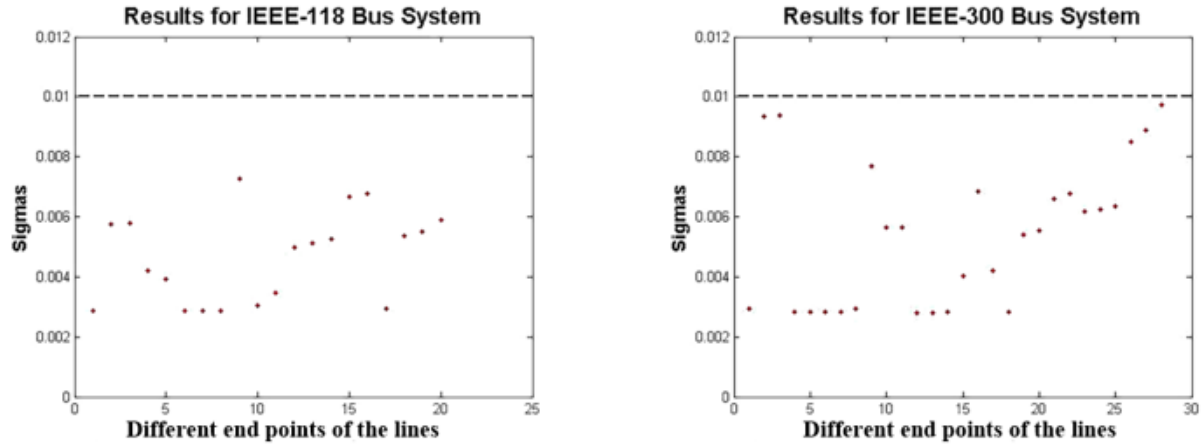


Figure 2.7: All the standard deviations (σ) for both test systems are below the pre-defined threshold (T_0) where $T_0 = 0.01$

This chapter presents a methodology for calibrating voltage transducers without having to take them off-line, in the presence of PMU errors and a good quality VT at a tie-line. The complications thus introduced were resolved by placing multiple good quality measurements at optimal locations inside the network so that all calibration errors stay below a desired threshold. The results indicate that the methodology described here provides a simple and effective solution to the online VT calibration problem.

The next chapter talks about a new methodology for online calibration of both VTs and CTs in the presence of PMU errors and starting from good quality VTs at the tie-lines.

CHAPTER 3: A NEW APPROACH TO INSTRUMENT TRANSFORMER CALIBRATION

In the field of power engineering, calibration has a variety of applications [28]-[45]. Improving instrument transformer's performance is one such application. This chapter describes one such method to calibrate both VTs and CTs.

In order to get a feel of what the data in real systems look like, field data obtained from a utility for a 500 kV network were plotted in the complex plane as shown in figs. 3.1 and 3.2. These are the plots of the data obtained from a utility plotted in the complex plane.

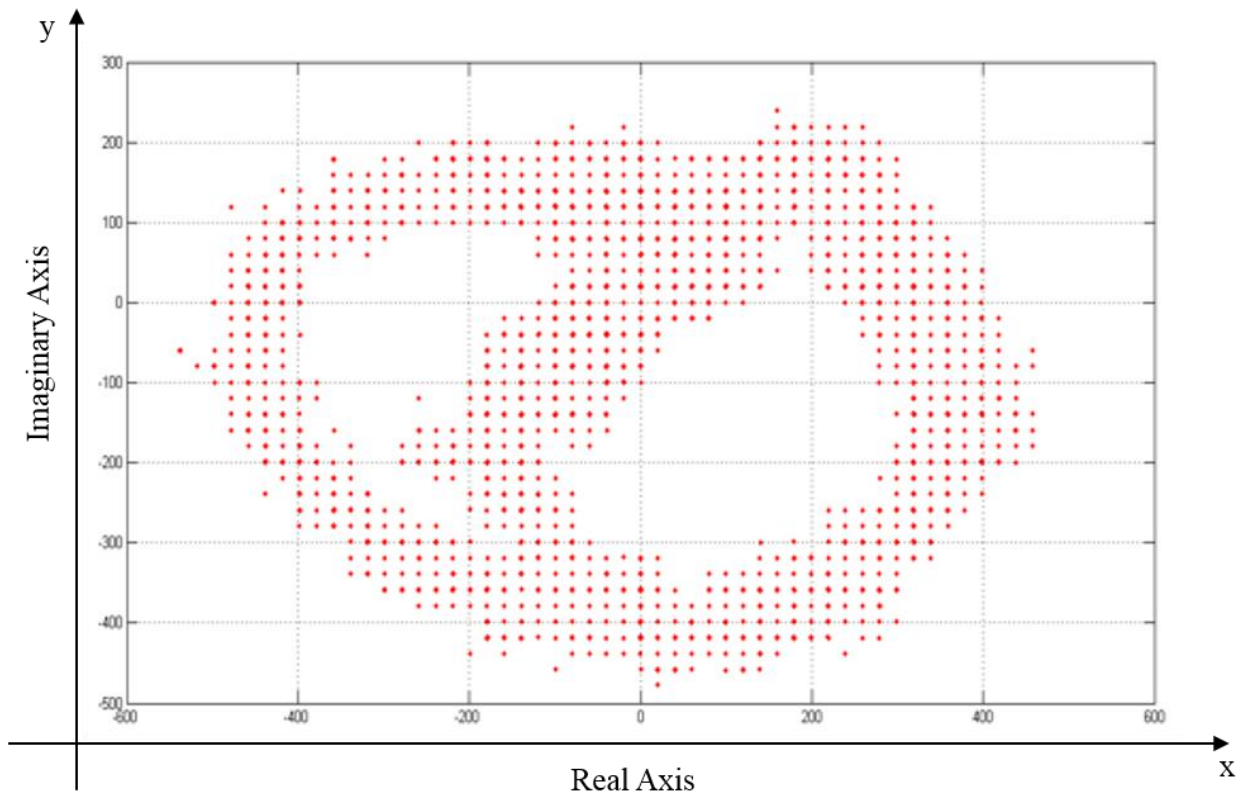


Figure 3.1(a): Field data-Voltages

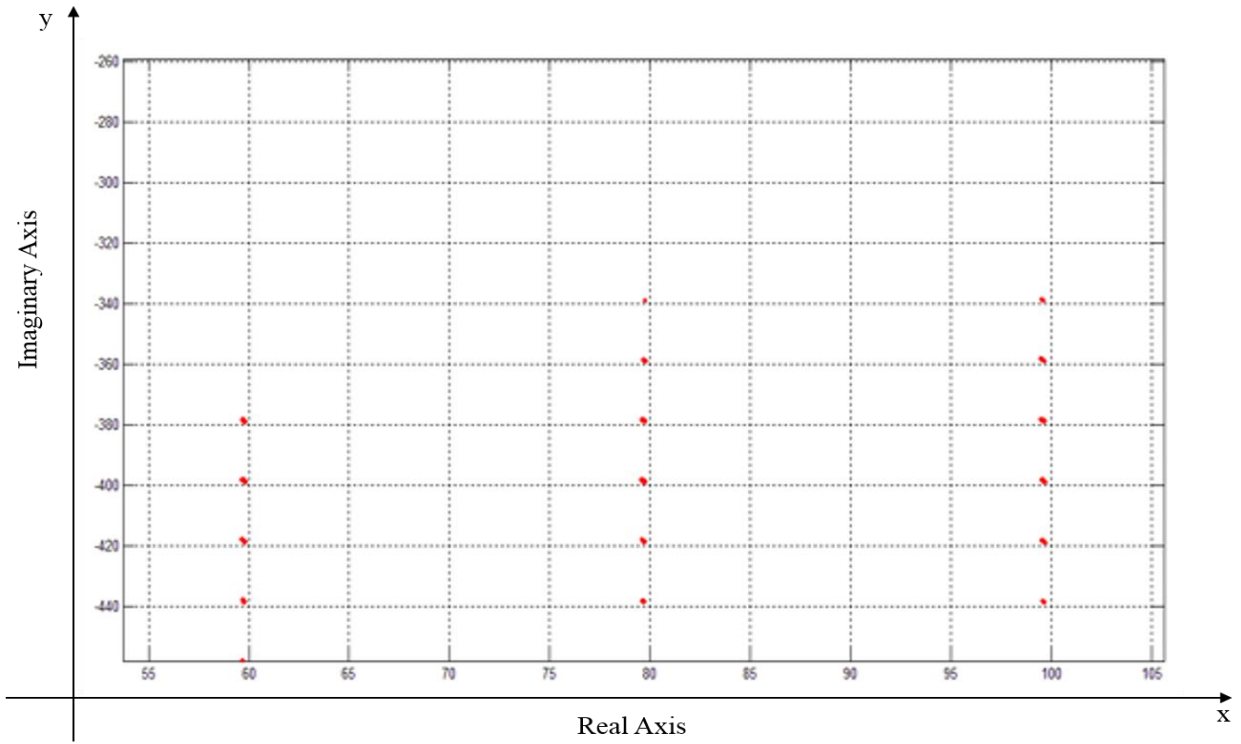


Figure 3.1(b): Field data-Voltages (magnified view)

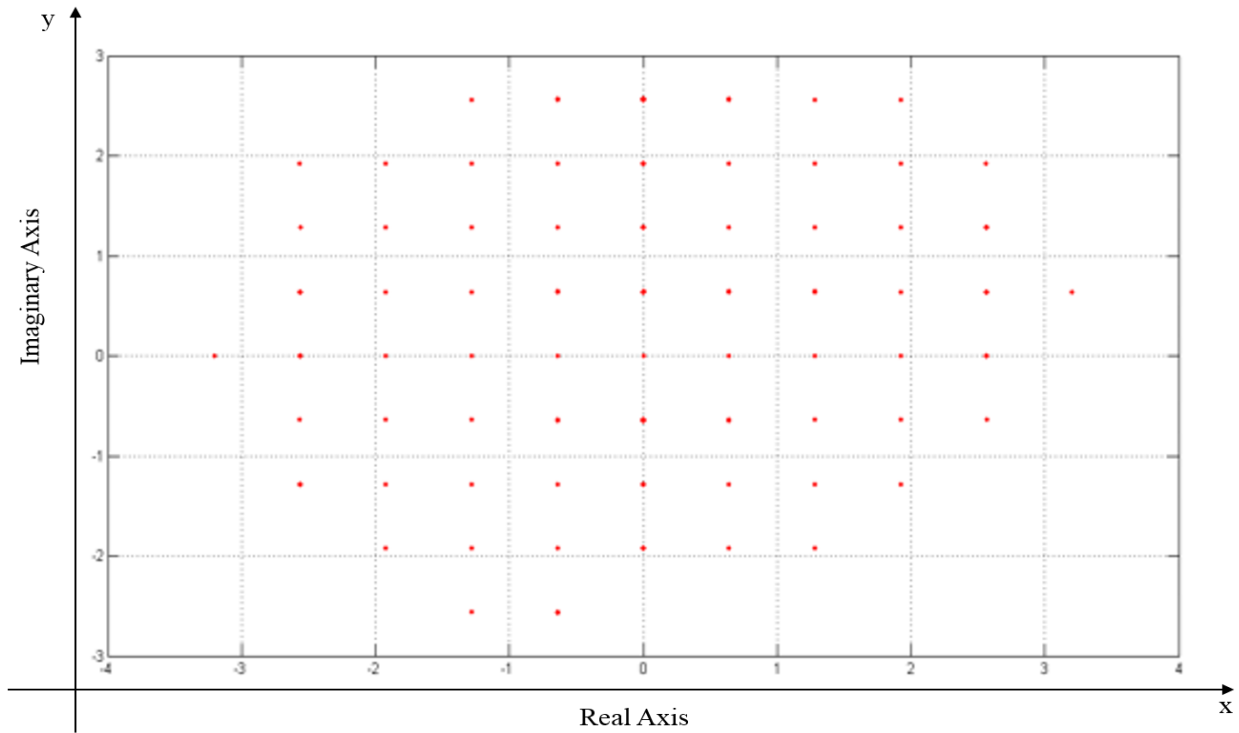


Figure 3.2(a): Field data-Currents

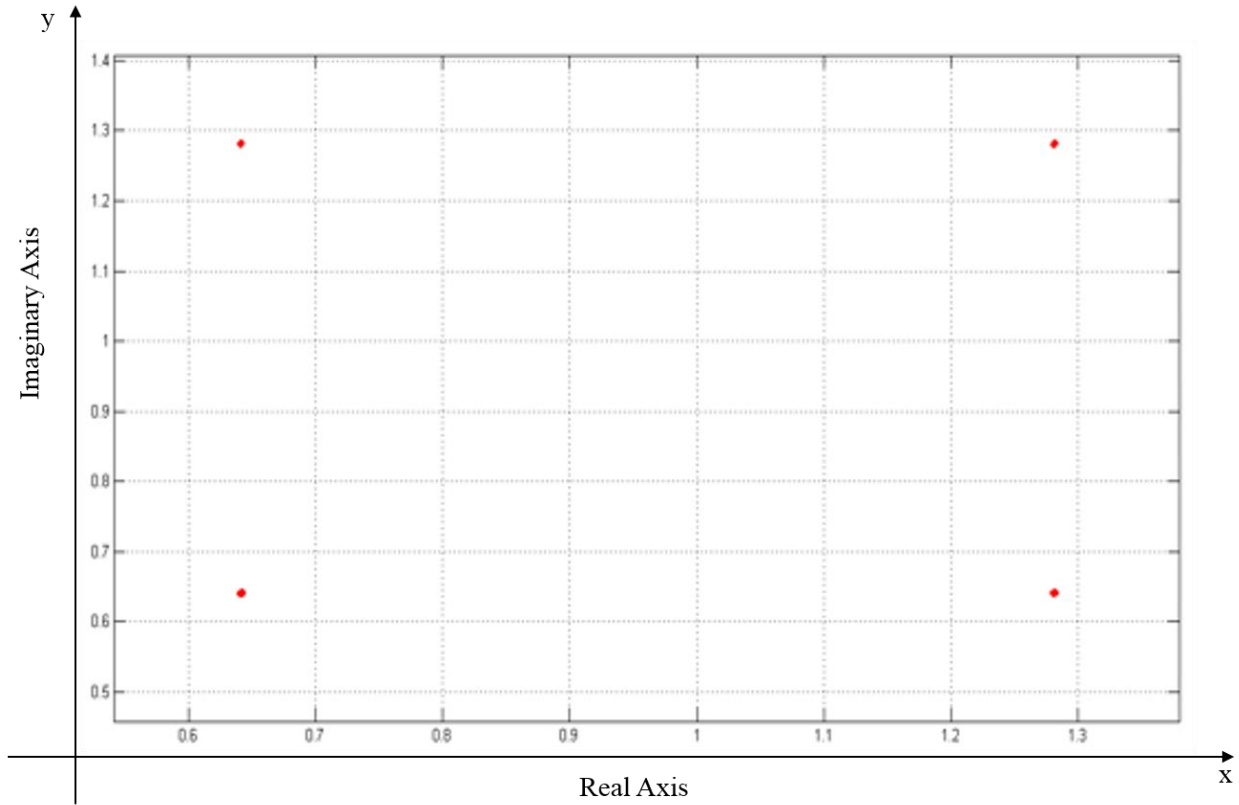


Figure 3.2(b): Field data-Currents (magnified view)

Analyzing these plots, an error of a constant value is observed between consecutive measurements. This error is introduced due to the standards applied on the analog to digital convertors present in the PMUs [46]. The data plotted here shows the presence of a quantized difference of 20 V in the voltage plots and 0.64 A in the currents. The presence of these errors have been explained in the next section.

3.1 Error Model

It has been observed from real world data that there exists some error in both the voltages and currents measured by PMUs. These errors can, in turn, be divided into two components, ratio errors arising from the instrument transformers and PMU errors introduced by the PMUs. The instrument transformers are essentially step-down transformers used to step down high-voltages/currents from the transmission lines to low voltages/currents suitable for the PMU devices, as these devices have electronic components which can only handle very low voltages/currents. The nominal transformer

ratios mentioned on the nameplates of the transformers do not remain constant over a period of time. They change due to various external factors such as age, weather conditions, etc, thus introducing an error termed as the ratio error.

The PMUs, on the other hand, have errors which have been observed to be quantization errors. In most commercially available PMUs, the output is of 16-bits. 1 bit out of the 16-bits is used to store the signs of the phasors. For the case of voltage transformers, 1 extra bit is also saved for determining if there an overvoltage, thus leaving 14 bits for the rest of its operation. Thus, the quantization error present in voltage measurements at the 500 kV level is calculated to be $\Delta V = 500 \text{ kV} / (\sqrt{3} \times 2^{14}) \sim 20 \text{ V}$. In the case of current transformers that extra bit is not required. For ease of understanding, a fault current of 20 kA has been assumed here. The quantization error present in current measurements is calculated to be $\Delta I = 20 \text{ kA} / 2^{15} \sim 0.64 \text{ A}$. These values of quantization error are supported by the field data obtained from a certain utility. Hence, these are the values which have been used for all the simulations done in this thesis.

3.2 PMU data based Voltage & Current Transformer Calibration

Majority of PMUs used in industries now a days are DULR PMUs. These instruments serve dual purposes and the following explanation is given on the basis of these devices. It is assumed here that DULR PMUs are placed on all transmission lines present in the high voltage network.

For ease of explanation, a single pi-section (fig.3.4) has been used for illustration purposes. The voltage transformer on end p is a revenue quality instrument transformer (for the simulations done for this thesis, *error in magnitude* = $\pm 0.15\%$ and *error in angle* = $\pm 0.104^\circ$).

In order to find the ratio errors of the instrument transformers on the side q as well as calculate the ratio errors for the current transformer on side p , the following set of equations are solved.

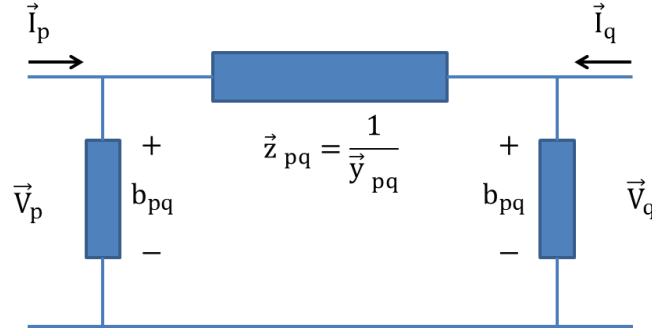


Figure 3.3: Two-bus π -network model of the power system

$$V_{pq_m} = V_{pq} \times REV_{pq} \Rightarrow V_{pq} = \frac{V_{pq_m}}{REV_{pq}} = V_{pq_m} \times KV_{pq} \quad (3.1)$$

$$V_{qp} = \frac{V_{qp_m}}{REV_{qp}} = V_{qp_m} \times KV_{qp} \quad (3.2)$$

$$I_{pq} = \frac{I_{pq_m}}{REI_{pq}} = I_{pq_m} \times KI_{pq} \quad (3.3)$$

$$I_{qp} = \frac{I_{qp_m}}{REI_{qp}} = I_{qp_m} \times KI_{qp} \quad (3.4)$$

The voltages and currents with subscript m are the voltages and currents measured by the DULR PMUs, while the other voltages and currents in the above equations are the original values of voltages and currents, in the absence of ratio errors. It is important to mention here that the quantization errors are already present, since the values are obtained from PMUs. REV s are the ratio errors in the voltages while REI s are the ratio errors in the currents. The inverse of the ratio errors are referred to as ratio correction factors and denoted by KV s and KI s, respectively. Using Kirchhoff's Laws on the pi-section, we get,

$$\begin{bmatrix} I_{pq} \\ I_{qp} \end{bmatrix} = \begin{bmatrix} b_{pq} + y_{pq} & -y_{pq} \\ -y_{pq} & b_{pq} + y_{pq} \end{bmatrix} \begin{bmatrix} V_{pq} \\ V_{qp} \end{bmatrix} = \begin{bmatrix} b_{pq} + \frac{1}{z_{pq}} & -\frac{1}{z_{pq}} \\ -\frac{1}{z_{pq}} & b_{pq} + \frac{1}{z_{pq}} \end{bmatrix} \begin{bmatrix} V_{pq} \\ V_{qp} \end{bmatrix} \quad (3.5)$$

Eq. (3.5) can be re-written for ease of calculation, as shown below. Taking the transpose of eq. (3.5),

$$[I_{pq} \quad I_{qp}] = [V_{pq} \quad V_{qp}] \begin{bmatrix} b_{pq} + \frac{1}{z_{pq}} & -\frac{1}{z_{pq}} \\ -\frac{1}{z_{pq}} & b_{pq} + \frac{1}{z_{pq}} \end{bmatrix} \quad (3.5(a))$$

This equation is in the form $\mathbf{AX} = \mathbf{B}$, where $\mathbf{A} = [V_{pq} \quad V_{qp}]$, $\mathbf{X} = \begin{bmatrix} b_{pq} + \frac{1}{z_{pq}} & -\frac{1}{z_{pq}} \\ -\frac{1}{z_{pq}} & b_{pq} + \frac{1}{z_{pq}} \end{bmatrix}$

and $\mathbf{B} = [I_{pq} \quad I_{qp}]$. Multiplying the inverse of $\begin{bmatrix} b_{pq} + \frac{1}{z_{pq}} & -\frac{1}{z_{pq}} \\ -\frac{1}{z_{pq}} & b_{pq} + \frac{1}{z_{pq}} \end{bmatrix}$ on both sides of eq.

(3.5(a)),

$$[I_{pq} \quad I_{qp}] \begin{bmatrix} b_{pq} + \frac{1}{z_{pq}} & -\frac{1}{z_{pq}} \\ -\frac{1}{z_{pq}} & b_{pq} + \frac{1}{z_{pq}} \end{bmatrix}^{-1} = [V_{pq} \quad V_{qp}] \quad (3.5(b))$$

Eq. (3.5(b)) also takes the form $\mathbf{AX} = \mathbf{B}$, where $\mathbf{A} = [I_{pq} \quad I_{qp}]$, $\mathbf{X} =$

$$\begin{bmatrix} b_{pq} + \frac{1}{z_{pq}} & -\frac{1}{z_{pq}} \\ -\frac{1}{z_{pq}} & b_{pq} + \frac{1}{z_{pq}} \end{bmatrix}^{-1} \text{ and } \mathbf{B} = [V_{pq} \quad V_{qp}].$$

\mathbf{X} in eq. (3.5(a)) is the admittance matrix while in eq. (3.5(b)) it is the impedance matrix. To solve these equations, it is best to use the impedance matrix instead of the admittance matrix, since the \mathbf{A} matrix in eq. (3.5(b)) has a better condition number than that in eq. (3.5(a)), as shown in fig. 3.5.

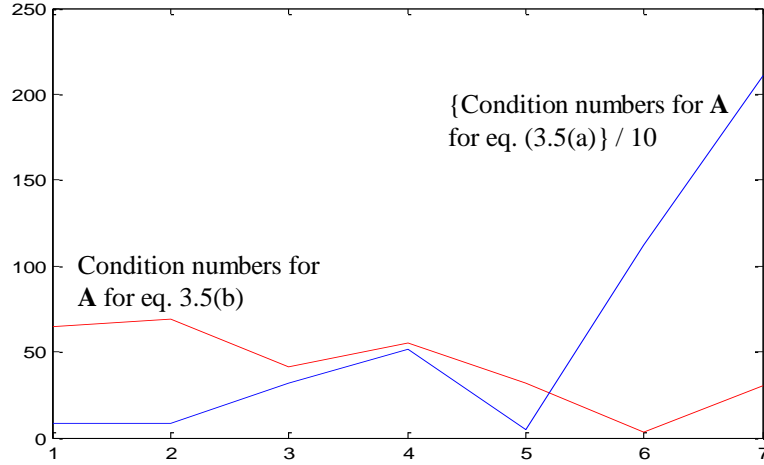


Figure 3.4: A Comparison of condition numbers when A is voltages (blue) instead of currents (red)

Next, replacing the actual voltages and currents by the measured quantities as shown in eq. (3.1) to (3.4) in eq. (3.5(b)), and solving the same we can get an equation of the form $\mathbf{AX} = \mathbf{B}$ as shown in eq. (3.6).

$$\begin{aligned}
 & \begin{bmatrix} I_{pq_m} & I_{qp_m} \end{bmatrix} \begin{bmatrix} \left(\frac{(b_{pq}z_{pq} + 1)}{b_{pq}(b_{pq}z_{pq} + 2)} \right) \left(\frac{kI_{pq}}{kV_{pq}} \right) & \left(\frac{1}{b_{pq}(b_{pq}z_{pq} + 2)} \right) \left(\frac{kI_{qp}}{kV_{pq}} \right) \\ \left(\frac{1}{b_{pq}(b_{pq}z_{pq} + 2)} \right) \left(\frac{kI_{pq}}{kV_{qp}} \right) & \left(\frac{(b_{pq}z_{pq} + 1)}{b_{pq}(b_{pq}z_{pq} + 2)} \right) \left(\frac{kI_{qp}}{kV_{qp}} \right) \end{bmatrix}^{-1} \\
 & = \begin{bmatrix} V_{pq_m} & V_{qp_m} \end{bmatrix} \tag{3.6}
 \end{aligned}$$

Replacing $b_{pq}z_{pq} + 1$ by w_{pq} for simplification, we get eq. (3.7).

$$\begin{aligned}
 & \begin{bmatrix} I_{pq_m} & I_{qp_m} \end{bmatrix} \begin{bmatrix} \left(\frac{w_{pq}}{b_{pq}(w_{pq} + 1)} \right) \left(\frac{kI_{pq}}{kV_{pq}} \right) & \left(\frac{1}{b_{pq}(w_{pq} + 1)} \right) \left(\frac{kI_{qp}}{kV_{pq}} \right) \\ \left(\frac{1}{b_{pq}(w_{pq} + 1)} \right) \left(\frac{kI_{pq}}{kV_{qp}} \right) & \left(\frac{w_{pq}}{b_{pq}(w_{pq} + 1)} \right) \left(\frac{kI_{qp}}{kV_{qp}} \right) \end{bmatrix}^{-1} \\
 & = \begin{bmatrix} V_{pq_m} & V_{qp_m} \end{bmatrix} \tag{3.7}
 \end{aligned}$$

Thus the equation can be written as $\mathbf{I}_m \mathbf{Z}_m = \mathbf{V}_m$, i.e. $\mathbf{A} = \mathbf{I}_m$, $\mathbf{X} = \mathbf{Z}_m$ and $\mathbf{B} = \mathbf{V}_m$. As the measured values of the phases are known, we have the matrices \mathbf{A} and \mathbf{B} are known completely while the matrix \mathbf{X} is unknown. The best way to solve this equation is to solve for \mathbf{X} in the least-squares sense. This is done in MATLAB using the command *lscov* as shown in eq. (3.8).

$$\mathbf{Z}_m = \text{lscov}(\mathbf{I}_m, \mathbf{V}_m) = \begin{bmatrix} a_0 & b_0 \\ c_0 & d_0 \end{bmatrix} \quad (3.8)$$

Eq. (3.7) is a versatile equation. It can be molded according to the requirement of the utility. In a utility, the tie-lines normally have revenue quality metering. Starting from such instrument transformers the high voltage network of the utility can be calibrated using this equation. If there are good quality voltage transformers available, both the voltage and current of the entire network can be calibrated, provided we know the line parameters. On the other hand, in the presence of a good quality current transformer along with a good voltage transformer, the line parameters can be estimated as well.

3.2.1 Voltage and Current Transformer Calibration

In the pi-section model shown in fig. 3.3, if p is an end of a tie-line, then the voltage transformer at that bus will be revenue quality. If the line parameters are known, then solving eqs. (3.7) and (3.8), the following equations can be obtained.

$$KI_{pq} = a_0 KV_{pq} \left(\frac{b_{pq}(w_{pq} + 1)}{w_{pq}} \right) \quad (3.9)$$

$$KI_{qp} = c_0 KV_{pq} (b_{pq}(w_{pq} + 1)) \quad (3.10)$$

$$KV_{qp} = \frac{KI_{pq}}{b_0} \left(\frac{1}{b_{pq}(w_{pq} + 1)} \right) = \left(\frac{a_0}{b_0} \right) KV_{pq}(w_{pq}) \quad (3.11)$$

In any network, one pi-section is connected to the next. Once the first pi-section has been solved, as shown above, the process of moving to the next one to estimate the ratio errors in the other PMUs is shown below.

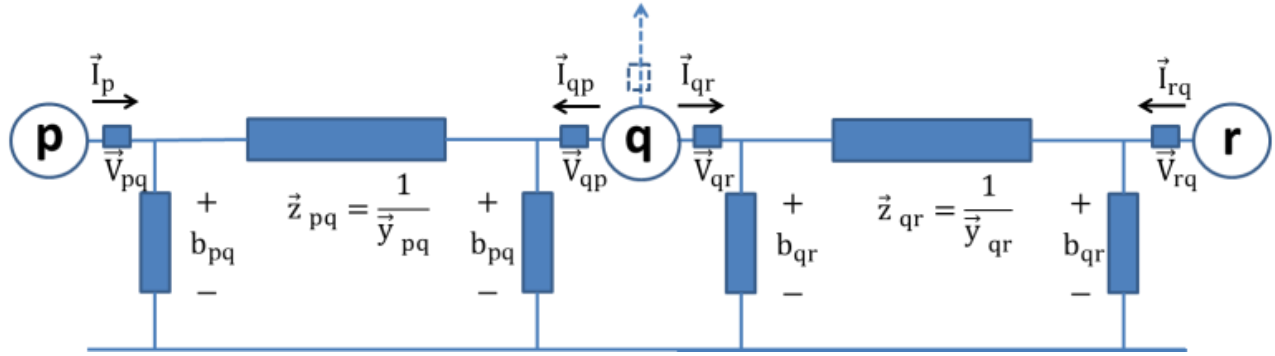


Figure 3.5: Two pi-sections with dual-use line relays acting as PMUs

Using fig.3.6 as an illustration, the true voltage at the node q should be the same, seen from any direction. But, due to the presence of ratio errors, that will not be the case for the measured phasors. To overcome this issue, a new term, γ , has been introduced. γ is the ratio of the two voltages obtained by the two DULR PMUs on either side of the node q .

$$\gamma = \frac{V_{qp_m}}{V_{qr_m}} = \frac{V_{qp} \times REV_{qp}}{V_{qr} \times REV_{qr}} = \frac{REV_{qp}}{REV_{qr}} \left\{ \text{Since } V_{qp} = V_{qr} = \text{Actual voltage at node } q \right\} \quad (3.12)$$

Solving eqs. (3.11) and (3.12), the following equation can be obtained.

$$REV_{qr} = \frac{REV_{qp}}{\gamma} = REV_{qp} \times \frac{V_{qr_m}}{V_{qp_m}} \quad (3.13)$$

Thus this process can be repeated and the entire network can be solved by moving from one pi-section to the next.

3.2.2 Simulation and Results for Voltage and Current Transformer Calibration

For the problem solved here, data for the morning load pickup has been assumed, which has unknown ratio errors and quantization errors. Ratio errors normally remain constant for an extended period of time, like over a period of six months. Quantization is modeled as additive noise in signal processing [14] but the signals change rapidly and over large ranges. As such, a staircase like data plot is obtained. To get a smooth data set, the data has been interpolated and this new data has been used to perform the rest of the calculation.

For simulation purposes, the IEEE 118 bus and 300 bus systems have been used to demonstrate the logic developed. The data for both these systems was created using MATPOWER [47]. This was assumed to be the actual data. The measured data was created from this data by introducing random ratio errors in the range of $\pm 0.15\%$ for magnitude and $\pm 0.104^\circ$ for angle in the good quality voltage measurement placed at bus 10, while the random ratio errors introduced had a range of $\pm 6\%$ for magnitude and $\pm 4^\circ$ for angle in the rest of the voltage measurements and $\pm 10\%$ for magnitude and $\pm 6.67^\circ$ for angle in all of the current measurements. Next, the quantization errors were introduced, as discussed in section 3.1 of this chapter. Eqs. (3.9) through (3.11) were then applied to this “measured data” to be able to get an estimate of the ratio errors. Once the ratio errors are estimated, they are compared to the original ratio errors that had been originally introduced into the data. The errors in estimating ratio errors is calculated from there and then the standard deviation (σ) of these errors are calculated. The plots thus obtained for standard deviation of the ratio errors for both voltage and current transformers have been shown below.

Figs. 3.7 and 3.8 show the standard deviation of the ratio errors in all the voltage transformers placed on the high-voltage networks of the IEEE 118 and 300 bus systems. As is seen in the plots, the standard deviation of the ratio errors are well within the pre-defined threshold of 0.01 *or* 1%. It has been assumed that there exists one good quality voltage transformer at bus 10 for the IEEE 118 bus system and one at bus 242 for the IEEE 300 bus system, which is one end of a tie line. The rest of them have been estimated using this knowledge.

Figs. 3.9 and 3.10, on the other hand, show the ratio errors present in all the current transformers associated with the high voltage networks, again, for both the test systems, with only one good quality voltage measurement present in the system. These plots, however, show that there are two instrument transformers in each system which have ratio errors well above the threshold of 0.01 *or* 1%. Though the rest of them lie within the threshold, these outliers may cause computational complication down the line.

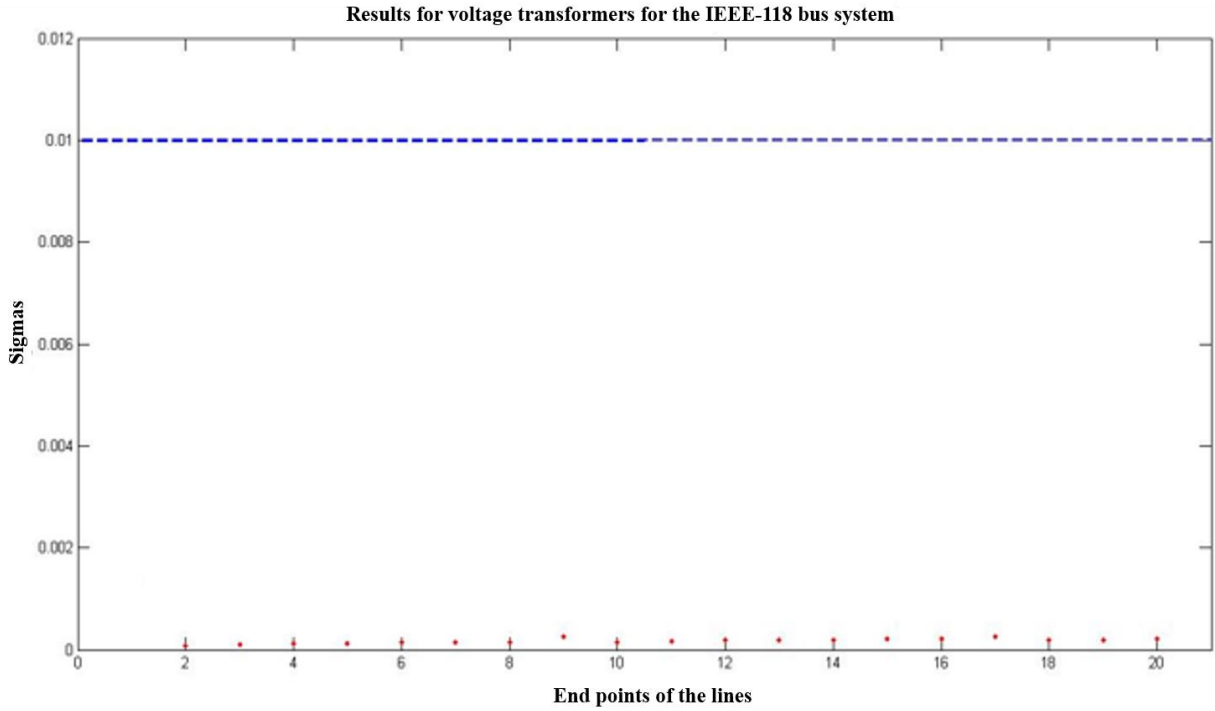


Figure 3.6: Standard deviation (σ) of the ratio errors in voltage transformers of the IEEE 118 bus system with good quality measurements only at bus 10

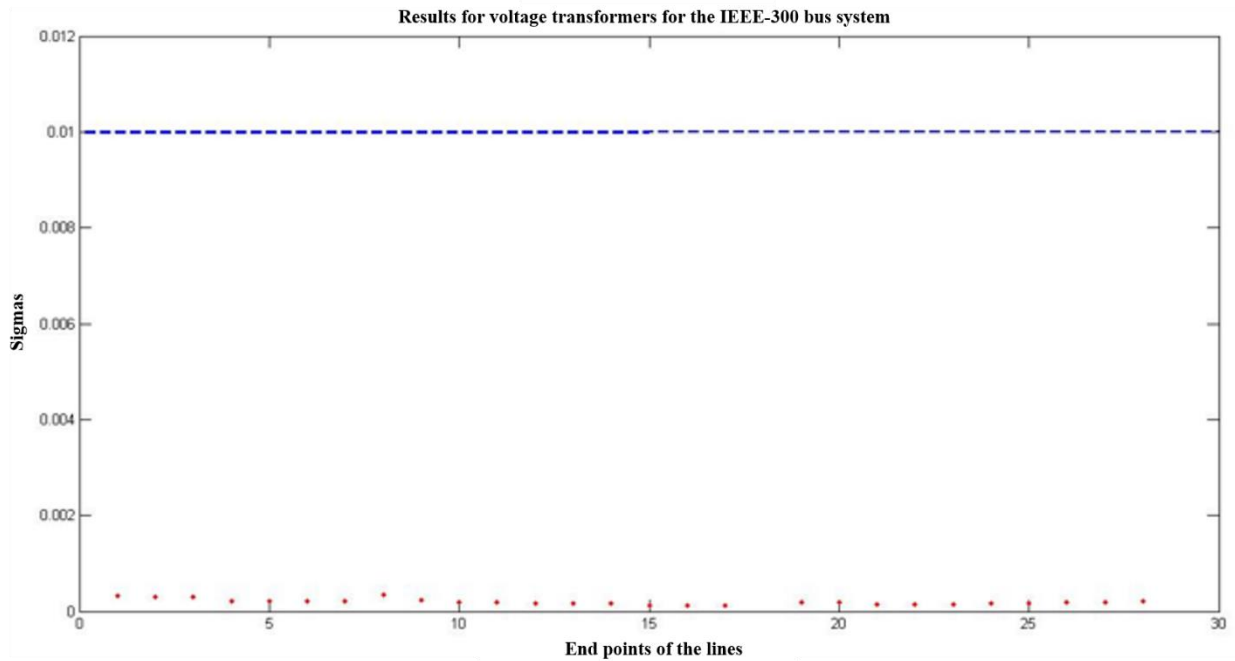


Figure 3.7: Standard deviation (σ) of the ratio errors in voltage transformers of the IEEE 300 bus system with good quality measurements only at bus 242

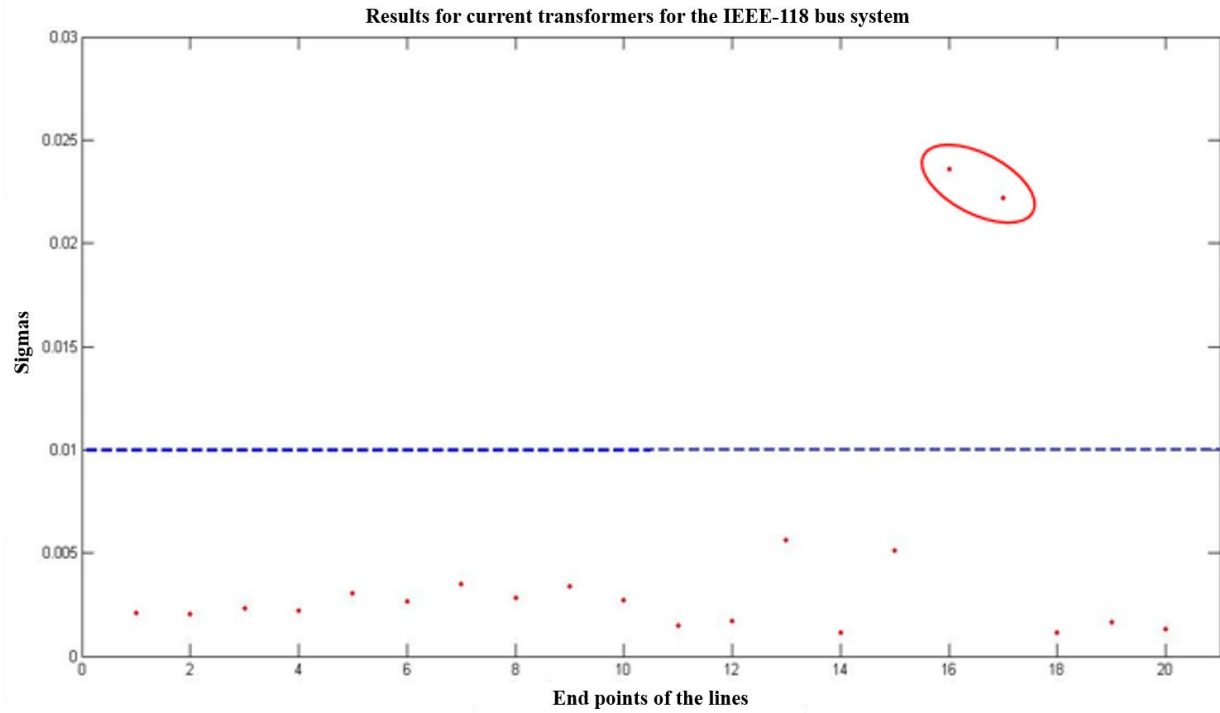


Figure 3.8: Standard deviation (σ) of the ratio errors in current transformers of the IEEE 118 bus system with good quality measurements only at bus 10

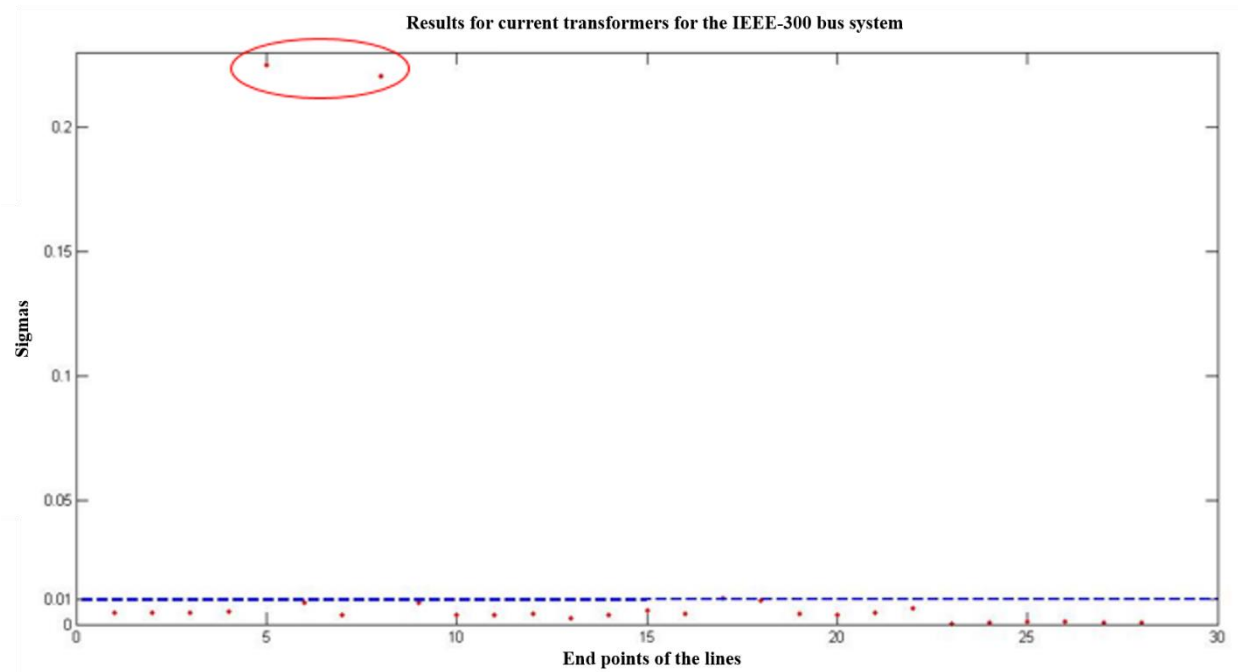


Figure 3.9: Standard deviation (σ) of the ratio errors in current transformers of the IEEE 300 bus system with good quality measurements only at bus 242

The reason behind this anomaly was identified to be the line parameters of some particular pi-sections. Due to extremely low impedance values in the lines, the ratio errors in the current transformers rose rapidly. Such kind of line parameters will not be observed in real systems. In these test systems, for the ease of simulations, some step-up transformers have been represented as high voltage transmission lines. Though, in real systems, this issue should not arise, since in real systems, the currents passing through these transformers will be monitored. As a result, they can be treated as injections into the high voltage network. For the rest of this thesis, all such pi-sections have been treated as injections and not real pi-sections.

Most real life systems have more than one tie-line. Thus in most systems, there will be more than one revenue quality voltage transformers present. This aids the process of calibration further. To illustrate this point, the IEEE-300 bus system has been calibrated in the presence of two good voltage quality measurements and the results have been shown in the following plots.

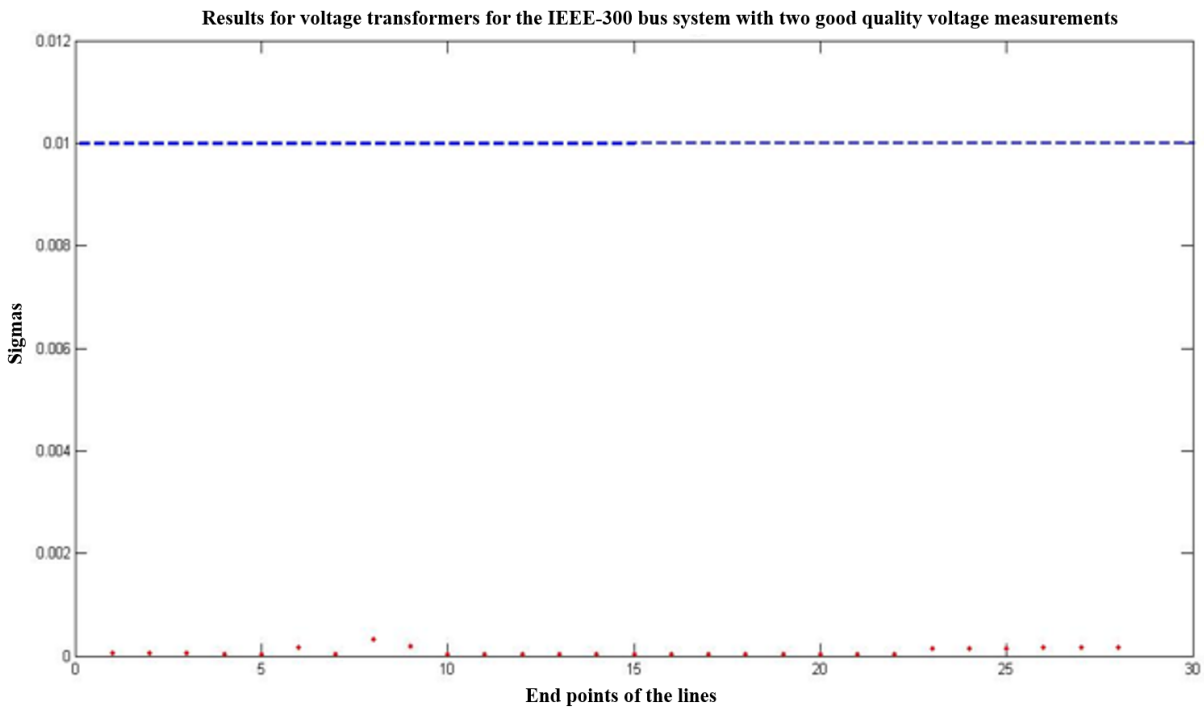


Figure 3.10: Standard deviation (σ) of the ratio errors in voltage transformers of the IEEE 300 bus system with good quality VT at bus 242 and bus 28

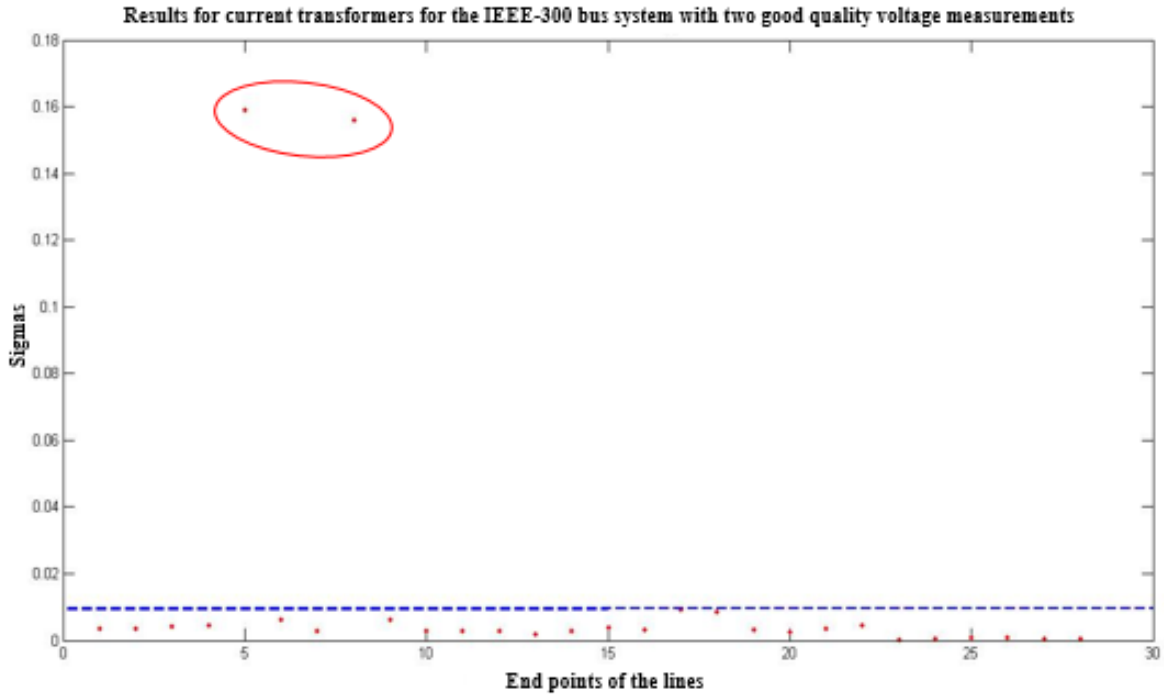


Figure 3.11: Standard deviation (σ) of the ratio errors in current transformers of the IEEE 300 bus system with good quality VT at bus 242 and bus 28

The next chapter talks about yet another derivative of the calibration method developed in this chapter, which calibrates all the instrument transformers of a network with only one good quality measurement at a tie-line even when the data obtained from the field is incomplete or has some garbage values in it.

Chapter 4: Calibrating Instrument Transformers in Presence of Incomplete Data

To maintain an optimal economic balance between demand and supply, utilities often have to take some lines off the grid. At other times certain lines need to be taken offline for the purpose of maintenance as well. As such it gets extremely difficult to collect and store the data for an entire transmission network at any point in time. That is, some of the data is either missing or tainted (for example voltage magnitude of in-service buses ≤ 0 , voltage or current angles = 9999 etc.). Therefore, it is a very rare occurrence that all the instrument transformers of the transmission network will be calibrated in one go.

The biggest challenge that arises from insufficient data availability is calibrating the voltage and current transformers of the entire high voltage network in the presence of only one good quality voltage transformer placed at the end of a tie-line. So far all the methods discussed in this thesis required a connected tree for their calculation processes. Unfortunately, with insufficient or garbage data, the connected tree can no longer be formed at any given point in time. This chapter describes a method to work around the missing or garbage data problem in order to calibrate the entire high voltage network.

4.1 Methodology

For the issue at hand, all the line parameters of the transmission system must be known, as well as the position of the good quality voltage transformer. The error model used in this chapter is the same as the one developed in the previous chapter. Also, all the PMUs used are DULR PMUs.

When a utility collects data, there are certain pockets of data missing since certain lines are out of service. The method developed in this chapter evaluates the ratios of ratio errors of individual pi-sections, irrespective of the presence or absence of a connected tree. It looks for the two voltages and two currents for a pi-section available at a given time and solves for that particular pi-section and stores the results. It keeps repeating the process for the data collected over the period of days or weeks. Once it solves for all the pi-sections in the entire network, at different times, it puts the

solution together like a jigsaw puzzle and provides a look at the entire network which is now calibrated completely.

The proposed methodology is described as follows. To solve for the pi-section shown in fig. 3.4, the basic data required are \vec{V}_{pq_m} , \vec{V}_{qp_m} , \vec{I}_{pq_m} and \vec{I}_{qp_m} , i.e., the measured values of voltages and currents from either ends of the pi-section. Now, only one group of the measured values of these four quantities is not enough. For the calculations done in this chapter, a set of m data points for each quantity over a period of h hours was assumed to be available. If the good voltage measurement is placed at p , the ratio errors can be calculated as shown in equations (3.1) to (3.4). The field data obtained from a utility is loaded, as it is, into the database. When the database encounters voltage magnitude values for in-service buses as zero, near-zero, or negative, or if the current or voltage angles are found to be 9999, then it identifies those values as garbage. Such inappropriate values along with missing data points are replaced by NaN (not a number) in the database. From this modified information it is found out which pi-sections in the network can be solved, i.e., a set of at least m data points for each of the four quantities needed to solve a pi-section are available (these data points have to be spread out evenly and not consecutive in order to be able to calibrate the system without running into numerical problems). The pi-section in question can then be solved by using the eqs. (3.5) through (3.8). For ease of calculation, eqs. (3.9) through (3.11) are modified as shown below.

Eq. (3.9) can be modified into:

$$\overline{KI}_{pq} = a_0 \overline{KV}_{pq} \left(\frac{\vec{b}_{pq}(\vec{w}_{pq} + 1)}{\vec{w}_{pq}} \right) \text{ or } \overline{REI}_{pq} = \frac{\overline{REV}_{pq}}{a_0} \left(\frac{\vec{w}_{pq}}{\vec{b}_{pq}(\vec{w}_{pq} + 1)} \right) \quad (4.1a)$$

Hence,

$$\frac{\overline{REI}_{pq}}{\overline{REV}_{pq}} = \frac{1}{a_0} \left(\frac{\vec{w}_{pq}}{\vec{b}_{pq}(\vec{w}_{pq} + 1)} \right) \quad (4.1b)$$

Similarly, eq. (3.10) can be modified as:

$$\overline{KI}_{qp} = c_0 \overline{KV}_{pq} \left(\vec{b}_{pq}(\vec{w}_{pq} + 1) \right) \text{ or } \overline{REI}_{qp} = \frac{\overline{REV}_{pq}}{c_0} \left(\frac{1}{\vec{b}_{pq}(\vec{w}_{pq} + 1)} \right) \quad (4.2a)$$

Hence,

$$\frac{\overline{\text{REI}}_{qp}}{\overline{\text{REV}}_{pq}} = \frac{1}{c_0} \left(\frac{1}{\vec{b}_{pq}(\vec{w}_{pq} + 1)} \right) \quad (4.2b)$$

Finally, eq. (3.11) can be modified into:

$$\overline{\text{KV}}_{qp} = \frac{\vec{k}_{pq}}{b_0} \left(\frac{1}{\vec{b}_{pq}(\vec{w}_{pq} + 1)} \right) = \left(\frac{a_0}{b_0} \right) \overline{\text{KV}}_{pq} \left(\frac{1}{\vec{w}_{pq}} \right) \text{ or } \overline{\text{REV}}_{qp} = \left(\frac{b_0}{a_0} \right) \overline{\text{REV}}_{pq} \vec{w}_{pq} \quad (4.3a)$$

Hence,

$$\frac{\overline{\text{REV}}_{qp}}{\overline{\text{REV}}_{pq}} = \left(\frac{b_0}{a_0} \right) \vec{w}_{pq} \quad (4.3b)$$

The above equations explain the process of solving the first pi-section that has the good quality voltage measurement at p . But, this is also how the other pi-sections are individually solved as well. To explain this further, the second pi-section of fig. (3.6) is considered. If, for example, in the data collected for a particular day does not have enough data for the pi-section pq to be solved, but qr can be solved, the eqs. (4.1) though (4.3) can be modified as follows.

$$\frac{\overline{\text{REI}}_{qr}}{\overline{\text{REV}}_{qr}} = \frac{1}{a_1} \left(\frac{\vec{w}_{qr}}{\vec{b}_{qr}(\vec{w}_{qr} + 1)} \right) \quad (4.4)$$

$$\frac{\overline{\text{REI}}_{rq}}{\overline{\text{REV}}_{qr}} = \frac{1}{c_1} \left(\frac{1}{\vec{b}_{qr}(\vec{w}_{qr} + 1)} \right) \quad (4.5)$$

$$\frac{\overline{\text{REV}}_{rq}}{\overline{\text{REV}}_{qr}} = \left(\frac{b_1}{a_1} \right) \vec{w}_{qr} \quad (4.6)$$

where, $\begin{bmatrix} a_1 & b_1 \\ c_1 & d_1 \end{bmatrix} = \text{lscov} \left(I_{qr_m}, V_{qr_m} \right) = \mathbf{Z}_{qr_m}$

Here, the ratio errors of this pi-section have all been calculated with respect to the one for the voltage transformer on the end qr . Once all the pi-sections have been solved in this manner, the results can be put together to form the picture of the entire high voltage network.

Now, from eq. (3.12), it is known that,

$$\vec{\gamma} = \frac{\vec{V}_{qp_m}}{\vec{V}_{qr_m}} = \frac{\overline{REV}_{qp}}{\overline{REV}_{qr}} \text{ or } \overline{REV}_{qr} = \overline{REV}_{qp} \left(\frac{\vec{V}_{qr_m}}{\vec{V}_{qp_m}} \right) \quad (4.7)$$

Dividing eq. (4.7) by \overline{REV}_{pq} ,

$$\frac{\overline{REV}_{qr}}{\overline{REV}_{pq}} = \frac{\overline{REV}_{qp}}{\overline{REV}_{pq}} \left(\frac{\vec{V}_{qr_m}}{\vec{V}_{qp_m}} \right) \quad (4.8)$$

Therefore, using eq. (4.8), the ratio errors of the second pi-section can be found with respect to that of the good voltage measurement at p . This process can be repeated as many times as needed to solve for the entire network. The simulations done in this thesis were all run in MATLAB, and they have been discussed in details in the next section along with the results that were obtained.

4.2 Simulation and Results

The method developed in the previous section has been demonstrated here with the help of two test systems, the high voltage networks of the IEEE 118 bus and 300 bus systems. The use of each of these test systems have been described in details below.

The IEEE-118 bus system has 11 high voltage buses connected by 10 lines, as shown in fig. 3.7(a). As before, the good quality voltage measurement was placed at bus 10. A data file consisting of 6000 measurements for each of the 11 bus voltages of the high voltage network of the 118 bus system was created using MATPOWER [47]. This data file was used to create measurements that mimicked those obtained in the field. As the line parameters of the system are known, the currents in the transmission lines were calculated using the voltage data created. Hence, the measured data was created by introducing random ratio errors in the range of $\pm 0.015\%$ for magnitude and $\pm 0.104^\circ$ for angle in the good quality voltage measurement placed at bus 10, while the random ratio errors introduced had a range of $\pm 0.06\%$ for magnitude and $\pm 4^\circ$ for angle in the rest of the voltage measurements and $\pm 0.1\%$ for magnitude and $\pm 6.67^\circ$ for angle in all of the current measurements. Next, the quantization errors were introduced, as discussed in the error model of Chapter 3, to create data resembling those obtained in the field. Hence, the final data created was a (6000x20) matrix for both voltages and currents, as there are 20 bus voltages (since

each bus voltage had two looks from the DULR PMUs placed on the lines) and 20 line currents being measured by the DULR PMUs.

Fig. 4.1 shows a snapshot of how a typical data file consisting of field data obtained from a utility would look like. It can be seen from this figure that there are certain parts of data which has garbage or missing values. To make the simulated data created so far for the 118 bus system resemble that shown in fig. 4.1, NaNs were introduced in the simulated data at random locations. For the purpose of this simulation, 25% of the data was replaced by NaNs. Though in a real life scenario, any utility will not have more than 10% NaNs in their data. This means that the methodology developed here is robust enough for field data from any utility.

	A	B	C	D	E	F	G	H
1	V1Mag	V1Ang	I1Mag	I1Ang	V2Mag	V2Ang	I2Mag	I2Ang
22	526.2685	-109.2674	364.6409	-99.61131	527.7143	-111.3042	360.6214	62.25095
23	526.247	-109.4194	364.2256	-99.82694	527.723	-111.4607	361.7863	62.11856
24	526.2501	-109.5667	365.0776	-100.008	527.7102	-111.6102	362.0865	62.02892
25	526.2684	-109.7175	365.1895	-100.107	527.7137	-111.7632	362.1244	61.80226
26	526.2579	-109.8695	365.4166	-100.3048	527.6891	-111.9175	362.7318	61.62383
27	526.2835	-110.0203	366.2782	-100.4842	527.7132	-112.074	362.4736	61.48656
28	526.248	-110.1737	366.3954	-100.5827	527.7151	-112.2235	363.0872	61.30884
29	526.269	-110.3209	366.5136	-100.6812	527.7207	-112.373	363.3953	61.2202
30	526.2408	-110.4743	367.504	-100.9572	NaN	-9999	NaN	-9999
31	526.2488	-110.6264	366.9974	-101.0745	527.687	-112.6867	364.0141	61.04337
32	526.2281	-110.7798	367.8743	-101.2512	527.6719	-112.8377	364.0767	60.81805
33	526.199	-110.9297	367.3716	-101.3687	NaN	-9999	NaN	-9999
34	526.218	-111.0817	367.4984	-101.4667	527.6526	-113.1396	364.145	60.59282
35	526.2087	-111.2351	367.7553	-101.6624	527.6938	-113.2925	364.2188	60.36766
36	526.2351	-111.3872	367.3894	-101.8784	NaN	-9999	NaN	-9999
37	526.1818	-111.5469	366.895	-101.9969	527.661	-113.6043	363.7426	60.09235
38	526.1965	-111.7038	367.1635	-102.1926	527.6506	-113.7602	364.3834	59.91765
39	526.2025	-111.8572	367.2994	-102.2903	NaN	-9999	NaN	-9999
40	526.1931	-112.0155	367.5744	-102.4355	527.6238	-114.077	364.7979	59.6059
41	526.1688	-112.1787	367.2284	-102.7023	527.6078	-114.2378	364.8965	59.38139
42	526.1806	-112.3405	367.5124	-102.8973	NaN	-9999	NaN	-9999
43	526.1462	-112.5086	367.6559	-102.9946	527.5713	-114.5645	364.4505	59.10536

Figure 4.1: Snapshot of a part of the field data obtained from a utility with data missing from it

For ease of calculation, as well as to improve the accuracy of the results obtained, these 6000 data points were divided into groups of 12 data sets for each voltage and current of the entire

network. A 3 dimensional matrix was created by clumping together every 500th data point ($\frac{6000}{12} = 500$) into one set, thereby creating a (500x12x20) matrix for both voltage and current.

The fig. 4.2 illustrates how the 3 dimension matrix can be assumed to resemble a stack of laminated sheets. So, for the IEEE-118 bus system, 20 lines being measured, 12 data points of each of the lines clumped together (i.e., (1st, 501st, 1001st...), (2nd, 502nd, 1002nd...) and so on) resulted in 500 of such laminated data sheets. Two 3 dimensional matrices, A_{vol} and A_{curr} , were then created which consisted of ones in the places where data is available and zeros in places where there is missing or garbage data (depicted by NaN). Taking one laminated sheet at a time, the A matrices were used to determine which pi-section could be solved as explained in the previous section.

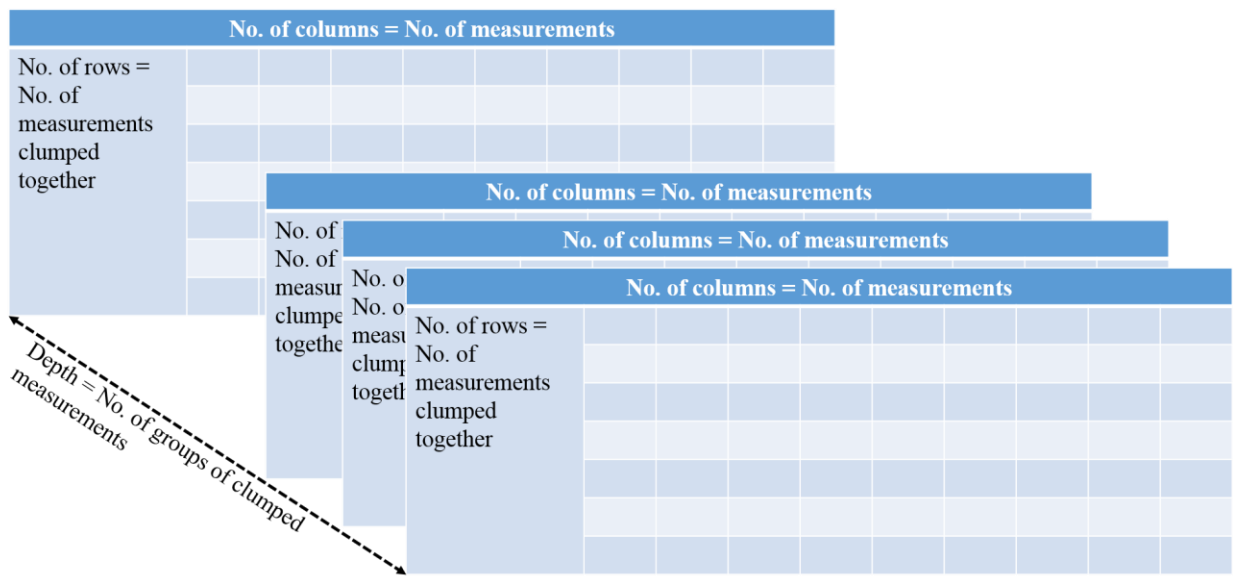


Figure 4.2: The 3D matrix created for both voltages and currents

If all the rows of the line voltages and line currents of a particular pi-section were available, that pi-section was solved using eqs. (4.1) through (4.6) and the results were stored, else they were left blank. To solve for each pi-section this way, an assumption had to be made here. One bus of each of these pi-sections were supposed to be a good quality measurement and the rest of the ratio errors were estimated with respect to the ratio error (voltage) at that bus. This entire process was

repeated for each of the laminated sheets and this provided the pieces of a jigsaw puzzle, as shown in fig. 4.3.

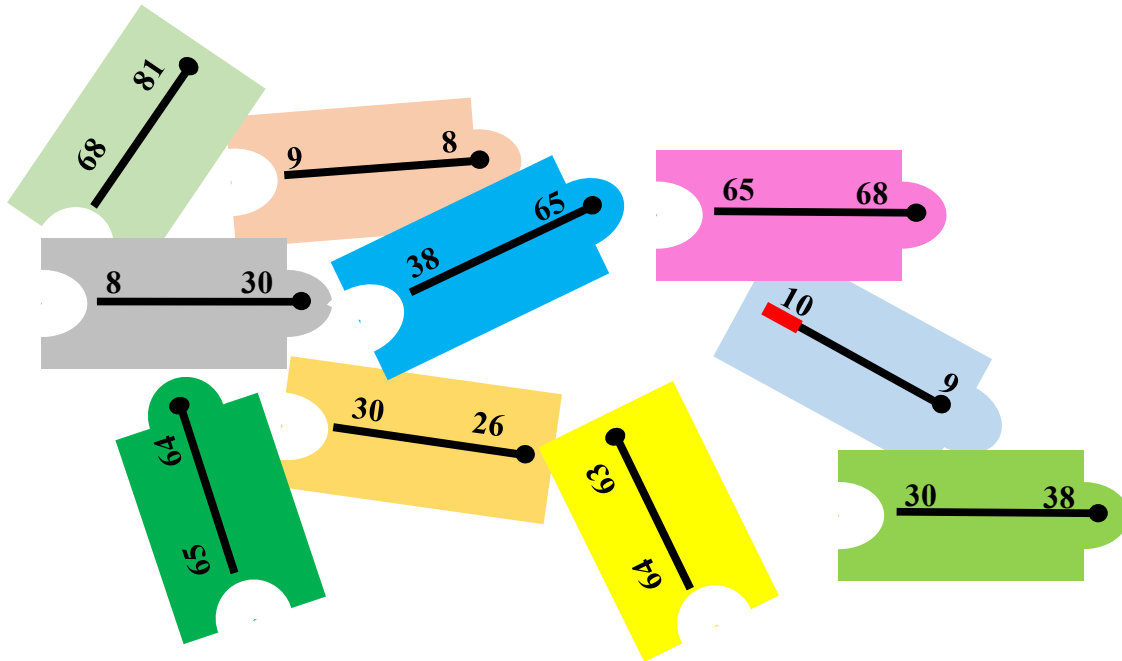


Figure 4.3: Solution of each pi-section available as pieces of a jigsaw puzzle

The solution for each pi-section was obtained multiple times, since there was always more than one laminated sheet where all the data for a particular pi-section was available. These values were then averaged to get a better estimate and finally all the data was put together to complete the jigsaw puzzle, as explained in the previous section using eq. (4.8). This way, the assumption previously made regarding the presence of a good quality voltage measurement at each pi-section, is not required any more, and hence can be ignored. Thus, for the 118 bus system a (1x20) matrix consisting of all the ratio errors with respect to the ratio error of the good quality voltage measurement (at the tie-line) was created.

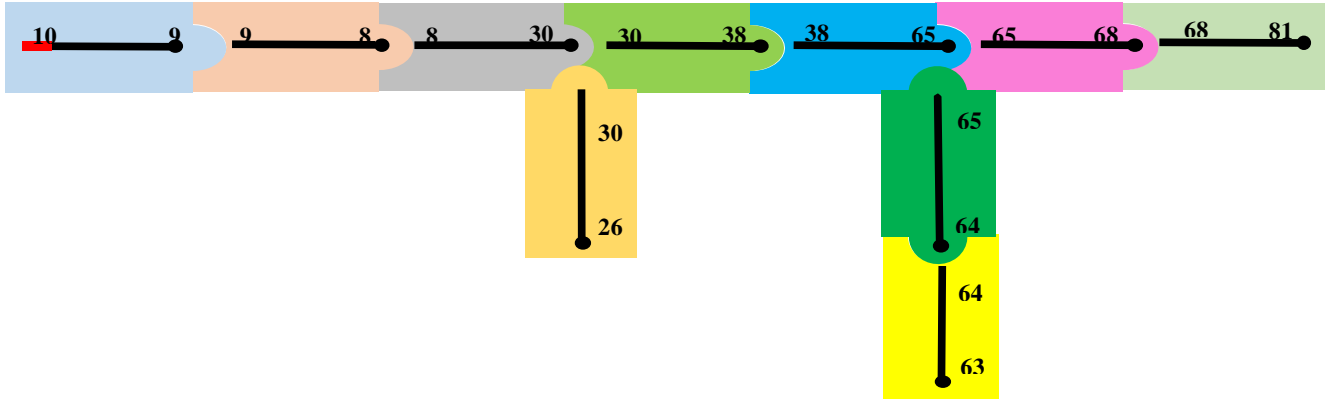


Figure 4.4: Putting the jigsaw puzzle together

This entire process was repeated 1000 times and the ratios of ratio errors were compiled. To compare with the ratio errors that were originally added into the data, a matrix was created which subtracted the calculated values from the original values and plotted the standard deviation of these errors. To give an example, tables 4.1 and 4.2 show the results for the first and the 1000th iterations.

TABLE 4.1: RATIO OF RATIO ERRORS IN VOLTAGES FOR THE IEEE-118 BUS SYSTEM FOR THE FIRST ITERATION

Original Ratio of Ratio Errors introduced	Ratio of Ratio Errors estimated in the simulation	Difference between the Ratio of Ratio Errors
1.0199-0.0561i	1.0199-0.0561i	-5.22505437006160e-06 + 3.67220742400476e-06i
0.9462-0.0439i	0.9463-0.044i	-6.00019774319449e-05 + 6.34274842384042e-05i
0.9552-0.0358i	0.9553-0.0358i	-6.80411301069439e-05 + 5.75846210854950e-05i
0.9571-0.0125i	0.9571-0.0137i	-1.52221284810405e-05 + 0.00122620737809760i
0.9952-0.0427i	0.9952-0.044i	2.48697299639611e-05 + 0.00126890511124770i
1.0223+0.0655i	1.0224+0.0643i	-0.000105318329399973 + 0.0011418235028648i
0.9606+0.0083i	0.9606+0.0083i	-1.15241383039644e-05 - 2.45384743135096e-05i
0.9723-0.022i	0.9724-0.0231i	-1.73091798579827e-05 + 0.00107540103338690i
0.9776+0.0645i	0.9777+0.0645i	-1.25558698970130e-05 - 2.54714746664025e-05i
0.969+0.0006i	0.969+0.001i	-1.56294501809651e-05 - 0.000371237923711419i
0.9622-0.0215i	0.9622-0.0212i	-2.46939827730497e-05 - 0.000362601089176400i
1.0583+0.0525i	1.0583+0.0524i	-2.19193249300087e-05 + 0.000107819477463904i
0.9858-0.025i	0.9859-0.0249i	-2.18914572739370e-05 - 9.10039216851996e-05i
0.9555+0.0192i	0.9555+0.0191i	-1.18928745539426e-05 + 9.76678062755976e-05i
0.9476-0.0429i	0.9476-0.0433i	4.93325341199835e-06 + 0.000386726020931698i
1.0121+0.0615i	1.0122+0.0611i	-4.30303077898486e-05 + 0.000418664422958098i
1.0051-0.0429i	1.0051-0.0428i	-2.27956847200783e-05 - 9.18558583004048e-05i
1.0189-0.0673i	1.0189-0.0675i	-1.07083570399791e-05 + 0.000171664788914394i
1.0125-0.0342i	1.0125-0.0344i	-1.47234326199897e-05 + 0.000166326655906400i

TABLE 4.2: RATIO OF RATIO ERRORS IN VOLTAGES FOR THE IEEE-118 BUS SYSTEM FOR THE THOUSANDTH ITERATION

Original Ratio of Ratio Errors introduced	Ratio of Ratio Errors estimated in the simulation	Difference between the Ratio of Ratio Errors
0.9751-0.0279i	0.9751-0.0279i	1.08293494294198e-06 - 2.24194548140155e-06i
1.0387+0.051i	1.0386+0.0533i	0.000133107455110082 - 0.00227670113587430i
0.9604+0.0029i	0.9604+0.005i	2.82400465390076e-05 - 0.00211048800061918i
0.9806-0.0379i	0.9806-0.038i	3.19444770829902e-05 + 9.41012535409999e-05i
0.9967+0.0485i	0.9966+0.0484i	2.03172046870925e-05 + 0.000100434030943501i
0.9478-0.0309i	0.9478-0.032i	4.29572905169540e-05 + 0.00111632022724630i
1.0007+0.002i	1.0007+0.0027i	3.98203040399281e-05 - 0.000726794374587830i
1.0416-0.023i	1.0416-0.0242i	2.98151321100892e-05 + 0.00124172051633330i
0.9664-0.0303i	0.9664-0.0296i	1.59282622690382e-05 - 0.000699961208135997i
1.0299-0.0164i	1.0299-0.0151i	2.92894331799243e-05 - 0.00133427898931080i
0.9585+0.0425i	0.9584+0.0437i	9.83544294990146e-05 - 0.00123255441682120i
0.9738+0.0364i	0.9737+0.0365i	5.21670634099358e-05 - 0.000127075650277898i
1.0161+0.0723i	1.0161+0.072i	3.08324488900169e-05 + 0.000204961080674304i
0.9971+0.0333i	0.9971+0.0334i	5.48360358409994e-05 - 0.000133189914436199i
0.9738-0.0042i	0.9737-0.0045i	4.91731793280659e-05 + 0.000334898696840070i
1.0159+0.0652i	1.0159+0.0649i	2.02338772699040e-05 + 0.000337812333245702i
0.9749+0.056i	0.9749+0.0558i	3.40181183600130e-05 + 0.000196787795956201i
1.0348-0.0326i	1.0348-0.0325i	5.07257151300955e-05 - 8.70159340944018e-05i
0.9523-0.059i	0.9522-0.0589i	4.65385176879884e-05 - 7.92423675890011e-05i

Similarly, the results for the ratios of ratio errors for currents can be obtained. Once all these results have been compiled, the standard deviation (σ) of the errors in ratios of ratio errors were calculated. Figs. 4.5 and 4.6 show the plots of the standard deviation of the ratio of ratio errors calculated with respect to the ratio error of the good quality voltage measurement placed at bus 10 for both the voltage as well as the current measurements of the entire high voltage network of the IEEE-118 bus system.

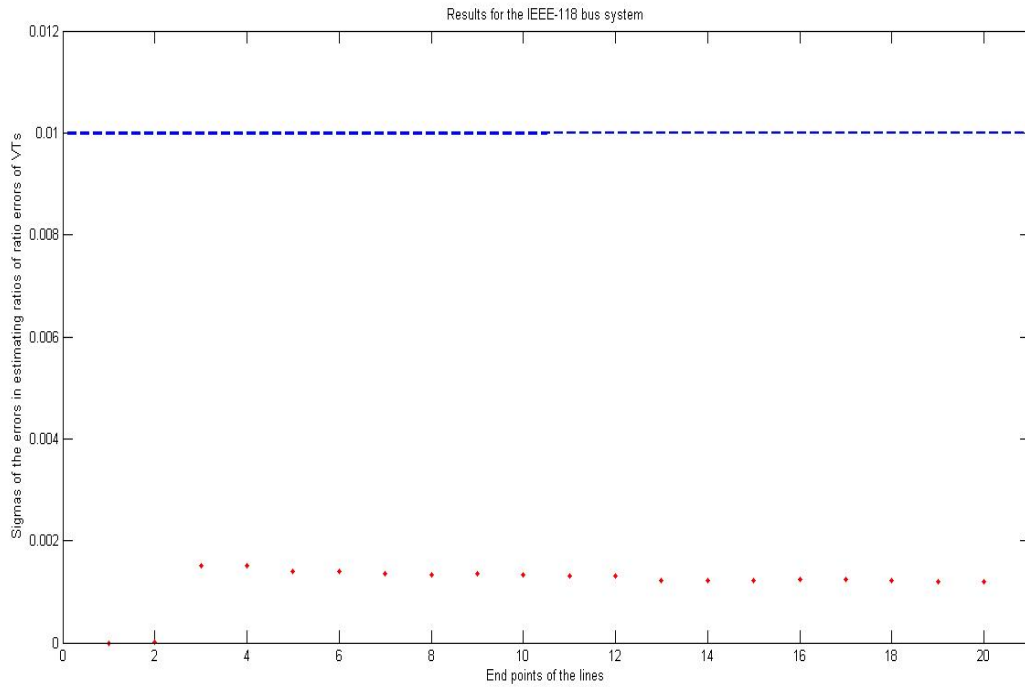


Figure 4.5: Standard deviation (σ) of the errors in estimating the ratios of ratio errors of the voltage transformers in the IEEE-118 bus system

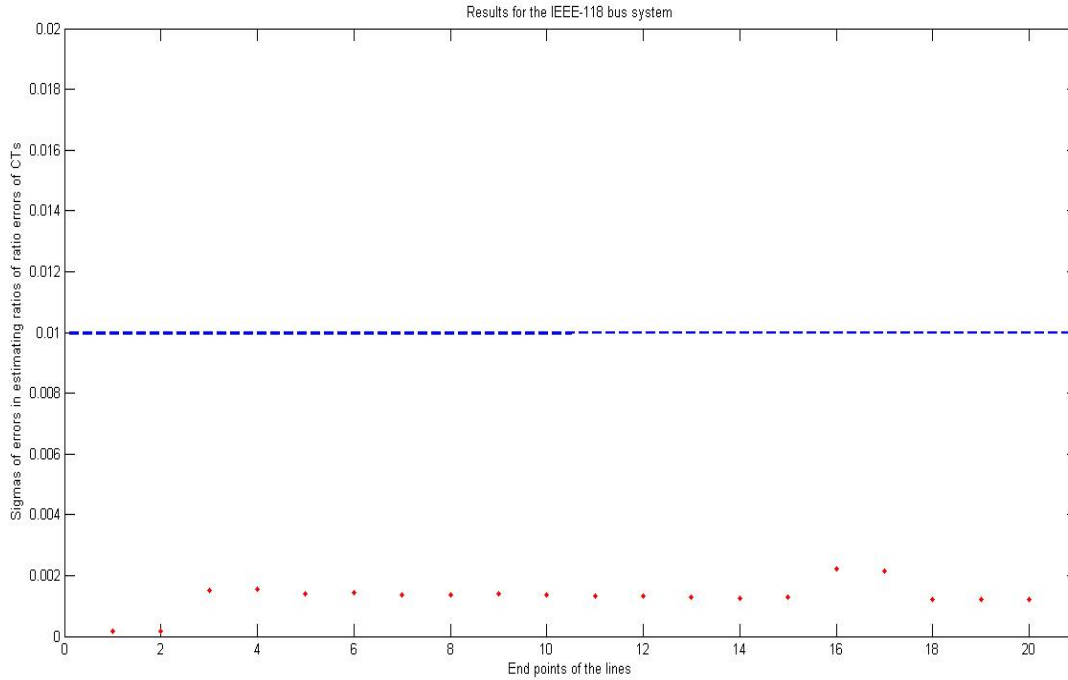


Figure 4.6: Standard deviation (σ) of the errors in estimating the ratios of ratio errors of the current transformers in the IEEE-118 bus system

The same method was repeated for the IEEE-300 bus system and the results obtained for the standard deviation of the errors in the ratio errors with respect to the ratio errors of the good quality voltage measurement placed at bus 242 for both the voltage as well as current transformers in the high voltage network were plotted in figs. 4.7 and 4.8.

The simulation provided in Appendix II illustrates the method described in this chapter to estimate the standard deviations of the ratios of ratio errors (standard deviation) of both voltage and current transformers when some measurements are absent.

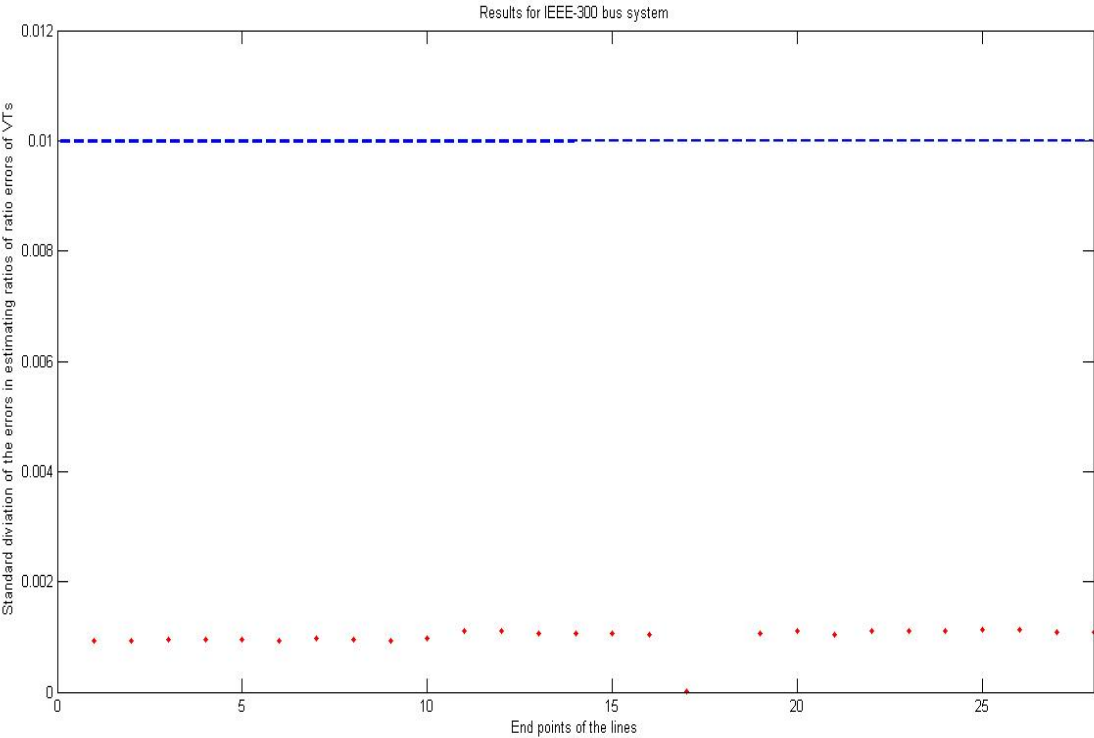


Figure 4.7: Standard deviation (σ) of the errors in estimating the ratios of ratio errors of the voltage transformers in the IEEE-300 bus system

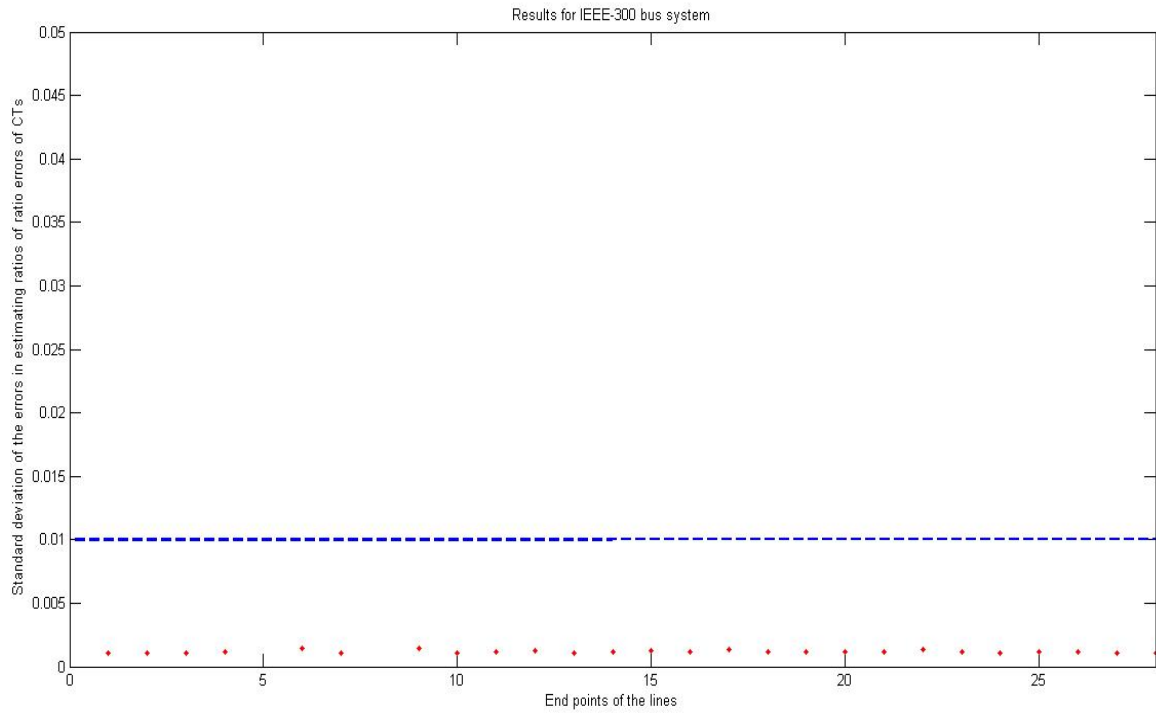


Figure 4.8: Standard deviation (σ) of the errors in estimating the ratios of ratio errors of the current transformers in the IEEE-300 bus system

This chapter provided a new technique to overcome the issue of insufficient data obtained from the field for calibration purposes. The method developed can calibrate both voltage and current transformers using data collected over a few days or even weeks. Unfortunately, if a line remains offline for the entire period of data collection, it cannot be calibrated. For this method to work, every line of the network has to be online for some duration of time during the data collection period for the purpose of calibration.

Chapter 5: Conclusion and Future Scope of Work

5.1 *Thesis Summary*

This thesis is aimed at solving the problem of instrument transformer calibration in presence of practical constraints. The blackout of 1965, one of the biggest blackouts in the history of the United States, made power engineers realize the need to automate the power grid. This major blackout resulted in the elevation of the power market from a traditional nascent market to a developing market. The gap between the target to be achieved and what it was at that point in time, opened up a host of opportunities for growth. Till date, the strong growth potential for power generation and distribution emanates from factors like growth in economy and propensity for increased electricity consumption. Gradually, transcendence from a developing market to a matured market called for more initiatives and measures to fully leverage the inherent potential of the market.

The power plant operators needed to be able to view the entire system at every time instant to be able to make decisions to address system viability in order to avoid the risk of cascading non-performing assets. To that end, Fred Schweppe's static state estimator algorithm [3] in the late 1960's-early 70's, the invention of microprocessors in 1982, followed by the creation of PMUs in 1983 [4] and their commercial availability by 1988 [5][6] were a huge leap forward. With the advent of PMUs, monitoring, control and protection of a power system became much more simplified.

This, in turn, helped power engineers to be able to understand what the current power system lacked and the field was thus poised to attract more investment and innovation. The need for calibrating instrument transformers in transmission networks was one such issue that surfaced soon after. Instrument transformers are basically step-down transformers that feed voltage and/or currents into PMUs for downstream applications. Just like any other piece of machinery, they have a tendency to deteriorate over time either due to the weather conditions they are forced to face or due to age. Thus, it has been seen that an error creeps into the voltages and currents that pass through them. Not just the instrument transformers, but even the PMUs, by virtue of their construction seem to introduce a small but inherent error into the measurements. All these errors

and the reasons of their existence have already been discussed in details in this thesis. To eliminate the downstream issues caused by these errors, a need for online calibration was felt.

The earliest attempts for calibrating these instrument transformers have been discussed in details in the second chapter of this thesis. It also talks about a relatively new and robust method for calibrating voltage transformers by placing optimal number of good quality measurements in a high voltage transmission network in order to keep the standard deviation of estimating these errors below a pre-defined threshold.

The next chapter developed a new error model based on what was observed in the field data. The concept of a PMU error being a quantization error was also introduced in this chapter. It then described a methodology where all the instrument transformers of an entire high voltage network could be calibrated with the presence of only one good voltage measurement located at the end of a tie-line. The major requirement for this method to work was the presence of a connected tree whose line parameters were known.

A new problem was faced when the field data for a certain utility was observed to have missing or incomplete data or even garbage data at some places. This resulted in a disconnected tree. Chapter 4 of this thesis deals with that issue. A methodology was developed in this chapter which calibrates all the instrument transformers of a high voltage transmission network with the presence of only one good quality voltage measurement on a tie-line, as before. However, this method solves for different pi-sections, one at a time, and puts all the result together like a jigsaw puzzle. This *trick* circumvented the incomplete data or garbage data problem.

All the simulations for the methods proposed in this thesis were implemented using positive sequence measurements of the IEEE 118 and 300 bus networks. The relevant results obtained have been presented in the respective chapters.

5.2 *Future Scope of work*

Striving towards betterment and constant innovation is what research is all about. Just like any other avenue of research, the work on calibration can be further extended in new directions. An extension to the current work can be the simultaneous estimation of line parameters of the high

voltage transmission network. All the methods developed in this thesis have assumed the line parameters to be known quantities. But, in reality, due to age, weather conditions and various other factors, the actual parameters of the transmission lines can be different from the values mentioned in the datasheets. One such method, that estimates line parameters, has been discussed in [43]. This method, however needs pre-calibrated voltage and current measurements which may not be available in practice.

A new method can be developed which takes into account good voltage and current measurements at a tie-line in the presence of PMU errors and extend the methodologies developed in this thesis to calibrate the line parameters as well. In order to be able to do that, however, all the injections to the pi-sections must be known. Since utilities mostly monitor the injections into the high voltage network, it can be presumed that line-parameter estimation will be limited to the high voltage network. Work is currently being done in this direction and it is expected to come to fruition soon.

Though it is known that the quantization error is being introduced either in the PMUs or maybe in the phasor data concentrators (PDCs) and not the instrument transformers, its source is still under debate. One avenue of research could be the investigation of these quantization errors and figure out where they originate from. Finding out the source of these errors could be a significant find and could also potentially provide a solution to eradicate them.

Another direction in which this idea can be extended further is by considering three-phase measurements instead of positive sequence components. Although the computations will become more cumbersome, the logic will remain the same and therefore, its implementation can be expected to be done without much ado. Other channels of research which seem elusive as of now, may open up in future when other scholars and researchers work on this topic. Hopefully, the work done in this thesis explains the problem at hand and sets into motion wheels of thought that will drive power systems towards a brighter future.

REFERENCES

1. Wikipedia [Online]. Available: https://en.wikipedia.org/wiki/Northeast_blackout_of_1965
2. Friedlander, G. D., "What went wrong VIII: The Great Blackout of '65: Could the 'long night' happen again? What was learned from the dramatic six-state (plus Ontario) outage of November 9-10, 1965?" in *IEEE Spectrum*, vol.13, no.10, pp.83-88, Oct. 1976.
3. Schweppe, F. C., Wildes, J., "Power System Static-State Estimation, Part I: Exact Model", *IEEE Trans. Power App. Syst.*, vol. PAS-89, no. 1, Jan. 1970.
4. Phadke, A. G., Thorp, J. S., Adamiak, M. G., "A New Measurement Technique for Tracking Voltage Phasors, Local System Frequency, and Rate of Change of Frequency," in *IEEE Trans. Power App. Syst.*, vol.PAS-102, no.5, pp.1025-1038, May 1983.
5. Phadke, A. G., Thorp, J. S., "History and applications of Phasor Measurements", *IEEE PES Power systems conf. expo.*, pp. 331-335, 2006.
6. Phadke, A. G, Thorp, J. S., "Synchronized Phasor Measurements and Their Applications", January, 2008, New York: Springer
7. Zhou, M., Centeno, V. A., Thorp, J. S. and Phadke, A. G., "An alternative for including phasor measurements in state estimators," *IEEE Trans. Power Syst.*, vol. 21, no. 4, pp. 1930-1937, Nov. 2006.
8. Valverde, G., Chakrabarti, S., Kyriakides, E., and Terzija, V., "A constrained formulation for hybrid state estimation," *IEEE Trans. Power Syst.*, vol. 26, no. 3, pp. 1102-1109, Aug. 2011.
9. Costa, A. S., Albuquerque, A., and Bez, D., "An estimation fusion method for including phasor measurements into power system real-time modeling," *IEEE Trans. Power Syst.*, vol. 28, no. 2, pp. 1910-1920, May 2013.
10. Jones, K. D., Thorp, J. S., and Gardner, R. M., "Three-phase linear state estimation using phasor measurements," in *Proc. IEEE Power Eng. Soc. Gen. Meeting*, Vancouver, BC, Canada, pp. 1-5, 21-25 Jul. 2013.
11. Jones, K. D., Pal, A., and Thorp, J. S., "Methodology for performing synchrophasor data conditioning and validation," *IEEE Trans. Power Syst.*, vol. 30, no. 3, pp. 1121-1130, May 2015.
12. Gao, F., Thorp, J. S., Gao, S., Pal, A., and Vance, K. A., "A voltage phasor based fault classification method for phasor measurement unit only state estimator output," *Elect. Power Compon. Syst.*, vol. 43, no. 1, pp. 22-31, Jan. 2015.
13. Chatterjee, P., Pal, A., Thorp, J. S., De La Ree Lopez, J., "Partitioned Linear State Estimation", in *Proc. IEEE PES Innovative Smart Grid Technologies Conference (ISGT)*, Washington DC, pp. 1-5, 18-20 Feb., 2015.

14. Pal, A., and Thorp, J. S., "Co-ordinated control of inter-area oscillations using SMA and LMI," in *Proc. IEEE Power Eng. Soc. Conf. Innovative Smart Grid Technol.*, Washington D.C., pp. 1-6, 16-20 Jan. 2012.
15. Pal, A., Thorp, J. S., Veda, S. S., and Centeno, V. A., "Applying a robust control technique to damp low frequency oscillations in the WECC," *Int. J. Elect. Power Energy Syst.*, vol. 44, no. 1, pp. 638-645, Jan. 2013.
16. Vance, K., Pal, A., Thorp, J.S., "A robust control technique for damping inter-area oscillations", *IEEE Power and Energy conference*, Illinois, pp.1-8, 24-25 Feb, 2012.
17. Wang, T., Pal, A., Thorp, J.S., Wang, Z., Liu, J., Yang, Y., "Multi-Polytope-Based adaptive robust damping control in power systems using CART", *IEEE Transactions on Power Systems*, vol.30, no.4, July 2015.
18. Phadke, A. G., and Horowitz, S. H., "Adaptive Relaying", *IEEE Comput. Applicat. Power*, vol.3, issue.3, pp.47-51, July 1990.
19. Li, M., Pal, A., Phadke, A. G., and Thorp, J. S., "Transient stability prediction based on apparent impedance trajectory recorded by PMUs," *Int. J. Elect. Power Energy Syst.*, vol. 54, pp. 498-504, Jan. 2014.
20. Pal, A., Singh, I., and Bhargava, B., "Stress assessment in power systems and its visualization using synchrophasor based metrics," in *Proc. IEEE 2014 North American Power Symposium (NAPS)*, Pullman, WA, pp. 1-6, 7-9 Sep. 2014.
21. Gao, F., Thorp, J. S., Pal, A., and Gao, S., "Dynamic state prediction based on Auto-Regressive (AR) model using PMU data," in *Proc. IEEE Power and Energy Conference at Illinois (PECI)*, Champaign, IL, pp. 1-5, 24-25 Feb. 2012.
22. Federal Power Comm., "Northeast Power Failure: Nov. 9 and 10, 1965," 1965.
23. Bernabeu, E.E., Thorp, J.S., Centeno, V, "Methodology for a security/dependability adaptive protection scheme based on data mining", *IEEE Trans. Power Del.*, vol.27, no.1, pp.104-111, January 2012.
24. Pal, A., Thorp, J. S., Khan, T., Young, S. S., "Classification trees for complex synchrophasor data", *Elect. Power Compon. Syst.*, vol. 41, no. 14, pp. 1381-1396, Sep. 2013.
25. IEEE Standard Requirements for Instrument Transformers, IEEE Std. C57.13-2008, pp. c1-82, Jul. 2008.
26. Pal, A., "PMU-Based Applications for Improved Monitoring and Protection of Power Systems," Ph.D. Dissertation, Bradley Dept. Elect. Comput. Eng., Virginia Tech, Blacksburg, May. 2014.
27. IEEE 300 bus system diagram [Online]. Available: <http://al-roomi.org/power-flow/300-bus-system>

28. Huang, Z., Du, P., Kosterev, D., and Yang, S., "Generator dynamic model validation and parameter calibration using phasor measurements at the point of connection," *IEEE Trans. Power Syst.*, vol. 28, no. 2, pp. 1939-1949, May 2013.
29. Hajnoroozi, A. A., Aminifar, F., and Ayoubzadeh, H., "Generating unit model validation and calibration through synchrophasor measurements," *IEEE Trans. Smart Grid*, vol. 6, no. 1, pp. 441-449, Jan. 2015.
30. Zoltan, I., "Impedance synthesis [instrument transformer calibration]," in *Proc. 18th IEEE Instrum. Meas. Technology Conf.*, Budapest, Hungary, vol. 3, pp. 1872-1874, 21-23 May, 2001.
31. Brandolini, A., Faifer, M., and Ottoboni, R., "A simple method for the calibration of traditional and electronic measurement current and voltage transformers," *IEEE Trans. Instrum. Meas.*, vol. 58, no. 5, pp. 1345-1353, May 2009.
32. Hajnoroozi, A., A., Aminifar, F. and Ayoubzadeh, H., "Generating unit model validation and calibration through synchrophasor measurements," *IEEE Trans. Smart Grid*, vol. 6, no. 1, pp. 441-449, Jan. 2015.
33. Tang, Y., Stenbakken, G. N. and Goldstein, A., "Calibration of phasor measurement unit at NIST," *IEEE Trans. Instrum. Meas.*, vol. 62, no. 6, pp. 1417-1422, Jun. 2013.
34. Shi, D., Tylavsky, D. J., and Logic, N., "An adaptive method for detection and correction of errors in PMU measurements," *IEEE Trans. Smart Grid*, vol. 3, no. 4, pp. 1575-1583, Dec. 2012.
35. Braun, J-P., Seigenthaler, S., "Calibration of PMUs with a reference grade calibrator", *IEEE Conference on Precision Electromagnetic Measurements (CPEM)*, Rio de Janeiro, Brazil, pp.678-679, 24-29 Aug. 2014.
36. Zhou, M., Centeno, V. A., Thorp, J. S., and Phadke, A. G., "Calibrating instrument transformers with phasor measurements," *Elect. Power Comp. Syst.*, vol. 40, no. 14, pp. 1605-1620, Oct. 2012.
37. Chakraborty, A., and Martin, C. F., "Optimal Measurement Allocation Algorithms for Parametric Model Identification of Power Systems," *IEEE Trans. Control Syst. Technol.*, vol.22, no.5, pp.1801-1812, Sept. 2014.
38. Lafond, C., Kamwa, I., Prevost J., and Nadeau, M., "Coherence verification of transmission line parameters with PMU measurements at its ends", in *Proc. IEEE 28th Canadian Conference on Electrical and Computer Engineering (CCECE)*, Halifax, NS, pp.519-524, 3-6 May 2015.
39. Mousavi-seyedi, S.S.; Aminifar, F.; Afsharnia, S., "Parameter Estimation of Multiterminal Transmission Lines Using Joint PMU and SCADA Data," *IEEE Trans. Power Del.*, vol.30, no.3, pp.1077-1085, June 2015.

40. Shi, D., Tylavsky, D. J., and Logic, N., "An adaptive method for detection and correction of errors in PMU measurements," *IEEE Trans. Smart Grid*, vol. 3, no. 4, pp. 1575-1583, Dec. 2012.
41. Mishra, C., Pal, A., and Centeno, V. A., "Kalman-filter based recursive regression for three-phase line parameter estimation using phasor measurements," in *Proc. IEEE Power Eng. Soc. General Meeting*, Denver, CO, pp. 1-5, 26-30 Jul. 2015.
42. Wu, Z., et al., "Three-phase instrument transformer calibration with synchronized phasor measurements," in *Proc. IEEE PES Innovative Smart Grid Technologies (ISGT)*, Washington D.C., pp. 1-6, 16-20 Jan. 2012.
43. Wu, Z., Zora, L. T., and Phadke, A. G., "Simultaneous transmission line parameter and PMU measurement calibration," accepted for publication in *2015 IEEE Power Eng. Soc. Gen. Meeting*.
44. Wu, Z., "Synchronized phasor measurement applications in three-phase power systems," Ph.D. Dissertation, Bradley Dept. Elect. Comput. Eng., Virginia Tech, Blacksburg, Mar. 2013.
45. Pal, A., Chatterjee, P., Thorp, J. S., and Centeno, V. A., "On-line calibration of voltage transducers using synchrophasor measurements", accepted for publication in *IEEE Trans. Power Del.*
46. Martin, K.E., et al, "IEEE Standard for Synchrophasors for Power Systems," in *Power Delivery*, IEEE Transactions on , vol.13, no.1, pp.73-77, Jan 1998
47. Zimmerman, R. D., Murillo-Sánchez, C. E., and Thomas, R. J., "MATPOWER steady-state operations, planning and analysis tools for power systems research and education," *IEEE Trans. Power Syst.*, vol. 26, no. 1, pp. 12-19, Feb. 2011.
48. The MathWorks Inc., "MATLAB version 7.10.0," (computer software), Natick, MA, 2010.
49. GUROBI Optimization, Inc., "GUROBI Optimizer Reference Manual," Version 6.0.2, Houston, Texas, Feb. 2015. [Online]. Available: <http://www.gurobi.com>
50. Kester, W., "Taking the Mystery out of the Infamous Formula, "SNR = 6.02N + 1.76dB," and Why You Should Care", MT-001 Tutorial, Analog Devices [Online]. Available: <http://www.analog.com/media/en/training-seminars/tutorials/MT-001.pdf>

APPENDICES

This section comprises of all the pseudo codes that have generated for the execution of the algorithms developed for the purpose of this thesis. Appendix I shows the steps followed to apply the methodology generated in Chapter 3 for the high voltage networks of both the IEEE 118 and 300 bus systems in the presence of only one good quality measurement (placed at bus 10 for the 118 bus system and at bus 242 for the 300 bus system). These simulations can also be extended to include more than one good quality measurements to start with at different tie-lines.

Appendix II illustrates the MATLAB program written in order to apply the methodology developed in Chapter 4 for both the test systems used in this thesis. Similar to the first half of Appendix I, only one good quality measurement has been assumed for each high voltage network for the simulations done. All the simulations shown here can be modified according to the requirements of the networks the methodologies are being applied to. The examples shown here are merely provided to aid the reader's understanding.

Appendix A

MATLAB simulations for Chapter-3

IEEE-118 bus system with good quality measurement at bus 10 in the presence of a connected tree

```
%%%%%%%%%%%%%%%%%%%%%%%%%%%%%%%%%%%%%%%%%%%%%%%%%%%%%%%%%%%%%%%%%%%%%%%%
%
% Program Name: Instrument Transformer Calibration for IEEE-118 bus system
%               for the pi-sections 10-9-8-30-26
%
% Description:  Generating standard deviations of the errors in estimating
%               ratio errors in the high voltage network of the IEEE 118
%               bus system following the methodology developed in Ch-3
%
% Author: Paroma Chatterjee
%          Virginia Polytechnic Institute and State University
%
% Last Modified: 12/21/2015; 11:20 PM
%
%%%%%%%%%%%%%%%%%%%%%%%%%%%%%%%%%%%%%%%%%%%%%%%%%%%%%%%%%%%%%%%%%%%%%%%%

% IEEE-118 bus system: 10, 9, 8, 30, 26

clc
clear
close all

% Creating data to mimic field data

load Vraw12 % Loading load flow voltages
load Iraw12 % Loading currents = voltages * line impedances

load REV % Loading Ratio errors in voltages
load REI % Loading Ratio errors in currents

N = size(REV,1);
[m,1] = size(I);

disp('Choose Location of Good Measurement')
disp('Possible Choices: 10,26,63,81')
Inp = input('Your choice:');
if(Inp==10)
    n = 1;
end
if(Inp==26)
    n = 9;
end
if(Inp==63)
    n = 17;
```

```

end
if(Inp==81)
    n = 20;
end
REV1 = zeros(1,N);

for i=1:N
    REV(i,n,1) = (0.9985 + 0.003*rand)*exp(1i*0.2*(rand-0.5)*pi/180);
    % For comparison purposes
    REV1(i) = REV(i,n,1);
end

% Inserting errors in measurements

Vm = zeros(N,m,1);
Im = zeros(N,m,1);
for i=1:N
    for j=1:m
        for k=1:l
            Vm(i,j,k) = V(j,LOC(k,2))*REV(i,k,1); % Ratio errors present
        end
    end
    for j=1:m
        for k=1:l
            Im(i,j,k) = I(j,k)*REI(i,k,1); % Ratio errors present
        end
    end
end
end

% Quantizing data

q_V = 20/345000; % Changing it to per unit
q_I = 0.64*345000/100000000;
Vmqr = zeros(N,m,1);
Imqr = zeros(N,m,1);
for i=1:N
    Vt(:,i,:) = Vm(i,:,:);
    Vmqr = quant(real(Vt),q_V);
    Vmqi = quant(imag(Vt),q_V);
    Vmqr(i,:,:)= Vmqr + 1i*Vmqi;
    It(:,i,:) = Im(i,:,:);
    Imqr = quant(real(It),q_I);
    Imqi = quant(imag(It),q_I);
    Imqr(i,:,:)= Imqr + 1i*Imqi;
end

Vmtotal = Vmqr;
Imtotal = Imqr;

clear Vm Im

% Estimating ratio errors in the system

% Pi-sections under study

```

```

Bus = [10 9 8 30 26 ]; % Pi-sections under study: 10-9-8-30-26

Z = [ 0.00258 + 1i*0.0322    % Line 10-9
      0.00244 + 1i*0.0305    % Line 9-8
      0.00431 + 1i*0.0504    % Line 8-30
      0.00799 + 1i*0.0860 ]; % Line 30-26

B = 1i*[ 1.230/2    % Line 10-9
         1.162/2    % Line 9-8
         0.514/2    % Line 8-30
         0.908/2 ]; % Line 30-26

order = [1,2,3,4,5,6,7,9];
l = length(order);
num_pie = length(Bus) - 1;
W = 1 + Z.*B; % W=1+ZB for different pie-sections

REVm = zeros(N,length(order));
REVe = zeros(N,length(order));

REVold = zeros(N,1);

REIm = zeros(N,length(order));
REIe = zeros(N,length(order));

for i=1:N
    Vm(:,i) = Vmtotal(i,order);
    Im(:,i) = Imtotal(i,order);

    REVm(i,1) = REV1(i);
    REVe(i,1) = REV1(i);
    REVold(i) = REV1(i);

% Estimation of ratio errors

for j = 1:num_pie-1;

    B0 = Vm(:,(2*j-1):(2*j));
    A = Im(:,(2*j-1):(2*j));
    X = lscov(A,B0);
% AX = B; IZ = V; Z = lscov(I,V); X = lscov(A,B) = [ao b0; c0 d0]

    REIm(i,(2*j-1)) = (REVold(i)*W(j,1))/(X(1,1)*B(j,1)*(W(j,1)+1));
% REIpq = (REVpq/a0)*(W/(B*(W+1)))
    REIm(i,2*j) = (REVold(i))/(X(2,1)*B(j,1)*(W(j,1)+1));
%REIqp = (REVpq/c0)*(1/(B*(W+1)))

    REVm(i,(2*j)) = REVold(i)*W(j,1)*X(1,2)/X(1,1);
% REVqp = (b0/a0)*REVpq*W
    REVm(i,(2*j+1)) = REVm(i,(2*j))*median(Vm(:,(2*j)+1)./Vm(:,(2*j)));
% REVqr = REVqp*gamma = REVqp*(Vqr(measured)/Vqp(measured))

    REIe(i,(2*j-1)) = REI(i,order(2*j-1),1)-REIm(i,(2*j-1));
% REIpq(difference) = REIpq(original)-REIpq(calculated)

```

```

REIE(i,2*j) = REI(i,order(2*j),1)-REIm(i,2*j);

REVe(i,(2*j)) = REV(i,order(2*j),1)-REVm(i,(2*j));
% REVqp(difference) = REVqp(original)-REVqp(calculated)
REVe(i,(2*j+1)) = REV(i,order(2*j+1),1)-REVm(i,(2*j+1));

REVold(i) = REVm(i,(2*j+1));

end

for j=num_pie

    B1 = Vm(:,(2*j)-1:(2*j));
    A1 = Im(:,(2*j)-1:(2*j));
    X1 = lscov(A1,B1);
% AX = B; IZ = V; Z = lscov(I,V); X = lscov(A,B) = [a0 b0; c0 d0]

    REIm(i,(2*j-1)) = (REVold(i)*W(j,1))/(X1(1,1)*B(j,1)*(W(j,1)+1));
% REIqp = (REVpq/a0)*(W/(B*(W+1)))
    REIm(i,2*j) = (REVold(i))/(X1(2,1)*B(j,1)*(W(j,1)+1));
%REIqp = (REVpq/c0)*(1/(B*(W+1)))

    REVm(i,(2*j)) = REVold(i)*W(j,1)*X1(1,2)/X1(1,1);
% REVqp = (b0/a0)*REVpq*W

    REIE(i,(2*j-1)) = REI(i,order(2*j-1),1)-REIm(i,(2*j-1));
% REIqp(difference) = REIqp(original)-REIqp(calculated)
    REIE(i,2*j) = REI(i,order(2*j),1)-REIm(i,2*j);

    REVe(i,(2*j)) = REV(i,order(2*j),1)-REVm(i,(2*j));
% REVqp(difference) = REVqp(original)-REVqp(calculated)

end

end

VoltSTD = [(std(REV1,0,2)) % Standard deviation for the "good" measurement
std(REV21,0,2) % Standard deviation at the end of first Pi-section
std(REV23,0,2) % Standard deviation at the start of second Pi-section
std(REV32,0,2) % Standard deviation at the end of second Pi-section
std(REV34,0,2) % Standard deviation at the start of third Pi-section
std(REV43,0,2) % Standard deviation at the end of third Pi-section
std(REV45,0,2) % Standard deviation at the start of fourth Pi-section
std(REV54,0,2)]; % Standard deviation at the end of fourth Pi-section

CurrSTD = [std(REI12,0,2) % Standard deviation for the "good" measurement
std(REI21,0,2) % Standard deviation at the end of first Pi-section
std(REI23,0,2) % Standard deviation at the start of second Pi-section
std(REI32,0,2) % Standard deviation at the end of second Pi-section
std(REI34,0,2) % Standard deviation at the start of third Pi-section
std(REI43,0,2) % Standard deviation at the end of third Pi-section
std(REI45,0,2) % Standard deviation at the start of fourth Pi-section
std(REI54,0,2)]; % Standard deviation at the end of fourth Pi-section

```

IEEE-300 bus system with good quality measurement at bus 242 in the presence of a connected tree

```
%%%%%%%%%%%%%%%%%%%%%%%%%%%%%%%%%%%%%%%%%%%%%%%%%%%%%%%%%%%%%%%%%%%%%%%%%%%%%%
%
% Program Name: Instrument Transformer Calibration for IEEE-300 bus system
%               for the pi-sections 242-173-198-216-210-169
%
% Description:  Generating standard deviations of the errors in estimating
%               ratio errors in the high voltage network of the IEEE 300
%               bus system with only one good quality measurement available
%               at bus 242 following the methodology described in Ch-3
%
% Author: Paroma Chatterjee
%          Virginia Polytechnic Institute and State University
%
% Last Modified: 12/21/2015; 11:30 PM
%%%%%%%%%%%%%%%%%%%%%%%%%%%%%%%%%%%%%%%%%%%%%%%%%%%%%%%%%%%%%%%%%%%%%%%%%%%%%%

% IEEE-300 bus system: 242, 173, 198, 216, 210, 169

clc
clear
close all

load V
load IL

V = downsample(V,200);
I = downsample(IL,200);

load REV
load REI

N = size(REV,1);
[m,1] = size(I);

disp('Choose Location of Good Measurement')
disp('Possible Choices: 4,190,664')
Inp = input('Your choice:');

if(Inp==4)
    n = 1;
end
if(Inp==190)
    n = 28;
end
if(Inp==664)
    n = 18;
end
```

```

REV1 = zeros(1,N);

for i=1:N
    REV(i,n,1) = (0.9985 + 0.003*rand)*exp(1i*0.2*(rand-0.5)*pi/180);
    % For comparison purposes
    REV1(i) = REV(i,n,1);
end

% Inserting errors in measurements
Vm = zeros(N,m,1);
Im = zeros(N,m,1);

for i=1:N
    for j=1:m
        for k=1:l
            Vm(i,j,k) = V(j,LOC(k,2))*REV(i,k,1); % Only Ratio errors present
        end
    end
    for j=1:m
        for k=1:l
            Im(i,j,k) = I(j,k)*REI(i,k,1); % Only Ratio errors present
        end
    end
end

% Quantizing data
q_V = 20/345000;
q_I = 0.64*345000/100000000;
Vmqr = zeros(N,m,1);
Imqr = zeros(N,m,1);
for i=1:N
    Vt(:,i,:) = Vm(i,:,:);
    Vmqr = quant(real(Vt),q_V);
    Vmqi = quant(imag(Vt),q_V);
    Vmqr(i,:,:)= Vmqr + 1i*Vmqi;
    It(:,i,:) = Im(i,:,:);
    Imqr = quant(real(It),q_I);
    Imqi = quant(imag(It),q_I);
    Imqr(i,:,:)= Imqr + 1i*Imqi;
end

Vmtotal = Vmqr;
Imtotal = Imqr;

clear Vm Im

% Pi-section under study
Bus = [664 194 219 237 231 190]; % Pi-section under study: 664-194-219-237-
231-190
Z = [ 0.0024 + 1i*0.0355 % Line 664-194
      0.0031 + 1i*0.0286 % Line 194-219
      0.0003 + 1i*0.0018 % Line 219-237
      0.0001 + 1i*0.0006 % Line 237-231
      0.0004 + 1i*0.0022 ]; % Line 231-190

```

```

B = 1i*[ 0.360/2      % Line 664-194
         0.500/2      % Line 194-219
         5.200/2      % Line 219-237
         3.570/2      % Line 237-231
         6.200/2 ]; % Line 231-190
order = [18,17,16,21,23,24,25,26,27,28];
l = length(order);
num_pie = length(Bus) - 1;
W = 1 + Z.*B; % W=1+ZB for different Pi-sections

for i=1:N
    Vm(1:m,:) = Vmtotal(i,1:m,order);
    Im(1:m,:) = Imtotal(i,1:m,order);

    % Estimation of ratio errors

    j = 1; % First Pi-section

    B1 = Vm(:,(2*j)-1:(2*j));
    A1 = Im(:,(2*j)-1:(2*j));
    X1 = lscov(A1,B1);

    REIm12(i) = (REV1(i)*W(1,1))/(X1(1,1)*B(1,1)*(W(1,1)+1));
    REIm21(i) = (REV1(i))/(X1(2,1)*B(1,1)*(W(1,1)+1));

    REVm21(i) = REV1(i)*W(1,1)*X1(1,2)/X1(1,1);
    REVm23(i) = REVm21(i)*median(Vm(:,(2*j)+1)./Vm(:,(2*j)));

    REI12(i) = REI(i,order(2*j-1),1)-REIm12(i);
    REI21(i) = REI(i,order(2*j),1)-REIm21(i);

    REV21(i) = REV(i,order(2*j),1)-REVm21(i);
    REV23(i) = REV(i,order(2*j+1),1)-REVm23(i);

    j = 2; % Second Pi-section

    B2 = Vm(:,(2*j)-1:(2*j));
    A2 = Im(:,(2*j)-1:(2*j));
    X2 = lscov(A2,B2);

    REIm23(i) = (REVm23(i)*W(2,1))/(X2(1,1)*B(2,1)*(W(2,1)+1));
    REIm32(i) = (REVm23(i))/(X2(2,1)*B(2,1)*(W(2,1)+1));

    REVm32(i) = REVm23(i)*W(2,1)*X2(1,2)/X2(1,1);
    REVm34(i) = REVm32(i)*median(Vm(:,(2*j)+1)./Vm(:,(2*j)));

    REI23(i) = REI(i,order(2*j-1),1)-REIm23(i);
    REI32(i) = REI(i,order(2*j),1)-REIm32(i);

    REV32(i) = REV(i,order(2*j),1)-REVm32(i);
    REV34(i) = REV(i,order(2*j+1),1)-REVm34(i);

    j = 3; % Third Pi-section

```



```

B3 = Vm(:, (2*j)-1:(2*j));
A3 = Im(:, (2*j)-1:(2*j));
X3 = lscov(A3,B3);

REIm34(i) = (REVm34(i)*W(3,1))/(X3(1,1)*B(3,1)*(W(3,1)+1));
REIm43(i) = (REVm34(i))/(X3(2,1)*B(3,1)*(W(3,1)+1));

REVm43(i) = REVm34(i)*W(3,1)*X3(1,2)/X3(1,1);
REVm45(i) = REVm43(i)*median(Vm(:, (2*j)+1)./Vm(:, (2*j)));

REI34(i) = REI(i,order(2*j-1),1)-REIm34(i);
REI43(i) = REI(i,order(2*j),1)-REIm43(i);

REV43(i) = REV(i,order(2*j),1)-REVm43(i);
REV45(i) = REV(i,order(2*j+1),1)-REVm45(i);

j = 4; % Fourth Pi-section

B4 = Vm(:, (2*j)-1:(2*j));
A4 = Im(:, (2*j)-1:(2*j));
X4 = lscov(A4,B4);

REIm45(i) = (REVm45(i)*W(4,1))/(X4(1,1)*B(4,1)*(W(4,1)+1));
REIm54(i) = (REVm45(i))/(X4(2,1)*B(4,1)*(W(4,1)+1));

REVm54(i) = REVm45(i)*W(4,1)*X4(1,2)/X4(1,1);
REVm56(i) = REVm54(i)*median(Vm(:, (2*j)+1)./Vm(:, (2*j)));

REI45(i) = REI(i,order(2*j-1),1)-REIm45(i);
REI54(i) = REI(i,order(2*j),1)-REIm54(i);

REV54(i) = REV(i,order(2*j),1)-REVm54(i);
REV56(i) = REV(i,order(2*j+1),1)-REVm56(i);

j = 5; % Fifth Pi-section

B5 = Vm(:, (2*j)-1:(2*j));
A5 = Im(:, (2*j)-1:(2*j));
X5 = lscov(A5,B5);

REIm56(i) = (REVm56(i)*W(5,1))/(X5(1,1)*B(5,1)*(W(5,1)+1));
REIm65(i) = (REVm56(i))/(X5(2,1)*B(5,1)*(W(5,1)+1));

REVm65(i) = REVm56(i)*W(5,1)*X5(1,2)/X5(1,1);

REI56(i) = REI(i,order(2*j-1),1)-REIm56(i);
REI65(i) = REI(i,order(2*j),1)-REIm65(i);

REV65(i) = REV(i,order(2*j),1)-REVm65(i);

```

end

```
VoltSTD = [(std(REV1,0,2)) % Standard deviation for the "good" measurement
```

```

std(REV21,0,2) % Standard deviation at the end of first Pi-section
std(REV23,0,2) % Standard deviation at the start of second Pi-section
std(REV32,0,2) % Standard deviation at the end of second Pi-section
std(REV34,0,2) % Standard deviation at the start of third Pi-section
std(REV43,0,2) % Standard deviation at the end of third Pi-section
std(REV45,0,2) % Standard deviation at the start of fourth Pi-section
std(REV54,0,2) % Standard deviation at the end of fourth Pi-section
std(REV56,0,2) % Standard deviation at the start of fifth Pi-section
std(REV65,0,2)]; % Standard deviation at the end of fifth Pi-section

CurrSTD = [std(REI12,0,2) % Standard deviation for the "good" measurement
std(REI21,0,2) % Standard deviation at the end of first Pi-section
std(REI23,0,2) % Standard deviation at the start of second Pi-section
std(REI32,0,2) % Standard deviation at the end of second Pi-section
std(REI34,0,2) % Standard deviation at the start of third Pi-section
std(REI43,0,2) % Standard deviation at the end of third Pi-section
std(REI45,0,2) % Standard deviation at the start of fourth Pi-section
std(REI54,0,2) % Standard deviation at the end of fourth Pi-section
std(REI56,0,2) % Standard deviation at the start of fifth Pi-section
std(REI65,0,2)]; % Standard deviation at the end of fifth Pi-section

```

Appendix B

MATLAB simulations for Chapter-4

IEEE-118 bus system with a good quality measurement at bus 10 in the absence of a connected tree

```
%%%%%%%%%%%%%%%%%%%%%%%%%%%%%%%%%%%%%%%%%%%%%%%%%%%%%%%%%%%%%%%%%%%%%%%%%
%
% Program Name: Instrument Transformer Calibration for IEEE-118 bus system
%
% Description: Generating standard deviations of the errors in estimating
%              ratio errors in the high voltage network of the IEEE 118
%              bus system with only one good quality measurement available
%              at bus 10 following the methodology described in Ch-4
%
% Author: Paroma Chatterjee
%         Virginia Polytechnic Institute and State University
%
% Last Modified: 12/21/2015; 11:45 PM
%
%%%%%%%%%%%%%%%%%%%%%%%%%%%%%%%%%%%%%%%%%%%%%%%%%%%%%%%%%%%%%%%%%%%%%%%%%

clc
clear
close all

% Initial data input
load IL
load V
load REV
load REI

T = 1000; % No of times the simulation is run

RREVm = zeros(T,r/ds,1); % Ratio of ratio errors of voltages
RREVmMean = zeros(T,1); % Mean of the ratio of ratio errors of voltages
Vmeas = zeros(T,r/ds,1);
RREIm = zeros(T,r/ds,1); % Ratio of ratio errors of currents
RREImMean = zeros(T,1); % Mean of the ratio of ratio errors of currents

for f = 1:T
    for i = 1:r/ds
        for j = 1:ds
            for k = 1:l
                Vm(i,j,k) = V(i,j,k)*REV(f,k);
% Introducing the ratio errors in voltages
                Im(i,j,k) = IL(i,j,k)*REI(f,k);
% Introducing the ratio errors in currents
            end
        end
    end
end
```

```

% Introducing Quantization Errors
q_V = 20/345000; % Changing it to per unit
q_I = 0.64*345000/100000000; % Changing it to per unit
Vmqr = zeros(r/ds,ds,1);
Imqr = zeros(r/ds,ds,1);
for i=1:r/ds
    Vt(:, :) = Vm(i, :, :);
    Vmqr = quant(real(Vt), q_V);
    Vmqi = quant(imag(Vt), q_V);
    Vmq(i, :, :) = Vmqr + 1i*Vmqi; % Quantized voltages
    It(:, :) = Im(i, :, :);
    Imqr = quant(real(It), q_I);
    Imqi = quant(imag(It), q_I);
    Imq(i, :, :) = Imqr + 1i*Imqi; % Quantized currents
end

Vnew = Vmq;
Inew = Imq;

% Creating data to resemble that obtained from the field
for i = 1:r/ds
    j = randi([1 ds], ds/2, 1);
    k = randi([1 l], l/2, 1);
    for n = 1:length(j)
        for m = 1:length(k)
            Vnew(i, j(n), k(m)) = NaN;
            Inew(i, j(n), k(m)) = NaN;
        end
    end
end

% Creating matrices having ones in the places where data is available and
zeros for NaNs
Avol = isfinite(Vnew);
Acurr = isfinite(Inew);

for i = 1:r/ds

    % Solving for 1st Pi section: 10-9
    count = 0;
    count1 = 0;
    for j = 1:ds
        if Avol(i, j, 1) == 0
            count = count+1;
        end
        if Acurr(i, j, 2) == 0
            count1 = count1+1;
        end
    end
    if count == 0
        if count1==0
            B0(:, :) = [conj(Vnew(i, :, 1))' conj(Vnew(i, :, 2))'];
            A0(:, :) = [conj(Inew(i, :, 1))' conj(Inew(i, :, 2))'];
            X = lscov(A0, B0);
        end
    end
end
% AX = B; IZ = V; Z = lscov(I, V); X = lscov(A, B) = [ao b0; c0 d0]

```

```

RREIm(f,i,1) = W(1,1)/(X(1,1)*b(1,1)*(W(1,1)+1));
% REIpq/REVpq = (1/a0)*(W/(B*(W+1)))
RREIm(f,i,2) = 1/(X(2,1)*b(1,1)*(W(1,1)+1));
% REIqp/REVpq = (1/c0)*(1/(B*(W+1)))
RREVm(f,i,2) = W(1,1)*X(1,2)/X(1,1);
% REVqp/REVpq = (b0/a0)*W
Vmeas(f,i,2) = mean(Vnew(i,:,2));
end
end

% Solving for 2nd Pi section: 9-8
count = 0;
count1 = 0;
for j = 1:ds
    if Avol(i,j,3) == 0
        count = count+1;
    end
    if Avol(i,j,4) == 0
        count1 = count1+1;
    end
end
if count == 0
    if count1 == 0
        B0(:, :) = [conj(Vnew(i,:,3))' conj(Vnew(i,:,4))'];
        A0(:, :) = [conj(Inew(i,:,3))' conj(Inew(i,:,4))'];
        X = lscov(A0,B0);
% AX = B; IZ = V; Z = lscov(I,V); X = lscov(A,B) = [ao b0; c0 d0]
RREIm(f,i,3) = W(2,1)/(X(1,1)*b(2,1)*(W(2,1)+1));
% REIpq/REVpq = (1/a0)*(W/(B*(W+1)))
RREIm(f,i,4) = 1/(X(2,1)*b(2,1)*(W(2,1)+1));
% REIqp/REVpq = (1/c0)*(1/(B*(W+1)))
Vmeas(f,i,3) = mean(Vnew(i,:,3));
% Saving the mean voltage
Vmeas(f,i,4) = mean(Vnew(i,:,4));
% Saving the mean voltage
RREVm(f,i,4) = W(2,1)*X(1,2)/X(1,1);
% REVqp/REVpq = (b0/a0)*W
end
end

% Solving for 3rd Pi section: 8-30
count = 0;
count1 = 0;
for j = 1:ds
    if Avol(i,j,5) == 0
        count = count+1;
    end
    if Avol(i,j,6) == 0
        count1 = count1+1;
    end
end
if count == 0
    if count1 == 0
        B0(:, :) = [conj(Vnew(i,:,5))' conj(Vnew(i,:,6))'];
        A0(:, :) = [conj(Inew(i,:,5))' conj(Inew(i,:,6))'];
        X = lscov(A0,B0);

```

```

% AX = B; IZ = V; Z = lscov(I,V); X = lscov(A,B) = [ao b0; c0 d0]
    RREIm(f,i,5) = W(3,1)/(X(1,1)*b(3,1)*(W(3,1)+1));
% REIpq/REVpq = (1/a0)*(W/(B*(W+1)))
    RREIm(f,i,6) = 1/(X(2,1)*b(3,1)*(W(3,1)+1));
%REIqp/REVpq = (1/c0)*(1/(B*(W+1)))
    Vmeas(f,i,5) = mean(Vnew(i,:,5));
% Saving the mean voltage
    Vmeas(f,i,6) = mean(Vnew(i,:,6));
% Saving the mean voltage
    RREVm(f,i,6) = W(3,1)*X(1,2)/X(1,1);
% REVqp/REVpq = (b0/a0)*W
    end
end

% Solving for 4th Pi section: 30-26
count = 0;
count1 = 0;
for j = 1:ds
    if Avol(i,j,7) == 0
        count = count+1;
    end
    if Avol(i,j,9) == 0
        count1 = count1+1;
    end
end
if count == 0
    if count1 ==0
        B0(:, :) = [conj(Vnew(i,:,7))' conj(Vnew(i,:,9))'];
        A0(:, :) = [conj(Inew(i,:,7))' conj(Inew(i,:,9))'];
        X = lscov(A0,B0);
% AX = B; IZ = V; Z = lscov(I,V); X = lscov(A,B) = [ao b0; c0 d0]
    RREIm(f,i,7) = W(4,1)/(X(1,1)*b(4,1)*(W(4,1)+1));
% REIpq/REVpq = (1/a0)*(W/(B*(W+1)))
    RREIm(f,i,9) = 1/(X(2,1)*b(4,1)*(W(4,1)+1));
% REIqp/REVpq = (1/c0)*(1/(B*(W+1)))
    Vmeas(f,i,7) = mean(Vnew(i,:,7));
% Saving the mean voltage
    Vmeas(f,i,9) = mean(Vnew(i,:,9));
% Saving the mean voltage
    RREVm(f,i,9) = W(4,1)*X(1,2)/X(1,1);
% REVqp/REVpq = (b0/a0)*W
    end
end

% Solving for 5th Pi section 30-38
count = 0;
count1 = 0;
for j = 1:ds
    if Avol(i,j,8) == 0
        count = count+1;
    end
    if Avol(i,j,10) == 0
        count1 = count1+1;
    end
end
if count == 0

```

```

        if count1 == 0
            B0(:, :) = [conj(Vnew(i, :, 8))' conj(Vnew(i, :, 10))'];
            A0(:, :) = [conj(Inew(i, :, 8))' conj(Inew(i, :, 10))'];
            X = lscov(A0, B0);
% AX = B; IZ = V; Z = lscov(I, V); X = lscov(A, B) = [ao b0; c0 d0]
            RREIm(f, i, 8) = W(5, 1) / (X(1, 1) * b(5, 1) * (W(5, 1) + 1));
% REIpq/REVpq = (1/a0) * (W / (B * (W + 1)))
            RREIm(f, i, 10) = 1 / (X(2, 1) * b(5, 1) * (W(5, 1) + 1));
% REIqp/REVpq = (1/c0) * (1 / (B * (W + 1)))
            Vmeas(f, i, 8) = mean(Vnew(i, :, 8));
% Saving the mean voltage
            Vmeas(f, i, 10) = mean(Vnew(i, :, 10));
% Saving the mean voltage
            RREVM(f, i, 10) = W(5, 1) * X(1, 2) / X(1, 1);
% REVqp/REVpq = (b0/a0) * W
        end
    end

% Solving for 6th Pi section: 38-65
count = 0;
count1 = 0;
for j = 1:ds
    if Avol(i, j, 11) == 0
        count = count + 1;
    end
    if Avol(i, j, 12) == 0
        count1 = count1 + 1;
    end
end
if count == 0
    if count1 == 0
        B0(:, :) = [conj(Vnew(i, :, 11))' conj(Vnew(i, :, 12))'];
        A0(:, :) = [conj(Inew(i, :, 11))' conj(Inew(i, :, 12))'];
        X = lscov(A0, B0);
% AX = B; IZ = V; Z = lscov(I, V); X = lscov(A, B) = [ao b0; c0 d0]
        RREIm(f, i, 11) = W(6, 1) / (X(1, 1) * b(6, 1) * (W(6, 1) + 1));
% REIpq/REVpq = (1/a0) * (W / (B * (W + 1)))
        RREIm(f, i, 12) = 1 / (X(2, 1) * b(6, 1) * (W(6, 1) + 1));
% REIqp/REVpq = (1/c0) * (1 / (B * (W + 1)))
        Vmeas(f, i, 11) = mean(Vnew(i, :, 11));
% Saving the mean voltage
        Vmeas(f, i, 12) = mean(Vnew(i, :, 12));
% Saving the mean voltage
        RREVM(f, i, 12) = W(6, 1) * X(1, 2) / X(1, 1);
% REVqp/REVpq = (b0/a0) * W
    end
end

% Solving for 7th Pi section: 65-64
count = 0;
count1 = 0;
for j = 1:ds
    if Avol(i, j, 13) == 0
        count = count + 1;
    end
    if Avol(i, j, 15) == 0

```

```

        count1 = count1+1;
    end
end
if count == 0
    if count1 == 0
        B0(:, :) = [conj(Vnew(i, :, 13))' conj(Vnew(i, :, 15))'];
        A0(:, :) = [conj(Inew(i, :, 13))' conj(Inew(i, :, 15))'];
        X = lscov(A0, B0);
% AX = B; IZ = V; Z = lscov(I, V); X = lscov(A, B) = [ao b0; c0 d0]
        RREIm(f, i, 13) = W(7, 1) / (X(1, 1) * b(7, 1) * (W(7, 1) + 1));
% REIpq/REVpq = (1/a0) * (W / (B * (W + 1)))
        RREIm(f, i, 15) = 1 / (X(2, 1) * b(7, 1) * (W(7, 1) + 1));
% REIqp/REVpq = (1/c0) * (1 / (B * (W + 1)))
        Vmeas(f, i, 13) = mean(Vnew(i, :, 13));
% Saving the mean voltage
        Vmeas(f, i, 15) = mean(Vnew(i, :, 15));
% Saving the mean voltage
        RREVm(f, i, 15) = W(7, 1) * X(1, 2) / X(1, 1);
% REVqp/REVpq = (b0/a0) * W
    end
end

% Solving for 8th Pi section: 64-63
count = 0;
count1 = 0;
for j = 1:ds
    if Avol(i, j, 16) == 0
        count = count+1;
    end
    if Avol(i, j, 17) == 0
        count1 = count1+1;
    end
end
if count == 0
    if count1 == 0
        B0(:, :) = [conj(Vnew(i, :, 16))' conj(Vnew(i, :, 17))'];
        A0(:, :) = [conj(Inew(i, :, 16))' conj(Inew(i, :, 17))'];
        X = lscov(A0, B0);
% AX = B; IZ = V; Z = lscov(I, V); X = lscov(A, B) = [ao b0; c0 d0]
        RREIm(f, i, 16) = W(8, 1) / (X(1, 1) * b(8, 1) * (W(8, 1) + 1));
% REIpq/REVpq = (1/a0) * (W / (B * (W + 1)))
        RREIm(f, i, 17) = 1 / (X(2, 1) * b(8, 1) * (W(8, 1) + 1));
% REIqp/REVpq = (1/c0) * (1 / (B * (W + 1)))
        Vmeas(f, i, 16) = mean(Vnew(i, :, 16));
% Saving the mean voltage
        Vmeas(f, i, 17) = mean(Vnew(i, :, 17));
% Saving the mean voltage
        RREVm(f, i, 17) = W(8, 1) * X(1, 2) / X(1, 1);
% REVqp/REVpq = (b0/a0) * W
    end
end

% Solving for 9th Pi section 65-68
count = 0;
count1 = 0;
for j = 1:ds

```



```

        if Avol(i,j,14) == 0
            count = count+1;
        end
        if Avol(i,j,18) == 0
            count1 = count1+1;
        end
    end
    if count == 0
        if count1 == 0
            B0(:, :) = [conj(Vnew(i, :, 14))' conj(Vnew(i, :, 18))'];
            A0(:, :) = [conj(Inew(i, :, 14))' conj(Inew(i, :, 18))'];
            X = lscov(A0, B0);
% AX = B; IZ = V; Z = lscov(I, V); X = lscov(A, B) = [ao b0; c0 d0]
            RREIm(f, i, 14) = W(9, 1) / (X(1, 1) * b(9, 1) * (W(9, 1) + 1));
% REIpq/REVpq = (1/a0) * (W / (B * (W + 1)))
            RREIm(f, i, 18) = 1 / (X(2, 1) * b(9, 1) * (W(9, 1) + 1));
% REIqp/REVpq = (1/c0) * (1 / (B * (W + 1)))
            Vmeas(f, i, 14) = mean(Vnew(i, :, 14));
% Saving the mean voltage
            Vmeas(f, i, 18) = mean(Vnew(i, :, 18));
% Saving the mean voltage
            RREVM(f, i, 18) = W(9, 1) * X(1, 2) / X(1, 1);
% REVqp/REVpq = (b0/a0) * W
        end
    end

% Solving for 10th Pi section: 68-81
count = 0;
count1 = 0;
for j = 1:ds
    if Avol(i, j, 19) == 0
        count = count+1;
    end
    if Avol(i, j, 20) == 0
        count1 = count1+1;
    end
end
if count == 0
    if count1 == 0
        B0(:, :) = [conj(Vnew(i, :, 19))' conj(Vnew(i, :, 20))'];
        A0(:, :) = [conj(Inew(i, :, 19))' conj(Inew(i, :, 20))'];
        X = lscov(A0, B0);
% AX = B; IZ = V; Z = lscov(I, V); X = lscov(A, B) = [ao b0; c0 d0]
        RREIm(f, i, 19) = W(10, 1) / (X(1, 1) * b(10, 1) * (W(10, 1) + 1));
% REIpq/REVpq = (1/a0) * (W / (B * (W + 1)))
        RREIm(f, i, 20) = 1 / (X(2, 1) * b(10, 1) * (W(10, 1) + 1));
% REIqp/REVpq = (1/c0) * (1 / (B * (W + 1)))
        Vmeas(f, i, 19) = mean(Vnew(i, :, 19));
% Saving the mean voltage
        Vmeas(f, i, 20) = mean(Vnew(i, :, 20));
% Saving the mean voltage
        RREVM(f, i, 20) = W(10, 1) * X(1, 2) / X(1, 1);
% REVqp/REVpq = (b0/a0) * W
    end
end
end

```

```

end

RREVMold = RREVM;
RREImold = RREIm;

DummyV(:, :) = abs(RREVM(f, :, :));
DummyC(:, :) = abs(RREIm(f, :, :));
for j=1:r/ds
    for k = 1:l
        if DummyV(j, k)==0
            RREVM(f, j, k) = NaN;
        end
        if DummyC(j, k)==0
            RREIm(f, j, k) = NaN;
        end
    end
end
end
RREVMMean(f, :) = nanmean(RREVM(f, :, :));
RREImMean(f, :) = nanmean(RREIm(f, :, :));
clear DummyV DummyC

% 1st Pi section: 10-9: Everything remains the same

% 2nd Pi section: 9-8

% Voltage Ratio Errors
RREVMMean(f, 3) =
RREVMMean(f, 2) * ( (sum(Vmeas(f, :, 3) ./sum(Vmeas(f, :, 3)~=0)) ) / (sum(Vmeas(f, :, 2) ./
sum(Vmeas(f, :, 2)~=0)) ) );
RREVMMean(f, 4) = RREVMMean(f, 4) *RREVMMean(f, 3);
% Current Ratio Errors
RREImMean(f, 3) = RREVMMean(f, 3) *RREImMean(f, 3);
RREImMean(f, 4) = RREVMMean(f, 3) *RREImMean(f, 4);

% 3rd Pi section: 8-30

% Voltage Ratio Errors
RREVMMean(f, 5) =
RREVMMean(f, 4) * (sum(Vmeas(f, :, 5) ./sum(Vmeas(f, :, 5)~=0)) ) / (sum(Vmeas(f, :, 4) ./s
um(Vmeas(f, :, 4)~=0)) ) );
RREVMMean(f, 6) = RREVMMean(f, 6) *RREVMMean(f, 5);
% Current Ratio Errors
RREImMean(f, 5) = RREVMMean(f, 5) *RREImMean(f, 5);
RREImMean(f, 6) = RREVMMean(f, 5) *RREImMean(f, 6);

% 4th Pi section: 30-26

% Voltage Ratio Errors
RREVMMean(f, 7) =
RREVMMean(f, 6) * (sum(Vmeas(f, :, 7) ./sum(Vmeas(f, :, 7)~=0)) ) / (sum(Vmeas(f, :, 6) ./s
um(Vmeas(f, :, 6)~=0)) ) );
RREVMMean(f, 9) = RREVMMean(f, 9) *RREVMMean(f, 7);
% Current Ratio Errors
RREImMean(f, 7) = RREVMMean(f, 7) *RREImMean(f, 7);
RREImMean(f, 9) = RREVMMean(f, 7) *RREImMean(f, 9);

```

```

% 5th Pi section: 30-38

% Voltage Ratio Errors
RREVMean(f,8) =
RREVMean(f,6)*(sum(Vmeas(f,:,8)./sum(Vmeas(f,:,8)~=0)))/(sum(Vmeas(f,:,6)./sum(Vmeas(f,:,6)~=0)));
RREVMean(f,10) = RREVMean(f,10)*RREVMean(f,8);
% Current Ratio Errors
RREIMean(f,8) = RREVMean(f,8)*RREIMean(f,8);
RREIMean(f,10) = RREVMean(f,8)*RREIMean(f,10);

% 6th Pi section: 38-65

% Voltage Ratio Errors
RREVMean(f,11) =
RREVMean(f,10)*(sum(Vmeas(f,:,11)./sum(Vmeas(f,:,11)~=0)))/(sum(Vmeas(f,:,10)./sum(Vmeas(f,:,10)~=0)));
RREVMean(f,12) = RREVMean(f,12)*RREVMean(f,11);
% Current Ratio Errors
RREIMean(f,11) = RREVMean(f,11)*RREIMean(f,11);
RREIMean(f,12) = RREVMean(f,11)*RREIMean(f,12);

% 7th Pi section: 65-64

% Voltage Ratio Errors
RREVMean(f,13) =
RREVMean(f,12)*(sum(Vmeas(f,:,13)./sum(Vmeas(f,:,13)~=0)))/(sum(Vmeas(f,:,12)./sum(Vmeas(f,:,12)~=0)));
RREVMean(f,15) = RREVMean(f,15)*RREVMean(f,13);
% Current Ratio Errors
RREIMean(f,13) = RREVMean(f,13)*RREIMean(f,13);
RREIMean(f,15) = RREVMean(f,13)*RREIMean(f,15);

% 8th Pi section: 64-63

% Voltage Ratio Errors
RREVMean(f,16) =
RREVMean(f,15)*(sum(Vmeas(f,:,16)./sum(Vmeas(f,:,16)~=0)))/(sum(Vmeas(f,:,15)./sum(Vmeas(f,:,15)~=0)));
RREVMean(f,17) = RREVMean(f,17)*RREVMean(f,16);
% Current Ratio Errors
RREIMean(f,16) = RREVMean(f,16)*RREIMean(f,16);
RREIMean(f,17) = RREVMean(f,16)*RREIMean(f,17);

% 9th Pi section: 65-68

% Voltage Ratio Errors
RREVMean(f,14) =
RREVMean(f,12)*(sum(Vmeas(f,:,14)./sum(Vmeas(f,:,14)~=0)))/(sum(Vmeas(f,:,12)./sum(Vmeas(f,:,12)~=0)));
RREVMean(f,18) = RREVMean(f,18)*RREVMean(f,14);
% Current Ratio Errors
RREIMean(f,14) = RREVMean(f,14)*RREIMean(f,14);
RREIMean(f,18) = RREVMean(f,14)*RREIMean(f,18);

```

```

% 10th Pi section: 68-81

% Voltage Ratio Errors
RREVMean(f,19) =
RREVMean(f,18)*(sum(Vmeas(f, :,19)./sum(Vmeas(f, :,19)~=0)))/(sum(Vmeas(f, :,18)
)./sum(Vmeas(f, :,18)~=0)));
RREVMean(f,20) = RREVMean(f,20)*RREVMean(f,19);
% Current Ratio Errors
RREImMean(f,19) = RREVMean(f,19)*RREImMean(f,19);
RREImMean(f,20) = RREVMean(f,19)*RREImMean(f,20);

end

load RREV
load RREI

RREVe = zeros(T,1);
RREIe = zeros(T,1);

% Calculating the errors in estimating ratios of ratio errors
for f = 1:T
    for i = 2:1
        RREVe(f,i) = (RREV(f,i)) - (RREVMean(f,i));
    end
    for i = 1:1
        RREIe(f,i) = (RREI(f,i)) - (RREImMean(f,i));
    end
end

% Calculating the standard deviation of the errors in estimating ratios of
ratio errors
VoltSTD(1,:) = std(RREVe,0,1);
CurrSTD(1,:) = std(RREIe,0,1);

% Plotting the final results
x = 1:20;
plot(x,VoltSTD,'r.')
axis([0 21 0 0.012])
xlabel('End points of the lines')
ylabel('Error in estimating ratios of ratio errors of VTs')

figure

x = 1:20;
plot(x,CurrSTD,'r.')
axis([0 21 0 0.02])
xlabel('End points of the lines')
ylabel('Error in estimating ratios of ratio errors of CTs')

```

IEEE-300 bus system with a good quality measurement at bus 242 in the absence of a connected tree

```

%%%%%%%%%%%%%%%%%%%%%%%%%%%%%%%%%%%%%%%%%%%%%%%%%%%%%%%%%%%%%%%%%%%%%%%%
%
% Program Name: Instrument Transformer Calibration for IEEE-300 bus system %
%
% Description: Generating standard deviations of the errors in estimating %
%              ratio errors in the high voltage network of the IEEE 300 %
%              bus system with only one good quality measurement available %
%              at bus 242 following the methodology described in Ch-4 %
%
% Author: Paroma Chatterjee %
%         Virginia Polytechnic Institute and State University %
%
% Last Modified: 12/21/2015; 11:40 PM %
%
%%%%%%%%%%%%%%%%%%%%%%%%%%%%%%%%%%%%%%%%%%%%%%%%%%%%%%%%%%%%%%%%%%%%%%%%

```

```

clc
clear
close all

load V % loading the load flow voltages
load IL % loading the currents = voltages * line impedances

[row,ds,c] = size(V);
r = row*ds;

load REV % loading ratio errors in voltage transformers
load REI % loading ratio errors in current transformers

T = 1000;
RREVm = zeros(T,r/ds,1);
RREVmMean = zeros(T,1);
Vmeas = zeros(T,r/ds,1);
RREIm = zeros(T,r/ds,1);
RREImMean = zeros(T,1);

% Creating data to mimic field data

for f = 1:T
    for i = 1:r/ds
        for j = 1:ds
            for k = 1:1
                Vm(i,j,k) = V(i,j,k)*REV(f,k);
                Im(i,j,k) = IL(i,j,k)*REI(f,k);
            end
        end
    end
end

% Quantizing data
q_V = 20/345000; % Changing it to per unit

```

```

q_I = 0.64*345000/100000000;
Vmqr = zeros(r/ds,ds,1);
Imqr = zeros(r/ds,ds,1);
for i=1:r/ds
    Vt(:, :) = Vm(i, :, :);
    Vmqr = quant(real(Vt), q_V);
    Vmqi = quant(imag(Vt), q_V);
    Vmqr(i, :, :) = Vmqr + 1i*Vmqi;
    It(:, :) = Im(i, :, :);
    Imqr = quant(real(It), q_I);
    Imqi = quant(imag(It), q_I);
    Imqr(i, :, :) = Imqr + 1i*Imqi;
end

Vnew = Vmqr;
Inew = Imqr;

Vold = Vnew;
Iold = Inew;

% Solving for the ratios of ratio errors

for i = 1:r/ds
    j = randi([1 ds], ds/2, 1);
    k = randi([1 1], 1/2, 1);
    for n = 1:length(j)
        for m = 1:length(k)
            Vnew(i, j(n), k(m)) = NaN;
            Inew(i, j(n), k(m)) = NaN;
        end
    end
end

Avol = isfinite(Vnew);
Acurr = isfinite(Inew);

for i = 1:r/ds

    % 1st Pi section: 4-16
    count = 0;
    count1 = 0;
    for j = 1:ds
        if Avol(i, j, 1) == 0
            count = count+1;
        end
        if Avol(i, j, 2) == 0
            count1 = count1+1;
        end
    end
    if count == 0
        if count1==0
            B0(:, :) = [conj(Vnew(i, :, 1))' conj(Vnew(i, :, 2))'];
            A0(:, :) = [conj(Inew(i, :, 1))' conj(Inew(i, :, 2))'];
            X = lscov(A0, B0);
        end
    end
end
% AX = B; IZ = V; Z = lscov(I, V); X = lscov(A, B) = [ao b0; c0 d0]

```

```

        RREIm(f,i,1) = W(1,1)/(X(1,1)*b(1,1)*(W(1,1)+1));
% REIpq/REVpq = (1/a0)*(W/(B*(W+1)))
        RREIm(f,i,2) = 1/(X(2,1)*b(1,1)*(W(1,1)+1));
%REIqp/REVpq = (1/c0)*(1/(B*(W+1)))
        RREVm(f,i,2) = W(1,1)*X(1,2)/X(1,1);
% REVqp/REVpq = (b0/a0)*W
        Vmeas(f,i,2) = mean(Vnew(i,:,2));
    else
        RREIm(f,i,1) = 0;
        RREIm(f,i,2) = 0;
        RREVm(f,i,2) = 0;
    end
end

% 2nd Pi section: 16-42
count = 0;
count1 = 0;
for j = 1:ds
    if Avol(i,j,3) == 0
        count = count+1;
    end
    if Avol(i,j,4) == 0
        count1 = count1+1;
    end
end
if count == 0
    if count1 == 0
        B0(:, :) = [conj(Vnew(i,:,3))' conj(Vnew(i,:,4))'];
        A0(:, :) = [conj(Inew(i,:,3))' conj(Inew(i,:,4))'];
        X = lscov(A0,B0);
% AX = B; IZ = V; Z = lscov(I,V); X = lscov(A,B) = [ao b0; c0 d0]
        RREIm(f,i,3) = W(2,1)/(X(1,1)*b(2,1)*(W(2,1)+1));
% REIpq/REVpq = (1/a0)*(W/(B*(W+1)))
        RREIm(f,i,4) = 1/(X(2,1)*b(2,1)*(W(2,1)+1));
%REIqp/REVpq = (1/c0)*(1/(B*(W+1)))
        Vmeas(f,i,3) = mean(Vnew(i,:,3));
% Saving the mean voltage
        Vmeas(f,i,4) = mean(Vnew(i,:,4));
% Saving the mean voltage
        RREVm(f,i,4) = W(2,1)*X(1,2)/X(1,1);
% REVqp/REVpq = (b0/a0)*W
    else
        RREIm(f,i,3) = 0;
        RREIm(f,i,4) = 0;
        RREVm(f,i,4) = 0;
    end
end

% 3rd Pi section: 42-34
count = 0;
count1 = 0;
for j = 1:ds
    if Avol(i,j,5) == 0
        count = count+1;
    end
    if Avol(i,j,8) == 0

```

```

        count1 = count1+1;
    end
end
if count == 0
    if count1 == 0
        B0(:, :) = [conj(Vnew(i, :, 5))' conj(Vnew(i, :, 8))'];
        A0(:, :) = [conj(Inew(i, :, 5))' conj(Inew(i, :, 8))'];
        X = lscov(A0, B0);
% AX = B; IZ = V; Z = lscov(I, V); X = lscov(A, B) = [ao b0; c0 d0]
        RREIm(f, i, 5) = W(3, 1) / (X(1, 1) * b(3, 1) * (W(3, 1) + 1));
% REIpq/REVpq = (1/a0) * (W / (B * (W + 1)))
        RREIm(f, i, 8) = 1 / (X(2, 1) * b(3, 1) * (W(3, 1) + 1));
%REIqp/REVpq = (1/c0) * (1 / (B * (W + 1)))
        Vmeas(f, i, 5) = mean(Vnew(i, :, 5));
% Saving the mean voltage
        Vmeas(f, i, 8) = mean(Vnew(i, :, 8));
% Saving the mean voltage
        RREVM(f, i, 8) = W(3, 1) * X(1, 2) / X(1, 1);
% REVqp/REVpq = (b0/a0) * W
    else
        RREIm(f, i, 5) = 0;
        RREIm(f, i, 8) = 0;
        RREVM(f, i, 5) = 0;
        RREVM(f, i, 8) = 0;
    end
end

% 4th Pi section: 42-39
count = 0;
count1 = 0;
for j = 1:ds
    if Avol(i, j, 6) == 0
        count = count+1;
    end
    if Avol(i, j, 9) == 0
        count1 = count1+1;
    end
end
if count == 0
    if count1 == 0
        B0(:, :) = [conj(Vnew(i, :, 6))' conj(Vnew(i, :, 9))'];
        A0(:, :) = [conj(Inew(i, :, 6))' conj(Inew(i, :, 9))'];
        X = lscov(A0, B0);
% AX = B; IZ = V; Z = lscov(I, V); X = lscov(A, B) = [ao b0; c0 d0]
        RREIm(f, i, 6) = W(4, 1) / (X(1, 1) * b(4, 1) * (W(4, 1) + 1));
% REIpq/REVpq = (1/a0) * (W / (B * (W + 1)))
        RREIm(f, i, 9) = 1 / (X(2, 1) * b(4, 1) * (W(4, 1) + 1));
%REIqp/REVpq = (1/c0) * (1 / (B * (W + 1)))
        Vmeas(f, i, 6) = mean(Vnew(i, :, 6));
% Saving the mean voltage
        Vmeas(f, i, 9) = mean(Vnew(i, :, 9));
% Saving the mean voltage
        RREVM(f, i, 9) = W(4, 1) * X(1, 2) / X(1, 1);
% REVqp/REVpq = (b0/a0) * W
    else
        RREIm(f, i, 6) = 0;
        RREIm(f, i, 9) = 0;
    end
end

```



```

        RREVM(f,i,6) = 0;
        RREVM(f,i,9) = 0;
    end
end

% 5th Pi section 42-46
count = 0;
count1 = 0;
for j = 1:ds
    if Avol(i,j,7) == 0
        count = count+1;
    end
    if Avol(i,j,10) == 0
        count1 = count1+1;
    end
end
if count == 0
    if count1 == 0
        B0(:, :) = [conj(Vnew(i, :, 7))' conj(Vnew(i, :, 10))'];
        A0(:, :) = [conj(Inew(i, :, 7))' conj(Inew(i, :, 10))'];
        X = lscov(A0, B0);
% AX = B; IZ = V; Z = lscov(I, V); X = lscov(A, B) = [a0 b0; c0 d0]
        RREIm(f, i, 7) = W(5, 1) / (X(1, 1) * b(5, 1) * (W(5, 1) + 1));
% REIppq/REVppq = (1/a0) * (W / (B * (W + 1)))
        RREIm(f, i, 10) = 1 / (X(2, 1) * b(5, 1) * (W(5, 1) + 1));
%REIqp/REVppq = (1/c0) * (1 / (B * (W + 1)))
        Vmeas(f, i, 7) = mean(Vnew(i, :, 7));
% Saving the mean voltage
        Vmeas(f, i, 10) = mean(Vnew(i, :, 10));
% Saving the mean voltage
        RREVM(f, i, 10) = W(5, 1) * X(1, 2) / X(1, 1);
% REVqp/REVppq = (b0/a0) * W
    else
        RREIm(f, i, 7) = 0;
        RREIm(f, i, 10) = 0;
        RREVM(f, i, 7) = 0;
        RREVM(f, i, 10) = 0;
    end
end
end

% 6th Pi section: 46-81
count = 0;
count1 = 0;
for j = 1:ds
    if Avol(i, j, 11) == 0
        count = count + 1;
    end
    if Avol(i, j, 12) == 0
        count1 = count1 + 1;
    end
end
if count == 0
    if count1 == 0
        B0(:, :) = [conj(Vnew(i, :, 11))' conj(Vnew(i, :, 12))'];
        A0(:, :) = [conj(Inew(i, :, 11))' conj(Inew(i, :, 12))'];
        X = lscov(A0, B0);
    end
end

```

```

% AX = B; IZ = V; Z = lscov(I,V); X = lscov(A,B) = [a0 b0; c0 d0]
    RREIm(f,i,11) = W(6,1)/(X(1,1)*b(6,1)*(W(6,1)+1));
% REIpq/REVpq = (1/a0)*(W/(B*(W+1)))
    RREIm(f,i,12) = 1/(X(2,1)*b(6,1)*(W(6,1)+1));
%REIqp/REVpq = (1/c0)*(1/(B*(W+1)))
    Vmeas(f,i,11) = mean(Vnew(i,:,11));
% Saving the mean voltage
    Vmeas(f,i,12) = mean(Vnew(i,:,12));
% Saving the mean voltage
    RREVm(f,i,12) = W(6,1)*X(1,2)/X(1,1);
% REVqp/REVpq = (b0/a0)*W
    else
        RREIm(f,i,11) = 0;
        RREIm(f,i,12) = 0;
        RREVm(f,i,11) = 0;
        RREVm(f,i,12) = 0;
    end
end

% 7th Pi section: 81-194
count = 0;
count1 = 0;
for j = 1:ds
    if Avol(i,j,13) == 0
        count = count+1;
    end
    if Avol(i,j,15) == 0
        count1 = count1+1;
    end
end
if count == 0
    if count1 == 0
        B0(:, :) = [conj(Vnew(i,:,13))' conj(Vnew(i,:,15))'];
        A0(:, :) = [conj(Inew(i,:,13))' conj(Inew(i,:,15))'];
        X = lscov(A0,B0);
% AX = B; IZ = V; Z = lscov(I,V); X = lscov(A,B) = [a0 b0; c0 d0]
        RREIm(f,i,13) = W(7,1)/(X(1,1)*b(7,1)*(W(7,1)+1));
% REIpq/REVpq = (1/a0)*(W/(B*(W+1)))
        RREIm(f,i,15) = 1/(X(2,1)*b(7,1)*(W(7,1)+1));
%REIqp/REVpq = (1/c0)*(1/(B*(W+1)))
        Vmeas(f,i,13) = mean(Vnew(i,:,13));
% Saving the mean voltage
        Vmeas(f,i,15) = mean(Vnew(i,:,15));
% Saving the mean voltage
        RREVm(f,i,15) = W(7,1)*X(1,2)/X(1,1);
% REVqp/REVpq = (b0/a0)*W
        else
            RREIm(f,i,13) = 0;
            RREIm(f,i,15) = 0;
            RREVm(f,i,13) = 0;
            RREVm(f,i,15) = 0;
        end
    end
end

% 8th Pi section: 81-195
count = 0;

```

```

count1 = 0;
for j = 1:ds
    if Avol(i,j,14) == 0
        count = count+1;
    end
    if Avol(i,j,19) == 0
        count1 = count1+1;
    end
end
if count == 0
    if count1 == 0
        B0(:, :) = [conj(Vnew(i, :, 14))' conj(Vnew(i, :, 19))'];
        A0(:, :) = [conj(Inew(i, :, 14))' conj(Inew(i, :, 19))'];
        X = lscov(A0, B0);
% AX = B; IZ = V; Z = lscov(I, V); X = lscov(A, B) = [ao b0; c0 d0]
        RREIm(f, i, 14) = W(8, 1) / (X(1, 1) * b(8, 1) * (W(8, 1) + 1));
% REIppq/REVppq = (1/a0) * (W / (B * (W + 1)))
        RREIm(f, i, 19) = 1 / (X(2, 1) * b(8, 1) * (W(8, 1) + 1));
%REIqp/REVppq = (1/c0) * (1 / (B * (W + 1)))
        Vmeas(f, i, 14) = mean(Vnew(i, :, 14));
% Saving the mean voltage
        Vmeas(f, i, 19) = mean(Vnew(i, :, 19));
% Saving the mean voltage
        RREVM(f, i, 19) = W(8, 1) * X(1, 2) / X(1, 1);
% REVqp/REVppq = (b0/a0) * W
    else
        RREIm(f, i, 14) = 0;
        RREIm(f, i, 19) = 0;
        RREVM(f, i, 14) = 0;
        RREVM(f, i, 19) = 0;
    end
end
end

% 9th Pi section 194-219
count = 0;
count1 = 0;
for j = 1:ds
    if Avol(i, j, 16) == 0
        count = count + 1;
    end
    if Avol(i, j, 21) == 0
        count1 = count1 + 1;
    end
end
if count == 0
    if count1 == 0
        B0(:, :) = [conj(Vnew(i, :, 16))' conj(Vnew(i, :, 21))'];
        A0(:, :) = [conj(Inew(i, :, 16))' conj(Inew(i, :, 21))'];
        X = lscov(A0, B0);
% AX = B; IZ = V; Z = lscov(I, V); X = lscov(A, B) = [ao b0; c0 d0]
        RREIm(f, i, 16) = W(9, 1) / (X(1, 1) * b(9, 1) * (W(9, 1) + 1));
% REIppq/REVppq = (1/a0) * (W / (B * (W + 1)))
        RREIm(f, i, 21) = 1 / (X(2, 1) * b(9, 1) * (W(9, 1) + 1));
%REIqp/REVppq = (1/c0) * (1 / (B * (W + 1)))
        Vmeas(f, i, 16) = mean(Vnew(i, :, 16));
% Saving the mean voltage
        Vmeas(f, i, 21) = mean(Vnew(i, :, 21));
    end
end
end

```

```

% Saving the mean voltage
    RREVM(f,i,21) = W(9,1)*X(1,2)/X(1,1);
% REVqp/REVpq = (b0/a0)*W
    else
        RREIm(f,i,16) = 0;
        RREIm(f,i,21) = 0;
        RREVM(f,i,16) = 0;
        RREVM(f,i,21) = 0;
    end
end

% 10th Pi section: 194-664
count = 0;
count1 = 0;
for j = 1:ds
    if Avol(i,j,17) == 0
        count = count+1;
    end
    if Avol(i,j,18) == 0
        count1 = count1+1;
    end
end
if count == 0
    if count1 == 0
        B0(:, :) = [conj(Vnew(i, :, 17))' conj(Vnew(i, :, 18))'];
        A0(:, :) = [conj(Inew(i, :, 17))' conj(Inew(i, :, 18))'];
        X = lscov(A0, B0);
% AX = B; IZ = V; Z = lscov(I, V); X = lscov(A, B) = [ao b0; c0 d0]
        RREIm(f, i, 17) = W(10, 1) / (X(1, 1) * b(10, 1) * (W(10, 1) + 1));
% REIqp/REVpq = (1/a0)*(W/(B*(W+1)))
        RREIm(f, i, 18) = 1 / (X(2, 1) * b(10, 1) * (W(10, 1) + 1));
%REIqp/REVpq = (1/c0)*(1/(B*(W+1)))
        Vmeas(f, i, 17) = mean(Vnew(i, :, 17));
% Saving the mean voltage
        Vmeas(f, i, 18) = mean(Vnew(i, :, 18));
% Saving the mean voltage
        RREVM(f, i, 18) = W(10, 1) * X(1, 2) / X(1, 1);
% REVqp/REVpq = (b0/a0)*W
    else
        RREIm(f, i, 17) = 0;
        RREIm(f, i, 18) = 0;
        RREVM(f, i, 17) = 0;
        RREVM(f, i, 18) = 0;
    end
end

% 11th Pi section: 195-219
count = 0;
count1 = 0;
for j = 1:ds
    if Avol(i, j, 20) == 0
        count = count+1;
    end
    if Avol(i, j, 22) == 0
        count1 = count1+1;
    end
end

```

```

end
if count == 0
    if count1 == 0
        B0(:, :) = [conj(Vnew(i, :, 20))' conj(Vnew(i, :, 22))'];
        A0(:, :) = [conj(Inew(i, :, 20))' conj(Inew(i, :, 22))'];
        X = lscov(A0, B0);
% AX = B; IZ = V; Z = lscov(I, V); X = lscov(A, B) = [a0 b0; c0 d0]
        RREIm(f, i, 20) = W(10, 1) / (X(1, 1) * b(11, 1) * (W(11, 1) + 1));
% REIpq/REVpq = (1/a0) * (W / (B * (W + 1)))
        RREIm(f, i, 22) = 1 / (X(2, 1) * b(11, 1) * (W(11, 1) + 1));
% REIqp/REVpq = (1/c0) * (1 / (B * (W + 1)))
        Vmeas(f, i, 20) = mean(Vnew(i, :, 20));
% Saving the mean voltage
        Vmeas(f, i, 22) = mean(Vnew(i, :, 22));
% Saving the mean voltage
        RREVM(f, i, 22) = W(11, 1) * X(1, 2) / X(1, 1);
% REVqp/REVpq = (b0/a0) * W
    else
        RREIm(f, i, 17) = 0;
        RREIm(f, i, 18) = 0;
        RREVM(f, i, 17) = 0;
        RREVM(f, i, 18) = 0;
    end
end

% 12th Pi section: 219-237
count = 0;
count1 = 0;
for j = 1:ds
    if Avol(i, j, 23) == 0
        count = count + 1;
    end
    if Avol(i, j, 24) == 0
        count1 = count1 + 1;
    end
end
if count == 0
    if count1 == 0
        B0(:, :) = [conj(Vnew(i, :, 23))' conj(Vnew(i, :, 24))'];
        A0(:, :) = [conj(Inew(i, :, 23))' conj(Inew(i, :, 24))'];
        X = lscov(A0, B0);
% AX = B; IZ = V; Z = lscov(I, V); X = lscov(A, B) = [a0 b0; c0 d0]
        RREIm(f, i, 23) = W(12, 1) / (X(1, 1) * b(12, 1) * (W(12, 1) + 1));
% REIpq/REVpq = (1/a0) * (W / (B * (W + 1)))
        RREIm(f, i, 24) = 1 / (X(2, 1) * b(12, 1) * (W(12, 1) + 1));
% REIqp/REVpq = (1/c0) * (1 / (B * (W + 1)))
        Vmeas(f, i, 23) = mean(Vnew(i, :, 23));
% Saving the mean voltage
        Vmeas(f, i, 24) = mean(Vnew(i, :, 24));
% Saving the mean voltage
        RREVM(f, i, 24) = W(12, 1) * X(1, 2) / X(1, 1);
% REVqp/REVpq = (b0/a0) * W
    else
        RREIm(f, i, 17) = 0;
        RREIm(f, i, 18) = 0;
        RREVM(f, i, 17) = 0;
        RREVM(f, i, 18) = 0;
    end
end

```

```

end
end

% 13th Pi section: 237-231
count = 0;
count1 = 0;
for j = 1:ds
    if Avol(i,j,25) == 0
        count = count+1;
    end
    if Avol(i,j,26) == 0
        count1 = count1+1;
    end
end
if count == 0
    if count1 == 0
        B0(:, :) = [conj(Vnew(i,:,25))' conj(Vnew(i,:,26))'];
        A0(:, :) = [conj(Inew(i,:,25))' conj(Inew(i,:,26))'];
        X = lscov(A0,B0);
% AX = B; IZ = V; Z = lscov(I,V); X = lscov(A,B) = [ao b0; c0 d0]
        RREIm(f,i,25) = W(13,1)/(X(1,1)*b(13,1)*(W(13,1)+1));
% REIpq/REVPq = (1/a0)*(W/(B*(W+1)))
        RREIm(f,i,26) = 1/(X(2,1)*b(13,1)*(W(13,1)+1));
% REIqp/REVPq = (1/c0)*(1/(B*(W+1)))
        Vmeas(f,i,25) = mean(Vnew(i,:,25));
% Saving the mean voltage
        Vmeas(f,i,26) = mean(Vnew(i,:,26));
% Saving the mean voltage
        RREVm(f,i,26) = W(13,1)*X(1,2)/X(1,1);
% REVqp/REVPq = (b0/a0)*W
    else
        RREIm(f,i,25) = 0;
        RREIm(f,i,26) = 0;
        RREVm(f,i,25) = 0;
        RREVm(f,i,26) = 0;
    end
end
end

% 14th Pi section: 231-190
count = 0;
count1 = 0;
for j = 1:ds
    if Avol(i,j,27) == 0
        count = count+1;
    end
    if Avol(i,j,28) == 0
        count1 = count1+1;
    end
end
if count == 0
    if count1 == 0
        B0(:, :) = [conj(Vnew(i,:,27))' conj(Vnew(i,:,28))'];
        A0(:, :) = [conj(Inew(i,:,27))' conj(Inew(i,:,28))'];
        X = lscov(A0,B0);
% AX = B; IZ = V; Z = lscov(I,V); X = lscov(A,B) = [ao b0; c0 d0]
        RREIm(f,i,27) = W(14,1)/(X(1,1)*b(14,1)*(W(14,1)+1));

```

```

% REIpq/REVPq = (1/a0)*(W/(B*(W+1)))
                RREIm(f,i,28) = 1/(X(2,1)*b(14,1)*(W(14,1)+1));
% REIqp/REVPq = (1/c0)*(1/(B*(W+1)))
                Vmeas(f,i,27) = mean(Vnew(i,:,27));
% Saving the mean voltage
                Vmeas(f,i,28) = mean(Vnew(i,:,28));
% Saving the mean voltage
                RREVm(f,i,28) = W(14,1)*X(1,2)/X(1,1);
% REVqp/REVPq = (b0/a0)*W
                else
                    RREIm(f,i,27) = 0;
                    RREIm(f,i,28) = 0;
                    RREVm(f,i,27) = 0;
                    RREVm(f,i,28) = 0;
                end
            end
        end

end

RREVmold = RREVm;
RREImold = RREIm;

DummyV(:, :) = abs(RREVm(f, :, :));
DummyC(:, :) = abs(RREIm(f, :, :));
for j=1:r/ds
    for k = 1:l
        if DummyV(j,k)==0
            RREVm(f,j,k) = NaN;
        end
        if DummyC(j,k)==0
            RREIm(f,j,k) = NaN;
        end
    end
end

end
RREVmMean(f, :) = nanmean(RREVm(f, :, :));
RREImMean(f, :) = nanmean(RREIm(f, :, :));
clear DummyV DummyC

% 1st Pi section: 4-16: Everything remains the same

% 2nd Pi section: 16-42

% Voltage Ratio Errors
RREVmMean(f,3) =
RREVmMean(f,2)*( (sum(Vmeas(f,:,3) ./sum(Vmeas(f,:,3)~=0)))/(sum(Vmeas(f,:,2) ./
sum(Vmeas(f,:,2)~=0))));
RREVmMean(f,4) = RREVmMean(f,4)*RREVmMean(f,3);
% Current Ratio Errors
RREImMean(f,3) = RREVmMean(f,3)*RREImMean(f,3);
RREImMean(f,4) = RREVmMean(f,3)*RREImMean(f,4);

% 3rd Pi section: 42-34

% Voltage Ratio Errors

```

```

RREVMean(f,5) =
RREVMean(f,4)*(sum(Vmeas(f,:,5)./sum(Vmeas(f,:,5)~=0)))/(sum(Vmeas(f,:,4)./sum(Vmeas(f,:,4)~=0)));
RREVMean(f,8) = RREVMean(f,8)*RREVMean(f,5);
% Current Ratio Errors
RREImMean(f,5) = RREVMean(f,5)*RREImMean(f,5);
RREImMean(f,8) = RREVMean(f,5)*RREImMean(f,8);

% 4th Pi section: 42-39

% Voltage Ratio Errors
RREVMean(f,6) =
RREVMean(f,4)*(sum(Vmeas(f,:,6)./sum(Vmeas(f,:,6)~=0)))/(sum(Vmeas(f,:,4)./sum(Vmeas(f,:,4)~=0)));
RREVMean(f,9) = RREVMean(f,9)*RREVMean(f,6);
% Current Ratio Errors
RREImMean(f,6) = RREVMean(f,6)*RREImMean(f,6);
RREImMean(f,9) = RREVMean(f,6)*RREImMean(f,9);

% 5th Pi section: 42-46

% Voltage Ratio Errors
RREVMean(f,7) =
RREVMean(f,4)*(sum(Vmeas(f,:,7)./sum(Vmeas(f,:,7)~=0)))/(sum(Vmeas(f,:,4)./sum(Vmeas(f,:,4)~=0)));
RREVMean(f,10) = RREVMean(f,10)*RREVMean(f,7);
% Current Ratio Errors
RREImMean(f,7) = RREVMean(f,7)*RREImMean(f,7);
RREImMean(f,10) = RREVMean(f,7)*RREImMean(f,10);

% 6th Pi section: 46-81

% Voltage Ratio Errors
RREVMean(f,11) =
RREVMean(f,10)*(sum(Vmeas(f,:,11)./sum(Vmeas(f,:,11)~=0)))/(sum(Vmeas(f,:,10)./sum(Vmeas(f,:,10)~=0)));
RREVMean(f,12) = RREVMean(f,12)*RREVMean(f,11);
% Current Ratio Errors
RREImMean(f,11) = RREVMean(f,11)*RREImMean(f,11);
RREImMean(f,12) = RREVMean(f,11)*RREImMean(f,12);

% 7th Pi section: 81-194

% Voltage Ratio Errors
RREVMean(f,13) =
RREVMean(f,12)*(sum(Vmeas(f,:,13)./sum(Vmeas(f,:,13)~=0)))/(sum(Vmeas(f,:,12)./sum(Vmeas(f,:,12)~=0)));
RREVMean(f,15) = RREVMean(f,15)*RREVMean(f,13);
% Current Ratio Errors
RREImMean(f,13) = RREVMean(f,13)*RREImMean(f,13);
RREImMean(f,15) = RREVMean(f,13)*RREImMean(f,15);

% 8th Pi section: 81-195

% Voltage Ratio Errors

```



```

RREVMean(f,15) =
RREVMean(f,13)*(sum(Vmeas(f,:,15)./sum(Vmeas(f,:,15)~=0)))/(sum(Vmeas(f,:,13)
)./sum(Vmeas(f,:,13)~=0)));
RREVMean(f,19) = RREVMean(f,19)*RREVMean(f,15);
% Current Ratio Errors
RREImMean(f,15) = RREVMean(f,15)*RREImMean(f,15);
RREImMean(f,19) = RREVMean(f,15)*RREImMean(f,19);

% 9th Pi section: 194-219

% Voltage Ratio Errors
RREVMean(f,16) =
RREVMean(f,15)*(sum(Vmeas(f,:,16)./sum(Vmeas(f,:,16)~=0)))/(sum(Vmeas(f,:,15)
)./sum(Vmeas(f,:,15)~=0)));
RREVMean(f,21) = RREVMean(f,21)*RREVMean(f,16);
% Current Ratio Errors
RREImMean(f,16) = RREVMean(f,16)*RREImMean(f,16);
RREImMean(f,21) = RREVMean(f,16)*RREImMean(f,21);

% 10th Pi section: 194-664

% Voltage Ratio Errors
RREVMean(f,17) =
RREVMean(f,15)*(sum(Vmeas(f,:,17)./sum(Vmeas(f,:,17)~=0)))/(sum(Vmeas(f,:,15)
)./sum(Vmeas(f,:,15)~=0)));
RREVMean(f,18) = RREVMean(f,18)*RREVMean(f,17);
% Current Ratio Errors
RREImMean(f,17) = RREVMean(f,17)*RREImMean(f,17);
RREImMean(f,18) = RREVMean(f,17)*RREImMean(f,18);

% 11th Pi section: 195-219

% Voltage Ratio Errors
RREVMean(f,20) =
RREVMean(f,19)*(sum(Vmeas(f,:,20)./sum(Vmeas(f,:,20)~=0)))/(sum(Vmeas(f,:,19)
)./sum(Vmeas(f,:,19)~=0)));
RREVMean(f,22) = RREVMean(f,22)*RREVMean(f,20);
% Current Ratio Errors
RREImMean(f,20) = RREVMean(f,20)*RREImMean(f,20);
RREImMean(f,18) = RREVMean(f,20)*RREImMean(f,22);

% 12th Pi section: 219-237

% Voltage Ratio Errors
RREVMean(f,23) =
(RREVMean(f,21)*(sum(Vmeas(f,:,23)./sum(Vmeas(f,:,23)~=0)))/(sum(Vmeas(f,:,2
1) ./sum(Vmeas(f,:,21)~=0))))+
(RREVMean(f,22)*(sum(Vmeas(f,:,23)./sum(Vmeas(f,:,23)~=0)))/(sum(Vmeas(f,:,2
2) ./sum(Vmeas(f,:,22)~=0)))))/2 ;
RREVMean(f,24) = RREVMean(f,24)*RREVMean(f,23);
% Current Ratio Errors
RREImMean(f,23) = RREVMean(f,23)*RREImMean(f,23);
RREImMean(f,24) = RREVMean(f,23)*RREImMean(f,24);

% 13th Pi section: 237-231

```

```

    % Voltage Ratio Errors
    RREVMean(f,25) =
RREVMean(f,24)*(sum(Vmeas(f,:,25)./sum(Vmeas(f,:,25)~=0)))/(sum(Vmeas(f,:,24)
)./sum(Vmeas(f,:,24)~=0)));
    RREVMean(f,26) = RREVMean(f,26)*RREVMean(f,25);
    % Current Ratio Errors
    RREImMean(f,25) = RREVMean(f,25)*RREImMean(f,25);
    RREImMean(f,26) = RREVMean(f,25)*RREImMean(f,26);

    % 14th Pi section: 231-190

    % Voltage Ratio Errors
    RREVMean(f,27) =
RREVMean(f,26)*(sum(Vmeas(f,:,27)./sum(Vmeas(f,:,27)~=0)))/(sum(Vmeas(f,:,26)
)./sum(Vmeas(f,:,26)~=0)));
    RREVMean(f,28) = RREVMean(f,28)*RREVMean(f,27);
    % Current Ratio Errors
    RREImMean(f,27) = RREVMean(f,27)*RREImMean(f,27);
    RREImMean(f,28) = RREVMean(f,27)*RREImMean(f,28);

end

load RREV
load RREI

RREVe = zeros(T,1);
RREIe = zeros(T,1);

for f = 1:T
    for i = 1:l
        RREVe(f,i) = (RREV(f,i)) - (RREVMean(f,i));
    end
    for i = 1:l
        RREIe(f,i) = (RREI(f,i)) - (RREImMean(f,i));
    end
end

VoltSTD(1,:) = std(RREVe,0,1);
CurrSTD(1,:) = std(RREIe,0,1);

x = 1:28;
plot(x,VoltSTD,'r.')
axis([0 21 0 0.012])
xlabel('End points of the lines')
ylabel('Error in estimating ratios of ratio errors of VTs')

figure

x = 1:28;
plot(x,CurrSTD,'r.')
axis([0 21 0 0.02])
xlabel('End points of the lines')
ylabel('Error in estimating ratios of ratio errors of CTs')

```